



***Theoretical studies of silicon-
containing six-membered rings***

Kennilegir reikningar á kísilinnihaldandi sexhringjum

M.Sc. thesis

September 2008

Ragnar Björnsson

Academic dissertation

Submitted to the Department of Chemistry, Faculty of Science, University of Iceland

M.Sc. committee:

Prof. Ingvar Árnason (supervisor)

Department of Chemistry, University of Iceland

Prof. Ágúst Kvaran (co-supervisor)

Department of Chemistry, University of Iceland

Dr. Andras Bödi (external examiner)

Paul Scherrer Institute, Switzerland

Hér með lýsi ég því yfir að ritgerð þessi er samin af mér og að hún hefur hvorki að hluta né í heild verið lögð fram áður til hærri prófgráðu.

I hereby declare that this thesis is based on my own observations, is written by me and has neither in part nor whole been submitted for a higher degree

Ragnar Björnsson

Abstract

The conformational properties of six-membered heterocycles is an active field of study, yet silacyclohexanes have not been investigated nearly as thoroughly as other heterocycles. With the recent experimental data that has been obtained for the axial/equatorial energy difference of several mono- and disubstituted 1-silacyclohexanes, we carried out a computational study with the intent of reproducing the experimental results as well as possible. Density functional theory is a practical computational method but standard density functionals do not always yield accurate energies compared to experiment. Some severe problems of standard density functionals for simple organic systems, have been highlighted in the literature recently. New density functionals, designed to better describe medium-range correlation in molecules than previous functionals, were evaluated against coupled cluster (CCSD(T)) results for the axial/equatorial energy difference of several heterocyclic systems. The results show that the recent M06-2X and B2PLYP-D functionals are clearly superior to traditional functionals like B3LYP for conformational problems like ours and calculated free energy differences are in good agreement with experiments.

Using the M06-2X functional, we investigated systematically the effect of silicon substitution on a monosubstituted cyclohexane ring. The conformational energy difference was predicted for a large number of silacyclohexanes, ranging from 1 to 6 silicon atoms in the ring, most of which have never been studied experimentally or theoretically. The remarkably different conformational properties of silacyclohexanes compared to cyclohexanes and other heterocycles indicate that we do not yet fully understand conformational behaviour of simple organic molecules and identification of possible dominating stereoelectronic effects on the conformational behaviour would be of great interest.

A follow-up study on the potential energy surface of the parent (unsubstituted) disilacyclohexanes was undertaken and lowest energy pathways of ring inversion calculated. Geometries and enthalpies of formation were calculated and simulation attempted on the complicated ^1H NMR spectra of the disilacyclohexanes.

Ágrip

Rannsóknir á stellingajafnvægi kísilinnihaldandi sexhringja eru af skörum skammti ef borið er saman við rannsóknir á súrefnis- og niturinnihaldandi sexhringjum. Með tilkomu nýrra mæligagna fyrir stellingajafnvægi milli áslægrar og þverlægrar stellingar einsetinna og 1,1-tvísetinna 1-silacyclohexanafleiða, ákváðum við að framkvæma ítarlega rannsókn með tölvuútreikningum, með því takmarki að ná samræmi milli kennilegra reikninga og tilraunaniðurstaðna. Skammtafræðilegir tölvureikningar eru margs konar, en DFT reikningar eru sérlega hentugir fyrir mörg efnafræðileg vandamál. Hefðbundnar DFT aðferðir hafa hins vegar ekki alltaf gefið ásættanlegar niðurstöður og vandamál tengd DFT aðferðum á lífrænum sameindum hafa verið í brennidepli í fagtímaritum nýlega. Ný kynslóð DFT aðferða getur hins vegar spáð fyrir um orkumun stellinga mun nákvæmar en áður, skv. samanburði okkar við coupled cluster reikninga og tilraunaniðurstöður.

Einnig voru rannsökuð, áhrif þess að bæta kísilatómi inn í einsetinn cyclohexanhring á kerfisbundin hátt. Spáð var fyrir um orkumun fjölmargra silacyclohexana, sem innihéldu allt frá einu kísilatómi upp í sex og mismunandi sethópa. Sumar þessara sameinda hafa aldrei verið rannsakaðar, hvorki með tilraunum né reikningum. Stellingajafnvægi kísilinnihaldandi sexhringja er skv. reikningum okkar, töluvert frábrugðið því sem þekkt er fyrir cyclohexan og aðra heterohringi og niðurstöðurnar benda til þess að við eigum enn talsvert eftir í land með að skilja stellingajafnvægi einfaldra lífrænna sameinda.

Orkufirborð ósetinna disilacyclohexanafleiða hafa áður verið kortlögð og ferlar fyrir umhverfingu stólförms í annað verið reiknaðir. Með notkun nýrra reikniðferða til að finna söðulpunkta, voru ferlar endurbættir og reiknaðir á nákvæmari hátt en áður. Með tilkomu GED (gas electron diffraction) mælinga hafa byggingar sameindanna verið greindar og voru nýir tölvureikningar bornir saman við tengjalengdir og tengjahorn úr tilraunum. Þá voru reikningar á myndunarvarma efnanna framkvæmdir og tilraunir gerðar til að herma flókin ^1H NMR róf disilacyclohexana.

Acknowledgements

- Ingvar Árnason, for great supervision and allowing my transition from a synthetic organosilicon chemist to a computational organosilicon chemist.
- Andras Bödi, for showing me the ropes in computational chemistry.
- Sunna Ólafsdóttir Wallevik for sharing experimental results and discussions.
- Erlendur Jónsson, for many valuable discussions about computational chemistry and computational expertise.
- Ester Eyjólfsdóttir and Sunna Ólafsdóttir Wallevik, for great company throughout our graduate studies in the office, lab and Ottawa.
- Fellow grad students, project students, faculty and staff at the Science Institute for a friendly and supportive atmosphere.
- The computational facilities used for this project are gratefully acknowledged: the Apple Xserve G5 cluster of Hannes Jónsson's group and Jötunn, the Intel Linux cluster of Reiknistofnun, The University Computing Service, without which, this project simply would not have been possible.
- The Icelandic Research Fund and the University of Iceland Research Fund, for financial support.
- And finally my family, for at least pretending from time to time to show an interest in computational organosilicon chemistry.

Table of contents

	Page nr.
Introduction	1
Chapter 1 – Conformational properties of mono- and disubstituted 1-silacyclohexanes: Theory vs. experiment	
1.1 Introduction	9
1.2 Experimental conformational analysis	11
1.3 A short introduction to modern computational chemistry	12
1.4 Calculating accurate energy differences	23
1.4.1 Basis sets	25
1.4.2 Problems with DFT in computational organic chemistry	30
1.4.3 Recent functionals	33
1.4.4 Benchmarking density functionals	35
1.5 Obtaining accurate molecular geometries	42
1.5.1 Bond lengths	44
1.5.2 Angles	47
1.5.3 Effect of geometries on the single-point energy	47
1.6 Obtaining corrections to enthalpy and free energy	48
1.7 Modelling a low-temperature conformational equilibrium in solution	53
1.8 Comparing theory with experiment	55
Chapter 2 – Silicon substitution effects on the conformational properties of the cyclohexane ring: From cyclohexane to cyclohexasilane	
2.1 Introduction	59
2.2 Trends in ΔE values of silacyclohexane families	60
2.2.1 Choosing families and substituents	60
2.2.2 Monosilacyclohexane families	62
2.2.3 Disilacyclohexane families	66
2.2.4 Trisilacyclohexane families	70
2.2.5 The tetra- and penta-silacyclohexanes and cyclohexasilane	72
2.2.6 General observations	74
2.3 Stereoelectronic analysis	76

Chapter 3 – Disilacyclohexanes - physical properties and NMR spectra	
3.1 Introduction	79
3.2 Potential energy surfaces	80
3.3 Structure and stability	84
3.4 NMR spectra and attempted simulation	90
Summary	97
References	99
Publications and presentations regarding this thesis	106
Curriculum vitae	108
Appendices	111

List of figures

	Page nr.
Figure 1 The lowest energy path of the chair-chair inversion of cyclohexane.	2
Figure 2 The chair conformer of cyclohexane showing the axial and equatorial protons.	3
Figure 3 The axial/equatorial equilibrium of monosubstituted cyclohexane.	4
Figure 4 1,3-diaxial steric repulsion in axial tertbutylcyclohexane.	5
Figure 5 The hyperconjugation explanation of the anomeric effect in carbohydrates.	6
Figure 6 The monosubstituted silacyclohexane families investigated.	61
Figure 7 The monosilacyclohexane families and cyclohexane.	62
Figure 8 Graph showing the trends in ΔE values of the monosilacyclohexane families.	64
Figure 9 Plot of ΔE values of 1-silacyclohexane vs. cyclohexane.	65
Figure 10 Plot of ΔE values of 2-silacyclohexane vs. cyclohexane.	65
Figure 11 Plot of ΔE values of 3-silacyclohexane vs. cyclohexane.	65
Figure 12 Plot of ΔE values of 4-silacyclohexane vs. cyclohexane.	65
Figure 13 The disilacyclohexane families.	66
Figure 14 Trends in ΔE values of the mono- and disilacyclohexanes.	67
Figure 15 Plot of ΔE values of 1,4-disilacyclohexane vs. 1-silacyclohexane.	68
Figure 16 Plot of ΔE values of 1,4-disilacyclohexane vs. 4-silacyclohexane.	68
Figure 17 Plot of ΔE values of 2,6-disilacyclohexane vs. 1-silacyclohexane.	69
Figure 18 Plot of ΔE values of 3,5-disilacyclohexane vs. 3-silacyclohexane.	69
Figure 19 Plot of ΔE values of 2,6-disilacyclohexane vs. 1,4-disilacyclohexane.	69
Figure 20 Plot of ΔE values of 2,6-disilacyclohexane vs. 1-silacyclohexane.	69
Figure 21 The trisilacyclohexane families.	70
Figure 22 Trends in ΔE values of the trisilacyclohexane families.	71
Figure 23 Plot of ΔE values of 2,6-disilacyclohexane vs. 2,4,6-trisilacyclohexane.	71
Figure 24 Plot of ΔE values of 3,5-disilacyclohexane vs. 1,3,5-trisilacyclohexane.	72
Figure 25 The tetra- and pentasilacyclohexane families and cyclohexasilane.	72
Figure 26 Trends in ΔE values of the tetra- and pentasilacyclohexanes.	73
Figure 27 Lowest-energy path of 1,2-disilacyclohexane.	81
Figure 28 Lowest-energy path of 1,3-disilacyclohexane.	82
Figure 29 Lowest-energy path of 1,4-disilacyclohexane.	82
Figure 30 Calculated path between twistforms Twist-1a and Twist-1b of 1,3-disilacyclohexane.	83
Figure 31 Diagram for the calculation of enthalpies of formation of the disilacyclohexanes.	88
Figure 32 Simulated vs. measured NMR spectrum of 1,2-disilacyclohexane.	93
Figure 33 Ball-and-stick model of 1,2-disilacyclohexane.	93
Figure 34 Simulated vs. measured NMR spectrum of 1,3-disilacyclohexane.	94
Figure 35 Ball-and-stick model of 1,3-disilacyclohexane.	94
Figure 36 Simulated vs. measured NMR spectrum of 1,4-disilacyclohexane.	95
Figure 37 Ball-and-stick model of 1,4-disilacyclohexane.	95

List of tables

	Page nr.
Table 1 <i>A</i> values (in kcal/mol) of a few monosubstituted cyclohexanes.	5
Table 2 Physical properties of organosilicon compounds.	7
Table 3 Experimental data of monosubstituted 1-silacyclohexanes.	9
Table 4 The scaling of the HF and post-HF computational methods.	16
Table 5 Calculated vs. experimental <i>A</i> values of a few monosubstituted 1-silacyclohexanes.	24
Table 6 B3LYP calculated ΔE values of 1-silyl-1-silacyclohexane with different basis sets.	27
Table 7 B3LYP and M06-2X calculations using different grid settings.	36
Table 8 ΔE values of several heterocycles using different computational methods.	38
Table 9 ΔE values of 2-ethoxy-tetrahydropyran with different computational methods.	40
Table 10 Calculated geometric parameters of silacyclohexanes compared to GED parameters.	46
Table 11 M06-2X/pc-3 ΔE values on different geometries of 1-silyl-1-silacyclohexane.	47
Table 12 Relative corrections to enthalpy and free energy by different methods for 1-fluoro-1-methyl-1-silacyclohexane.	51
Table 13 <i>A</i> values from DNMR experiments compared with solvent-corrected <i>A</i> values (IPCM).	54
Table 14 ΔH values of monosubstituted 1-silacyclohexanes obtained from Raman experiments in different solvents.	54
Table 15 Experimental data of mono- and disubstituted 1-silacyclohexanes compared with quantum calculated data.	56
Table 16 Raman ΔH values compared to calculated ΔH values of monosubstituted 1-silacyclohexanes.	57
Table 17 M06-2X/pc-3 calculated ΔE values of different monosilacyclohexane families.	63
Table 18 M06-2X/pc-3 calculated ΔE values of different disilacyclohexane families.	66
Table 19 M06-2X/pc-3 calculated ΔE values of different trisilacyclohexane families.	70
Table 20 M06-2X/pc-3 calculated ΔE values of different tetrasilacyclohexane families.	73
Table 21 M06-2X/pc-3 calculated ΔE values of different pentasilacyclohexane and cyclohexasilane families.	73
Table 22 ΔE values of 1-CCl ₃ -2,3,4,5,6-pentasilacyclohexane with different computational methods.	75
Table 23 Relative energies of conformers of 1,2-disilacyclohexane with different methods.	84
Table 24 Relative energies of conformers of 1,3-disilacyclohexane with different methods.	84
Table 25 Relative energies of conformers of 1,4-disilacyclohexane with different methods.	84
Table 26 Experimental and calculated geometric parameters of 1,2-disilacyclohexane.	85
Table 27 Experimental and calculated geometric parameters of 1,3-disilacyclohexane.	86
Table 28 Experimental and calculated geometric parameters of 1,4-disilacyclohexane.	86
Table 29 The bond skeleton of the disilacyclohexanes.	87
Table 30 Calculated enthalpies of formation for the disilacyclohexanes using different methods.	89
Table 31 Relative enthalpy differences for the disilacyclohexanes.	89
Table 32 Simulated coupling constants and linewidths of 1,2-disilacyclohexane.	93
Table 33 Simulated coupling constants and linewidths of 1,3-disilacyclohexane.	94
Table 34 Simulated coupling constants and linewidths of 1,4-disilacyclohexane.	95

Introduction

The conformational properties of six-membered saturated heterocycles is the focus of this work. Conformational analysis of cycloalkanes and heterocycles is a field that has contributed much to the understanding of bonding and energy in organic chemistry. Understanding the conformational properties of cycloalkanes and heterocycles is crucial if one intends to study and understand the conformations of biological macromolecules like proteins and nucleic acids; some biomolecules like sugars and steroids even include 5- and 6-membered ring systems. Conformational analysis plays also a role in drug discovery. When a drug (that often includes a heterocycle) binds to an enzyme it doesn't necessarily react through the lowest energy conformation. The human body temperature, 37°C, can be sufficiently high for low energy minor conformers of a drug to be significantly populated [1]. One cannot but wonder how much attention is paid to this fact when screening large receptor databases (that probably only include the lowest energy conformer) to enzyme active sites.

Cyclohexane is the most stable of the simplest cycloalkanes, with an ΔH_f° of -29.9 kcal/mol, compared to -18.3, +6.7, and +12.7 to cyclopentane, cyclobutane, and cyclopropane, respectively [2]. The common explanation for this energy difference involves considering the lowest energy conformer of cyclohexane as having zero strain energy, with its almost perfect tetrahedral bond angles and staggered bonds, thus resulting in no torsional strain and minimal steric strain as compared to the smaller cycloalkanes.

Also in contrast to other cycloalkanes, the lowest energy conformer of cyclohexane, the chair form, dominates in general. Other known conformers are the half-chair, twist-boat and boat.

To understand the conformational landscape of cyclohexane it is informative to look at the chair-chair lowest energy path (figure 1).

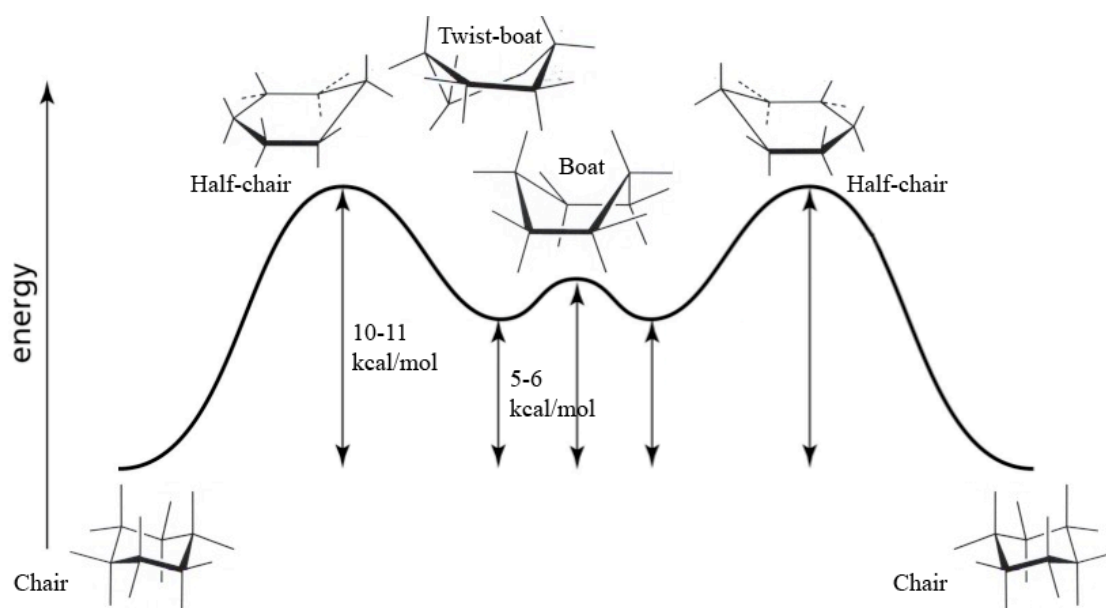


Figure 1. The lowest energy path of the chair-chair inversion of cyclohexane.

The twist-boat is another minimum on the potential energy surface (PES) of cyclohexane but lies 5-6 kcal/mol higher [2]. The half-chair and boat are both saddle points on the PES. The half-chair conformer constitutes the barrier to chair inversion, it lies at 10-11 kcal/mol on the PES, thus 10-11 kcal/mol being the activation energy of the chair-chair inversion. The half-chair connects the chair and the twist-boat. The twist-boat can then undergo conversion (through a transformation known as pseudorotation) to other twist-boats through a boat transition state; all twist-boat forms being equivalent due to symmetry (applies to cyclohexane but not necessarily to heterocycles).

The half-chair is strained due to the 5 carbons lying in one plane. This strain can be relieved by converting into the twist-boat. The boat form is higher in energy than the twist-boat, that can be explained as being due to hydrogen flagpole interactions (steric strain) and eclipsed bonds (torsional strain). The twist-boat also has similar steric and torsional strain but just not as much as the boat form.

It should also be noted that another possible conformer, planar cyclohexane, is never encountered in the chair-chair inversion and has never been encountered experimentally, as this would be a highly strained structure (calculations suggest > 25 kcal/mol higher in energy than the chair form).ⁱ

ⁱ M06-2X/pc-2//B3LYP/6-31G(d)

Another way of showing the conformational landscape of six-membered rings is the conformational globe by Cremer and Szabo [3], that can be very helpful in understanding the possible conformational pathways, especially when the ring system contains a heteroatom. An example for utilizing this model in our group involves 1-silacyclohexane [4]. Each point of the globe (of the volume of the sphere) corresponds to a specific conformation of cyclohexane but the energetically most favorable conformers are on the surface. Going from the north pole of the globe to the equator is e.g. the chair to twist-boat transformation. Transformation along the equator is the process of pseudorotation mentioned earlier.

Though the chair conformer is highly symmetric, there exist two different types of hydrogens, usually designated as axial and equatorial hydrogens; axial hydrogens sticking up and down from the “ring plane” (figure 2).

The difference between hydrogens or substituents in the axial and equatorial positions is an important part of cyclohexane and heterocyclic chemistry.

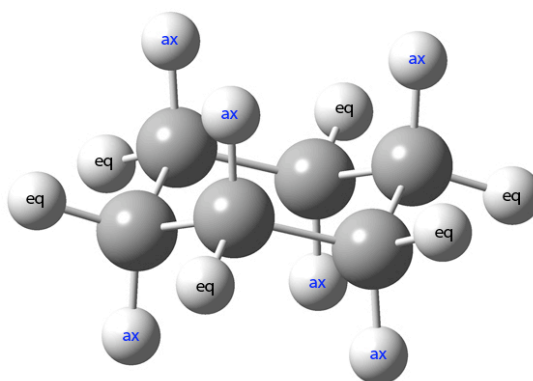


Figure 2. The chair conformer of cyclohexane showing the axial and equatorial protons.

Because of a low enough barrier, chair-chair inversion or ring flipping takes place at room temperature. During the ring inversion, the axial bonds become equatorial and vice versa. A single resonance is detected for all 12 protons in the nuclear magnetic resonance (NMR) experiment at room temperature, due to interconversion taking place at a timescale faster than the NMR timescale (ms range).

Lowering the temperature down to 200 K, the interconversion is slowed sufficiently down so separate resonances are detected for the axial and equatorial protons.

Conformational analysis of substituted cyclohexanes mainly involves the axial/equatorial equilibrium of the chair conformer; other conformers of cyclohexane can often be disregarded. A classic example of conformational analysis in general is that of methylcyclohexane. When measuring the conformational equilibrium of methylcyclohexane (ignoring twist-boat and boat forms), using integration of peaks from each conformer in an ^{13}C NMR spectrum for example, one would detect that the conformer with the methyl group in the equatorial position is in great excess (95 %) compared to the conformer where the methyl group possesses the axial position. Thermodynamically this can be described as $A = -\Delta G = RT \ln(K)$ where K is the equilibrium constant of the conformational equilibrium shown in figure 3.

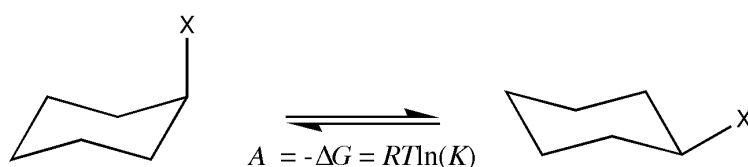


Figure 3. The axial/equatorial equilibrium of monosubstituted cyclohexane.

The A value is the free energy difference of the two conformers, for methylcyclohexane a value of ~ 1.7 kcal/mol [5]. A positive A value means that the equatorial conformer is more stable than the axial conformer, in this case by 1.7 kcal/mol while a negative value would mean that the axial conformer is in excess. It is important to realize what an energy difference of 1.7 kcal/mol means in terms of population of conformers. At room temperature the equatorial conformer is 95 % of the methylcyclohexane conformers and the axial conformer is only 5 %.

What is the nature of this energy difference between conformers, one might wonder?

The classical explanation is the one found in almost all organic chemistry textbooks from 1940-2006, the so called 1,3-diaxial repulsion [2], [6].

This constitutes steric strain between an axial substituent with the axial hydrogens of two carbons of the ring, thus destabilizing the axial conformer with respect to the equatorial conformer where this interaction is nonexistent (figure 4).

A more steric substituent in the axial position should thus result in the further destabilization of the axial conformer and thus a larger equilibrium constant and A value. And a less steric substituent should result in a smaller A value.

This simple model appears to be reasonable when considering the cases of *tert*-butylcyclohexane (a rather bulky substituent) and fluorocyclohexane (a very small substituent), see table 1. In fact, *A* values are often used as a measure of the steric bulkiness of a substituent.

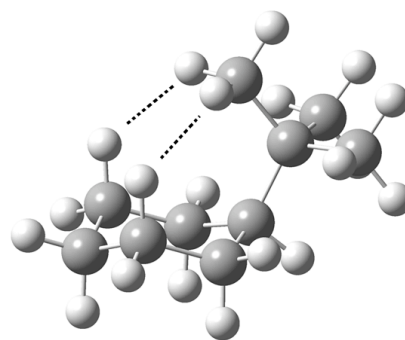


Figure 4. 1,3-diaxial steric repulsion in axial *tert*-butylcyclohexane.

Monosubstituted cyclohexanes thus have a general equatorial preference and with the rare exceptions of mercurybonded substituents, all monosubstituted cyclohexanes have positive *A* values [5].

Table 1. *A* values (in kcal/mol) of a few monosubstituted cyclohexanes [5].

Substituent	<i>A</i> value	% eq	Experiment
F	0.28-0.38	62-66 %	¹⁹ F NMR at 180-187 K
Me	1.74	95 %	¹³ C NMR at 300 K
CF ₃	2.5	99 %	¹⁹ F NMR at 300 K
SiH ₃	1.45	92 %	¹³ C NMR at 188 K
<i>t</i> -Bu	4.9	~100 %	¹³ C NMR at 153 K

The conformational analysis of heterocycles has mostly involved nitrogen and oxygen as heteroatoms, due to the availability of piperidine and piperazine rings in natural products like alkaloids and in pharmaceuticals, while oxygen-containing rings play a big role in carbohydrate chemistry where most common sugars are tetrahydropyran derivatives. An obvious consequence of heteroatom insertion is different bond lengths and both C-O and C-N bonds are shorter than C-C bonds. This often causes considerable strain in the rings and among with electronic effects this leads to different conformational properties. A very interesting conformational effect in heterocycles originates from carbohydrate chemistry, the anomeric effect. It can be described as a trend of the glycosidic linkage at the carbon next to the oxygen atom, to have an axial preference rather than an equatorial one. This preference seems to result from the alignment of the exocyclic C-O bond anti to the lone pair of the ring oxygen.

Explanations of the anomeric effect generally involve favorable orbital interaction, hyperconjugation, a stereoelectronic effect, where the lone pair of the ring oxygen acts as a donor towards the exocyclic acceptor C-O bond and stabilizes the axial conformer more due to greater orbital overlap (figure 5). Other factors have also been suggested, as for example that the axial arrangement of the exocyclic C-O bond cancels repulsive electrostatic interactions or that dipoles are more favorably aligned [7].

This hyperconjugative interaction as an explanation for the anomeric effect in carbohydrates has been widely accepted for some time, but has recently been questioned by recent QTAIM calculations (quantum theory of atoms in molecules) [8], [9].

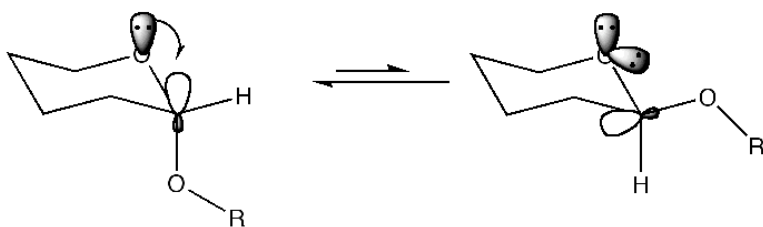


Figure 5. The hyperconjugation explanation of the anomeric effect in carbohydrates.

The anomeric effect has in later years been extended as the general description of the gauche preference of the C-Y bond in an X-C-Y-C system where X and Y are heteroatoms having lone pairs (known examples are O, N, S and F).ⁱⁱ One of the simplest systems where the anomeric effect takes place is dimethoxyethane. The conformational properties of tetrahydropyrans will be discussed more later.

This thesis is about the conformational analysis of heterocycles where the heteroatom is silicon and focuses mostly on the axial/equatorial equilibrium of mono- and disubstituted silacyclohexanes. The conformational properties of cyclohexanes and N- and O- heterocycles have been studied extensively for a long time but heterocycles containing silicon atoms have not been investigated nearly as thoroughly as is evident in a recent review of the conformational properties of six-membered heterocycles by Kleinpeter [10]. This is despite the fact that silicon is in the same group as carbon in the periodic table, has similar electronic structure with its 4 valence electrons and the atom usually forms 4 covalent bonds. It is thus interesting to study heteroatom effects of an atom so similar to carbon.

ⁱⁱ IUPAC Compendium of Chemical Terminology, Electronic version, <http://goldbook.iupac.org/A00372.html>.

Main differences between carbon and silicon, from a physical organic point of view, are less electronegativity and a greater atomic radius of silicon, silicon thus forms longer bonds in general. Some physical properties that highlight these differences are shown in table 2.

Table 2. Physical properties of organosilicon compounds.

	Bond length	Bond energy^a		Electronegativity^a	Covalent radius^c
C-C	1.54 Å ^a	80 kcal/mol	C	2.5	76 pm
C-H	1.09 Å ^a	99 kcal/mol	H	2.1	31 pm
Si-C	1.87 Å ^a	75 kcal/mol	Si	1.8	111 pm
Si-Si	2.34 Å ^a	47 kcal/mol			
Si-H	1.47 Å ^b	75 kcal/mol			

^a [11]

^b Bond length of SiH₄ [12].

^c [13]

The conformational properties of silacyclohexanes in the last few years have mostly come from research conducted in the group of Prof. Ingvar Arnason at the University of Iceland. Important milestones in the area of conformational analysis of silacyclohexanes are given below:

- Several papers in 1998-2001 investigated 1,3,5-trisilacyclohexanes that were synthesized, their NMR properties evaluated [14], [15], [16], conformational properties calculated [17], [18] and the structures measured by gas-phase electron diffraction [19].
- The conformational landscape of silacyclohexane was calculated for the first time in detail in 2000 [20] and confirmed in 2006 [4].
- The conformational analysis of the 1-methyl-1-silacyclohexane [21] was thoroughly reinvestigated in 2002 where contradicting old results were discussed and different experimental and theoretical methods were evaluated. The much smaller *A* value of 1-methyl-1-silacyclohexane (0.45 kcal/mol) as compared to 1-methylcyclohexane (1.74 kcal/mol) is an interesting result.

- Another paper in 2007 dealt with the conformational properties of 1-trifluoromethyl-1-silacyclohexane [22]. While the carbon analogue shows a clear preference ($A = 2.5$ kcal/mol) for the equatorial conformer the silicon analogue shows a small axial preference ($A = -0.19$ kcal/mol from GED). This is quite a surprising result as one would expect, based on the steric repulsion model, the A value to be smaller for the silicon analogue but certainly not of opposite sign.

The sharp contrast between the conformational equilibrium of the CF_3 -substituted cyclohexane and CF_3 -substituted silacyclohexane is one of the reasons why the conformational properties of silacyclohexanes continue to be of great interest in the group of Ingvar Arnason.

Using quantum chemical calculations as a tool to perform conformational analysis, we have investigated and reinvestigated several silacyclohexanes as well as cyclohexanes (for comparison) in this thesis. Our aim has been not only to achieve coherence with the results of the experimental methods but also to go a step further in the conformational analysis where ‘experiment’ cannot go and make an attempt at understanding what drives the conformational equilibrium of the various silacyclohexane families. This project was carried out at the same time as a sister project by Sunna Ólafsdóttir Wallevik that dealt with the synthesis and spectroscopic measurements of several mono- and disubstituted 1-silacyclohexanes [23].

Chapter 1 – Conformational properties of mono- and disubstituted 1-silacyclohexanes: Theory vs. experiment

1.1 Introduction

In the recent years conformational data has emerged for a few monosubstituted 1-silacyclohexanes using several experimental and theoretical methods.

The experimental methods involve gas-phase electron Diffraction (GED), dynamic nuclear magnetic resonance (DNMR), Raman spectroscopy and microwave spectroscopy. These different experimental methods offer different kind of conformational data: different thermodynamic properties and can be measured in different phases (gas, pure liquid, solvated). While we obtain molecular structures, vibrational frequencies, free energies of activation and other information from the experimental methods mentioned above, we are mainly interested in the conformational energy difference of the axial and equatorial conformers. The M.Sc. project of Sunna Ólafsdóttir Wallevik as well as work from previous M.Sc. student Pálmar Ingi Guðnason [24] has culminated in the synthesis of several mono- and disubstituted 1-silacyclohexanes. Experimental results of some of these molecules are summarized in table 3.

Table 3. Experimental data of monosubstituted 1-silacyclohexanes [23]. *A* values and ΔH values in kcal/mol.

	GED (<i>A</i> / mol % axial)	DNMR (<i>A</i> / mol % axial)	Raman (ΔH) ^c
CH ₃	0.45(14) / 32 (7) %	0.23 (2) / 26(1) % ^a	0.15 (neat) ^d
	<i>T</i> = 298 K	<i>T</i> = 110 K	0.15 (pentane) ^d 0.16 (CH ₂ Cl ₂) ^d
CF ₃	-0.19(29) / 58 (12) %	0.4 (1) / 17(2) % ^a	-0.53 (neat)
	<i>T</i> = 293 K	<i>T</i> = 113 K	-0.51 (pentane) -0.62 (CH ₂ Cl ₂)
F	-0.31(20) / 63 (8) %	-0.13 (2) / 64(2) % ^a	-0.25 (neat)
	<i>T</i> = 293 K	<i>T</i> = 112 K	-0.22 (pentane) -0.28 (CH ₂ Cl ₂)
SiH ₃	-0.17(15) / 57(7) %	0.12 (3) / 45(3) % ^b	-0.19 (neat)
	<i>T</i> = 321 K	<i>T</i> = 100 K ^c	-0.22 (heptane) -0.19 (THF)

^a Low temperature NMR measurements were performed in a 1:1:3 solvent mixture of CD₂Cl₂, CHFCl₂, and CHF₂Cl.

^b SiD₄ was used as solvent for the low temperature measurements.

^c Raman measurements were carried out at variable temperatures and the van't Hoff relation was used for analysis.

^d Raman measurements were carried out for 1-deuterium-1-methyl-silacyclohexane.

What is evident from the experimental data in table 3, is not only the dramatically different conformational properties of 1-silacyclohexanes compared to cyclohexanes (table 1), but also the general low energy difference between conformers (less than 0.5

kcal/mol). This is a problem for experimental methods as well as theoretical methods if one hopes to accurately acquire energy differences of conformers and then compare differently substituted molecules in order to understand what drives the conformational equilibrium.

One main objective in this thesis was to do a thorough analysis of what is needed to properly calculate accurate energy differences of the synthesized silacyclohexanes and understand the reason for the failure of some computational methods, as will be discussed later, and see if it is possible with one method to get reasonably accurate values that compare well with the experimental results. Such a method could be used to explore other similar systems and thus provide an (hopefully) economic and robust alternative tool to synthesis and measurement to get conformational data of silacyclohexanes and heterocycles in general.

A thorough investigation of the difference between data obtained from experiment and theory is important, not only for our main objective in understanding what drives the conformational equilibrium of the silacyclohexanes, but this work also serves as error analysis for computational chemistry. Development of computational methods (especially density functional theory and force-field modelling) depends on understanding why different methods do worse or fail dramatically for different chemical systems. Theoretical determination of thermodynamic properties like entropies, can even be more troublesome, as will be discussed later.

The different experimental methods provide different thermodynamic properties and are carried out in different environments. For theory to be able to successfully model all the different experiments is actually a formidable problem, we are looking at very small energy differences (compared with the total energy of the system), trying to account for zero-point energy, enthalpic and entropic effects due to many possible vibrations and even trying to model different environments. A short introduction to the experiments that we are modelling, follows.

1.2 Experimental conformational analysis

The gas-phase electron diffraction experiment involves obtaining a diffraction pattern from molecules being hit by an electron beam in the gas phase. It is one of the most valuable methods to get accurate molecular structures in the gas phase (that are unaltered by intermolecular effects) and by examining closely the diffraction pattern, usually with the help of theoretical methods, one can obtain the ratio of the different conformers present at room temperature. The resulting equilibrium constant is then related to the free energy difference, $\Delta G = -RT \ln(K)$. The experiment is carried out in the gas-phase, typically at room temperature or close to it.

In the dynamic NMR experiment the rate of the conformational equilibrium is slowed down by lowering the temperature (sometimes even down to 100 K) until one obtains different resonances from the nuclei of the different conformers. Magnetic resonances from ^1H , ^{13}C and ^{19}F can all be used successfully for conformational analysis although ^1H resonances from different conformers have often too small chemical shift differences to be of practical use. ^{29}Si nuclei, while having reasonably high abundance, have too low sensitivity to be useful for conformational analysis. By peak integration, one obtains the ratio of conformers and thus the free energy difference and by line shape analysis at the coalescence temperature one can also obtain the free energy of activation for the equilibrium. The experiment is carried out in the solvated phase, using solvents with very low freezing points (typically freons).

Temperature-dependent Raman spectroscopy can be used for conformational analysis by examining the line intensities of analogous vibrational frequencies from the different conformers. Using the van't Hoff relation, $\ln(A_a/A_c) = -\Delta H/RT + \text{constant}$, one obtains the enthalpy difference of the conformers; where A is the intensity of a vibrational frequency from either conformer. Entropy contributions are not obtained from the experiment due to the fact that we generally don't know the extinction coefficients of the spectral bands, thus the free energy difference is not obtained. The experiment can be carried out in the vapour phase, neat liquid or in a solvated phase [25].

1.3 A short introduction to modern computational chemistry

Our objective is aimed at getting relative energies between two conformers of small molecules. Modelling by molecular mechanics involves defining a molecule in terms of Newtonian mechanics where atoms are treated as single particles and bonds treated as springs. It is often the only theory available to model large biological molecules. Due to the general bad performance of molecular mechanics to model the conformational equilibrium we are interested in, as is demonstrated by Halgren [26], these methods will not be discussed further.

Using quantum mechanics we can obtain the total energy of a molecule, which is defined as containing the kinetic energies of the electrons and the nuclei, the attraction of the electrons to the nuclei and interelectronic and internuclear repulsions of the molecular system. As all of chemistry is essentially governed by quantum mechanics it is the most rigorous theory one can use to explain chemical problems of interest, like conformational equilibria.

As the performance of different quantum mechanical methods on the properties of chemical systems will be closely discussed in this thesis, an introduction to quantum chemistry follows.

Computational methods in quantum chemistry involve solving (approximately) the many-electron, non-relativistic, time-independent Schrödinger equation:

$$\hat{H}\Psi_i(\vec{x}_1, \vec{x}_2, \dots, \vec{x}_N, \vec{R}_1, \vec{R}_2, \dots, \vec{R}_M) = E_i \Psi_i(\vec{x}_1, \vec{x}_2, \dots, \vec{x}_N, \vec{R}_1, \vec{R}_2, \dots, \vec{R}_M) \quad (1-1)$$

where the Hamiltonian operator is defined as:

$$\hat{H} = -\frac{1}{2} \sum_{i=1}^N \nabla_i^2 - \frac{1}{2} \sum_{A=1}^M \frac{1}{M_A} \nabla_A^2 - \sum_{i=1}^N \sum_{A=1}^M \frac{Z_A}{r_{iA}} + \sum_{i=1}^N \sum_{j>i}^N \frac{1}{r_{ij}} + \sum_{A=1}^M \sum_{B>A}^M \frac{Z_A Z_B}{R_{AB}} \quad (1-2)$$

The Schrödinger equation can only be solved approximately for real chemical systems as the only exact analytical solutions known to the Schrödinger equation exist for the hydrogen atom, He^+ , H_2^+ and similar systems containing only a single electron.

Quantum chemistry thus involves different approximations to the Schrödinger equation. An almost universal approximation in quantum chemistry, that is applied to further simplify the Schrödinger equation, is the Born-Oppenheimer approximation. Due to the significant mass differences of the nuclei vs. the electron (even the proton weighs 1800 times more than the electron) the nuclei move much slower than the electrons and it is thus possible to disregard the kinetic energy term of the nuclei and look at the repulsion energy of the nuclei as a constant. The problem thus simplifies to solving only the electronic Schrödinger equation with the electronic Hamiltonian (equation 1-3) and adding the nuclear repulsion term to get the total energy (often called the electronic energy nonetheless).

$$\hat{H}_{\text{elec}} = -\frac{1}{2} \sum_{i=1}^N \nabla_i^2 - \sum_{i=1}^N \sum_{A=1}^M \frac{Z_A}{r_{iA}} + \sum_{i=1}^N \sum_{j>i}^N \frac{1}{r_{ij}} = \hat{T} + \hat{V}_{\text{Ne}} + \hat{V}_{\text{ee}} \quad (1-3)$$

The Born-Oppenheimer approximation is also vital with regard to chemistry, as without it we wouldn't have a potential energy surface (PES) in quantum chemistry, a frightening thought, as so much in chemistry can be explained by the concept of a PES. The validity of the Born-Oppenheimer approximation has actually been in the news recently ⁱⁱⁱ due to startling experimental evidence a few years ago that suggested failure of the approximation. A follow-up experimental and theoretical study, however, reconfirmed the validity of the Born-Oppenheimer approximation.

While we can set up the electronic Hamiltonian operator for a specific chemical system, the problem is finding the eigenfunctions ψ_i , i.e. the electronic wave functions of the chemical system. Once the eigenfunctions are determined, the operators of the Hamiltonian can be applied to the eigenfunctions and yield the energy eigenvalues. This is a problem because it isn't possible to find the eigenfunctions in a direct way. However, due to the variational principle there is a systematic way of approaching the ground state eigenfunction ψ_0 . It states that the energy computed by using an appropriate normalized trial wave function, will be an upper bound to the true energy of the ground state, as shown in equation 1-4.

ⁱⁱⁱ <http://www.rsc.org/chemistryworld/News/2008/January/03010802.asp>

$$\langle \Psi_{\text{trial}} | \hat{H} | \Psi_{\text{trial}} \rangle = E_{\text{trial}} \geq E_0 = \langle \Psi_0 | \hat{H} | \Psi_0 \rangle \quad (1-4)$$

The Hartree-Fock approximation involves constructing this N-electron trial wave function as an antisymmetrized product of N one-electron wave functions (that we can solve) that is called a Slater determinant, equation 1-5.

$$\Psi_0 \approx \Phi_{\text{SD}} = \frac{1}{\sqrt{N!}} \begin{vmatrix} \chi_1(\vec{x}_1) & \chi_2(\vec{x}_1) & \cdots & \chi_N(\vec{x}_1) \\ \chi_1(\vec{x}_2) & \chi_2(\vec{x}_2) & & \chi_N(\vec{x}_2) \\ \vdots & \vdots & & \vdots \\ \chi_1(\vec{x}_N) & \chi_2(\vec{x}_N) & \cdots & \chi_N(\vec{x}_N) \end{vmatrix} \quad (1-5)$$

Using the variational principle we can then find the best Slater determinant that yields the lowest energy (which will be closest to the true energy).

While we won't go into the specifics of the Hartree-Fock equations and the self-consistent field procedure of solving them, we note that this strategy can never yield the true wave function or the true ground state energy. The Hartree-Fock approximation neglects instantaneous electron-electron interaction or electron correlation as the Fock operator is only a simple one-electron operator with an average repulsive potential term, which means each electron interacts only with a mean field within the Hartree-Fock approximation. The difference between the true ground state energy and the Hartree-Fock energy is the electron correlation energy. The Hartree-Fock approximation is, however, variational. The total HF energy will always be higher than the exact total energy, never lower.

$$E_{\text{C}}^{\text{HF}} = E_0 - E_{\text{HF}} \quad (1-6)$$

The post Hartree-Fock methods involve how to calculate the electron correlation energy correctly. This is the so called wave function based *ab initio* quantum chemistry, *ab initio* meaning 'from the beginning' and means that empirical observations of chemical systems do not enter into the equations in any way.

A conceptually simple way of accounting for electron correlation is through the perturbation approach by Møller and Plesset. The HF wave function is mapped onto a perturbation theory formulation, becoming a first-order perturbation. Adding the second order level of perturbation, which results in the MP2 method, captures most of the correlation. MP2 is the most popular perturbation method. One can continue infinitely and the perturbation levels of MP3 and MP4 are also sometimes used. The sometimes oscillating convergence of the perturbational approach [27] is the reason that it is not used systematically for approaching the wave function by increasing gradually the order of perturbation. MP2 shows the most reliable convergence but it is not uncommon to find MP2 total energies being lower than the exact total energy. None of the MP n methods are variational.

Another way of accounting for electron correlation is by using a multiple determinant wave function. Configuration interaction and coupled cluster theory are two different approaches where the Hartree-Fock wave function is systematically expanded by taking into account excited Slater determinants and in principle one can approach the true wave function and energy in this way. Approximations are, however, almost always used. In the coupled cluster formulation the wave function is built in this way:

$$|\Psi\rangle = e^{\hat{T}}|\Phi_0\rangle \quad (1-7)$$

$$\hat{T} = \sum_{n=1}^{\infty} \hat{T}_n$$

The excitation operator is expressed as a sum of excitations. One of the most famous coupled cluster approximations is the CCSD(T) approach where the S and D stand for single and double excitations and the (T) means that triple excitations are accounted for in a perturbative way.

As electron correlation is such a vital part of almost all chemical systems the standard Hartree-Fock approximation as a computational method is often insufficient. All the procedures of going beyond the HF approximation have dramatic computational consequences, however. The formal scaling of HF calculations is N^4 where N can be for

example be a measure of molecular size^{iv}. This means that a calculation twice as big would take 16 times as long to complete. The more elaborate post HF methods have even more troubling scaling behaviour as shown in table 4.

Table 4. The scaling of the HF and post-HF computational methods.

	H₂O	2 H₂O	Scaling
HF	1	16	N ⁴
MP2	1	32	N ⁵
MP3, CCSD	1	64	N ⁶
MP4, CCSD(T)	1	128	N ⁷
MP7, CCSDTQ	1	1024	N ¹⁰

The orbitals used for building up the wave function must be specified somehow. A convenient starting point is to use the functions from the exact solution of the Schrödinger equation for the hydrogen atom (Slater-type orbitals). It is computationally more convenient, however, to use combinations of Gaussian functions to mimic the Slater-type orbitals. Multiple Gaussians are needed to accurately mimic each Slater-type orbital or basis function. A minimal basis would have one basis function (made out of 3 Gaussians for example) for each occupied orbital of an atom and is called a single-zeta basis set. It is usually inadequate as there isn't enough flexibility to describe different molecular environments. In a double-zeta basis set there are 2 basis functions to describe each orbital. Since most of chemistry is about the interaction of valence electrons, John Pople (coauthor of the Gaussian software [28] and Nobel laureate) developed the split-valence basis sets that are single-zeta in the core region and double- or triple-zeta in the valence region. To provide even more flexibility in the basis set to describe electron distribution in molecular systems, multi-zeta basis sets aren't enough. The basis set is thus expanded to include functions that mimic orbitals with angular momentum one higher than the valence region (sometimes even higher). These basis functions are called polarization functions and would involve adding *d* functions to p-block elements like carbon and *p* functions to hydrogens. When the molecule carries a negative charge (anions) the basis set is usually augmented with extra diffuse functions that allow the electron density to expand into a larger volume. The split-valence basis sets by Pople, which are shown below, are probably the best known basis set family and are still very much in use.

^{iv} Strictly, N is the number of basis functions required to approximate all the one-electron wave functions in a Slater determinant

STO-3G : A minimal single-zeta basis set.

6-31G : A double-zeta split-valence basis set.

6-31G(d) : A double-zeta split-valence basis set with d polarization functions.

6-31+G(d): Same as above but with diffuse functions.

6-311+G(d,p) : A triple-zeta basis set with diffuse functions and both d and p polarization functions.

6-311++G(3df,3pd): A triple-zeta basis set with many diffuse and higher order polarization functions.

As mentioned before, the scaling of the post-HF methods is clearly quite unfavorable and it turns out that these methods depend heavily on the number of basis functions to reach good accuracy; i.e. many basis functions are needed to achieve good accuracy and due to unfavorable scaling with respect to basis functions, such calculations will take a long time.

The composite methods were developed to achieve accurate energies by these post-HF methods, but by taking advantage of the additive effects of basis sets. Instead of doing one calculation with an expensive method like CCSD(T) and a large basis set, many smaller calculations are done with a less expensive method with several basis sets and an expensive method calculation is done with a small basis. Adding all these effects together the net outcome is an energy roughly equivalent to that of an expensive method/ large basis calculation in much less time. Well known composite methods are G3B3 theory [29], [30] and CBS-QB3 [31], [32].

Density functional theory is another way of solving the Schrödinger equation. Unlike HF and post-HF methods, DFT stays away from the complicated many-electron wave function. Instead its equations are based on the electron density, a quantity that is a function of only three spatial variables (compared to the N electron wave function that depends on $3N$ variables).

Although equations relating the electron density of a quantum system to its energy are almost as old as the Schrödinger equation itself, it wasn't until the arrival of the Hohenberg-Kohn theorems in 1964 where the ground state electron density was directly related to the ground state wave function, that density functional theory had a firm theoretical basis [33]. Furthermore they stated that the density that minimized the total

energy was the exact groundstate energy; DFT now had it's own variational principle as well.

While the Hohenberg-Kohn theorems showed that it was possible to solve the Schrödinger equation using the ground state density, they provided no way of how to get the ground state density. The equations of Kohn and Sham provided such a way a year later, in a 1965 paper where the problem was reformulated by taking as a starting point a fictitious system of non-interacting electrons that has the same overall density as the real interacting system [34]. This density can be expressed as a Slater determinant of one-electron functions.

The energy functional^v can be expressed [35]:

$$\begin{aligned}
 E[\rho(\vec{r})] &= T_s[\rho] + J[\rho] + E_{xc}[\rho] + E_{Ne}[\rho] \\
 &= T_s[\rho] + \frac{1}{2} \iint \frac{\rho(\vec{r}_1) \rho(\vec{r}_2)}{r_{12}} d\vec{r}_1 d\vec{r}_2 + E_{xc}[\rho] + \int V_{Ne} \rho(\vec{r}) d\vec{r} \\
 &= -\frac{1}{2} \sum_i^N \langle \phi_i | \nabla^2 | \phi_i \rangle + \frac{1}{2} \sum_i^N \sum_j^N \iint |\phi_i(\vec{r}_1)|^2 \frac{1}{r_{12}} |\phi_j(\vec{r}_2)|^2 d\vec{r}_1 d\vec{r}_2 \\
 &\quad + E_{xc}[\rho(\vec{r})] - \sum_i^N \int \sum_A^M \frac{Z_A}{r_{iA}} |\phi_i(\vec{r}_1)|^2 d\vec{r}_1
 \end{aligned} \tag{1-8}$$

where $T_s[Q]$ is the non-interacting kinetic energy functional, $J[Q]$ is the classical Coulomb electron-electron interaction, $E_{Ne}[Q]$ the nuclei-electron interaction and $E_{xc}[Q]$ is the exchange-correlation functional. The $E_{xc}[Q]$ term contains the quantum-mechanical contributions to the potential energy, that is the exchange energy and correlation energy and also the rest of the kinetic energy that isn't covered by T_s .

The Kohn-Sham approach thus involves calculating as much as possible of the density but putting everything that isn't known how to deal with directly, into the exchange-correlation term, $E_{xc}[Q]$. The above energy expression can be subjected to the variational principle with respect to the individual orbitals and the resulting equations solved self-consistently (very similar as the Hartree-Fock SCF procedure), if an expression for the E_{xc} term can be given.

^v A functional is a function of a function. The energy functional acts on the density (another function) yielding the energy (a number) as output.

This is the big unknown of density functional theory and it is important to realize that if the exact exchange correlation functional was known the Kohn-Sham strategy would lead to the exact energy and thus an exact solution to the Schrödinger equation [35]. Unfortunately it isn't.

Density functional development has thus mainly revolved around making approximations to the exchange-correlation functional in order to come up with an expression of the functional that is as close to the real, exact (and unknown) functional as possible. The different flavours of density functional theory available are thus usually only different approximations to the exchange-correlation functional. The functional is generally divided into two separate terms, an exchange term and a correlation term and an approximation made to each term individually:

$$E_{xc}[Q] = E_x[Q] + E_c[Q] \quad (1-9)$$

The simplest form of an approximate exchange-correlation functional is the local density approximation, LDA. It assumes that the exchange-correlation energy at any point in space is a function of the electron density at that point in space only and can be given by the electron density of a homogeneous electron gas of the same density.

The electron density of a molecular system is generally very different from a homogeneous electron gas. The LDA approximation isn't satisfactory for molecular systems (overbinding of chemical bonds and underestimation of barrier heights) and LDA-based DFT hardly made an impact on computational chemistry and was mainly used in solid-state physics [35].

In the early eighties, the generalized gradient approximation (GGA) was developed as an extension to the LDA approximation. Within the GGA approximation the exchange and correlation energies depend not only on the density but also on the gradient of the density. Density functionals based on GGA are a significant improvement over LDA and give much better total energies, atomization energies, structural energy differences and energy barriers. Examples are the BLYP, PBE, BP86, HCTH and mPWPW91 functionals.

Hybrid functionals give even better performance. By combining exchange-correlation from GGA with exact (Hartree-Fock) exchange in the hybrid functional one obtains the recipe for a class of functionals that have been the most successful for a large number of properties since they were introduced. Usually only a certain percentage of HF exchange is introduced and this introduces a degree of empiricism into the functional approximation as each component of the exchange functional now has a weight factor that cannot be determined from first-principles and is thus usually fitted to experimental data. It is informative to look at the formulation for the very popular B3LYP functional [36]:

$$E_{xc}^{B3LYP} = E_{xc}^{LDA} + a_0 (E_x^{HF} - E_x^{LDA}) + a_x (E_x^{B88} - E_x^{LDA}) + a_c (E_c^{LYP} - E_c^{LDA}) \quad (1-10)$$

$a_0 = 0.20$, $a_x = 0.72$ and $a_c = 0.81$ are the three empirical parameters. B3LYP thus has 20 % Hartree-Fock exchange.

Other examples of hybrid functionals include B3P86, B97-1, B98, PBE1PBE, BH&LYP, MPW1K, mPW3LYP etc.

The B3LYP functional, since its introduction in 1994 [36], is by far the most popular functional in chemistry today, with around 80 % usage in the chemistry literature of all density functionals [37]. This is a very interesting observation, that implies both that functional development since 1994 has not been as successful as people had hoped for, but perhaps also that chemists sometimes blindly choose B3LYP over other functionals that might be much more successful for several properties.

In the recent few years, a new class of density functionals have begun to appear, named meta-GGA functionals. They are dependent on higher order density gradients or the kinetic energy density. Examples are TPSS, BB95, VSXC.

Hybrid variants of the meta-GGA class have also appeared that include HF exchange and recent comparisons show them to be a general improvement over GGA and GGA-hybrids for several properties [37]. Examples are B1B95, TPSSh, BB1K, BMK.

Density functional theory is a nice alternative to the wave-function theories, its attractive scaling being one of the most important aspects. Keeping in mind the scaling of the wave function theories in table 4, DFT usually scales as N^3 (GGA and meta-GGA) or N^4 (hybrids) and one can generally use the same basis functions as the HF and post-HF

methods. In solid-state physics, plane-waves are often used instead of Gaussians, that are more convenient in systems with periodic boundary conditions.

Density functional theory is, however, not without its problems.

- Due to the exchange-correlation functional being an approximation and not the true exact functional, DFT as we know it, is non-variational; total energies less than the exact total energy can thus be obtained.
- The functionals used today, also have not reached “chemical accuracy”, the ultimate goal of most quantum mechanical methods, that involves calculating thermodynamical quantities like enthalpies of formation within 1 kcal/mol. The performance of B3LYP for the well known G3/99 database of 223 enthalpies of formations is a mean absolute error of 4.8 kcal/mol against experimental data [38].
- Current density functionals also experience something called the self-interaction error which can be described as the interaction of the electron with itself.
- Weak or nonbonding interactions are also a limitation of DFT with most functionals failing dramatically for van der Waals complexes for example. This limitation of DFT will be discussed more later.
- Perhaps the most serious problem of current density functional theory is that it cannot be systematically improvable. The exact density functional is not known, and although we have several clues about its nature, we have no real path towards finding it, unlike wave function theory where the wave function can be systematically improved by increasing the level of electron correlation (by excited determinants). Perdew, however, has recently categorized the current and future development of DFT into five different stages or rungs of a “Jacob’s ladder” [39]. The LDA and GGA approximations are the first two stages of the ladder while meta-GGA’s enter into the third stage. As one goes up the ladder, one approaches

“heaven” or the exact density functional. Much of DFT development is right now at the third rung but fourth and fifth rung functionals are starting to appear.

1.4 Calculating accurate energy differences

Popular tools for calculating conformational energy differences of small molecules have for the last few years, mainly been density functionals like B3LYP and the MP2 method. B3LYP and MP2 thus were the most obvious choices to try, to see if we could reproduce the recent experimental results for the synthesized 1-silacyclohexanes. Most calculations in chapter 1 and 2 were carried out with NWChem 5.1, the computational chemistry software package by Pacific Northwest National Laboratory [40].

The energetic quantities used in this thesis are shown below:

$\Delta E = E^{\text{ax}} - E^{\text{eq}}$: The electronic energy difference between conformers.

$\Delta H = H^{\text{ax}} - H^{\text{eq}}$: The enthalpy difference between conformers.

$H = E + H^{\text{corr}}$: The enthalpy that equals the electronic energy plus the thermal correction to energy and enthalpy (includes zero-point energy).

$H^{\text{corr}} = E_{\text{zpe}} + E_{\text{vib}} + E_{\text{rot}} + E_{\text{transl}} + RT$: Zero-point energy (ZPE), thermal corrections due to vibrations, rotations and translations.

$A = G^{\text{ax}} - G^{\text{eq}}$ = The free energy difference (or A value) between conformers.

$G = E + G^{\text{corr}}$ = The free energy equals the electronic energy plus the free energy correction.

$G^{\text{corr}} = H^{\text{corr}} - TS_{\text{tot}}$: The free energy correction consists of the correction to enthalpy plus a term containing the thermal correction to entropy.

Results of the MP2^{vi} and B3LYP calculations for several 1-silacyclohexanes, first presented at the *12th European symposium on gas electron diffraction* in Blaubeuren June 2007, compared with GED experimental results, are shown in table 5.

^{vi} MP2 and CCSD(T) calculations are usually performed using the frozen-core approximation where only the valence electrons are correlated while the core electrons are HF-approximated. All MP2 and CCSD(T) calculations mentioned in this thesis are frozen-core approximated.

Table 5. Calculated vs. experimental *A* values (in kcal/mol) of a few monosubstituted 1-silacyclohexanes, C₅H₁₀SiHX .

X=	GED results (<i>A</i> /mol % axial)	B3LYP^a (<i>A</i> /mol % axial)	MP2^a (<i>A</i> /mol % axial)
CH ₃	0.45(14) 32(7) %	0.66 25 %	0.35 36 %
CF ₃	-0.19(29) 58(12) %	0.13 45 %	-0.28 63 %
F	-0.31(20) 63(8) %	-0.24 60 %	-0.15 56 %
SiH ₃	-0.17(15) kcal/mol 57(7) %	0.52 kcal/mol 29 %	0.20 kcal/mol 42 %

^a Geometries and thermal corrections to free energy calculated at the B3LYP/6-311+G(d,p) level of theory in all cases. The MP2 electronic energies are calculated with the aug-cc-pVTZ basis set but the B3LYP calculations with the 6-311+G(d,p) basis set.

As shown in table 5, the popular B3LYP functional seems rather inconsistent in predicting *A* values of the molecules in question. While it predicts the energy difference for the 1-fluoro-1-silacyclohexane quite well, it predicts the wrong sign for the 1-trifluoromethyl molecule, and both wrong sign and significant deviation for 1-silyl-1-silacyclohexane. Generally, B3LYP appears to predict too much stabilization of the equatorial conformer.

The MP2 method seems more consistent, predicting in general smaller deviations from experiment than B3LYP (except 1-fluoro). It still predicts the wrong sign for 1-silyl-1-silacyclohexane though, but is much closer to the experimental result than B3LYP.

When comparing experimental free energies to computational free energies, the comparison can be quite risky since the computations involve several factors: calculation of a molecular geometry with one method and one basis set, calculation of a single-point energy with one method and one basis set and finally a frequency calculation with perhaps another method and basis set. Obviously errors are associated with each calculation that might build up or cancel out. However, in table 5, the same geometries and thermal corrections to free energy were used for both the B3LYP and MP2 calculations. Since the MP2 results generally seem to be better, the errors associated with the B3LYP results must mainly be due to the single-point energy B3LYP calculation and thus either a deficiency of the functional or the basis set used (6-311+G(d,p) vs. aug-cc-pVTZ).

One must of course also be aware that errors are associated with the experimental values as well and the uncertainties given for the GED *A* values are often considerable.

However, the tendency for equatorial-overstabilization of the B3LYP calculations and the much better results of the MP2 calculations (MP2 conformational energies are more reliable according to recent reports [41], [42]), seemed to point towards a deficiency of the DFT calculations.

This apparent failure of the B3LYP functional, the most popular density functional used in computational chemistry today, to predict consistent energy differences of these molecules, interested us. We wanted to understand whether this error was associated with our own calculations or if B3LYP or perhaps density functional theory in general was inadequate of predicting accurate conformational energy differences of this small magnitude.

Few studies have been reported, concerning the accuracy of density functionals to predict conformational energy differences [41].

1.4.1 Basis sets

We started to look at the basis set, as we wanted to see how large effect the basis set has on the calculation and if the basis we used before was inadequate in some way.

It is important to remember here that the concept of a basis set is an approximation and that ideally one would use as many basis functions as is needed until the energy has converged (a complete basis), instead of tailormade basis sets for specific calculations. This is not universal, as sometimes density functionals are parameterized for a specific basis set and are intended for use with that basis set only.

When the energy is converged in DFT calculations, all that remains is the error of the functional approximation. A complete basis is, however, obviously not practical.

One can, however, approach a complete basis by using basis set families designed to systematically approach the basis set limit, by including more functions of the correct nature in each step and then inspect if the difference between each step is low enough for one's purpose of accuracy. Sometimes it is also possible to extrapolate to the complete basis set limit.

The basis set family by Dunning, the correlation-consistent basis sets (cc-pVnZ, where n stands for the multi-zeta level of the basis set) [43], [44], are very popular for systematic expansion of the basis set. While designed for configuration interaction (and also intended for coupled cluster calculations) they have been used for MP2, HF and

DFT calculations as well. It has been pointed out though that these basis sets might not be ideal for DFT calculations and use of them can lead to unreliable convergence, despite them having more basis functions [45].

Recently, it has also been pointed out that the correlation-consistent basis sets are insufficient with regard to *d*-polarization functions of second-row elements (Al-Cl). This includes silicon. By adding extra tight *d*-functions and reoptimizing exponents of *d*-functions in the basis set, the energy of a second-row element containing molecule converges more normally. This has led to the cc-pV(*n*+*d*)Z basis sets by Wilson et al. and are generally recommended when calculating properties of molecules with second-row elements (Al-Ar) [46].

The polarization-consistent basis sets were introduced in 2001 by Jensen and are still being developed and evaluated [47-54]. This basis set family was designed for DFT and HF calculations, by noticing that the basis set convergence of DFT and HF is exponential [55], [56], as opposed to the inverse power series convergence of correlation energies of the post-HF methods [57]. By careful selection of angular momentum functions and optimization of constants in each basis set, the basis set family systematically approaches the complete basis set limit, but in a much more economic way than the correlation-consistent basis sets, i.e. less basis functions.

Systematically approaching the complete basis set limit was something we wanted to explore and to begin with we explored the basis set expansion of our molecules using the B3LYP functional. We are comparing the basis set convergence of relative energies of conformers (i.e. ΔE values) that few studies have been devoted to, although several recent studies on the behaviour of density functionals with respect to basis set have been carried out [58-62].

As a benchmark molecule we chose the 1-silyl-1-silacyclohexane molecule as this was one of the molecules in table 5 with significant deviations from the experimental results and it contained 2 silicon atoms (i.e. 2 second-row atoms).

Table 6. ΔE values (in kcal/mol) of the axial/equatorial equilibrium of 1-silyl-1-silacyclohexane^a.

B3LYP calculations with different basis sets.

Basis set ^b	ΔE	Nr. functions ^d
Split-valence basis sets		
6-31G(d)	0.464	134
6-31G(d,p)	0.466	176
6-31++G(d,p)	0.551	218
6-311G(d)	0.519	184
6-311G(d,p)	0.487	226
6-311++G(d,p)	0.482	268
6-311++G(2d,2p)	0.519	345
6-311++G(3df,3pd)	0.546	541
Correlation-consistent basis sets		
cc-pVDZ	0.531	176
cc-pVTZ	0.514	414
cc-pVQZ	0.547	813
aug-cc-pVDZ	0.432	295
aug-cc-pVTZ	0.546	652
aug-cc-pVQZ	0.535	1212
cc-pV(D+d)Z ^c	0.554	186
cc-pV(T+d)Z ^c	0.527	424
cc-pV(Q+d)Z ^c	0.555	823
Polarization-consistent basis sets ^c		
pc-0	0.184	99
pc-1	0.474	176
pc-2	0.520	414
pc-3	0.549	924
aug-pc-0	0.123	141
aug-pc-1	0.394	295
aug-pc-2	0.550	652
aug-pc-3	0.553	1323

^a $A = -\Delta G = -0.17(15)$ kcal/mol for 1-silyl-1-silacyclohexane, according to the GED experiment.

^b The aug-prefix means the basis set is augmented with diffuse functions.

^c Basis sets were obtained from the EMSL library at <https://bse.pnl.gov/bse/portal>.

^d Total number of basis functions for describing the atomic orbitals of 1-silyl-1-silacyclohexane in each basis set.

Several B3LYP single-point energy calculations on 1-silyl-1-silacyclohexane were carried out on a geometry optimized at the B3LYP/6-311+G(d,p) level, using several different basis sets. Results are shown in table 6 where one can see the effect of increasing basis set on the electronic energy difference. The ΔE values for the split-

valence basis sets show some zig-zag behaviour when diffuse functions (+) and polarization functions are added. The largest split-valence basis set is 6-311++G(3df, 3pd) that should be the closest to the basis set limit (judged by the number of basis functions) but the path from the smallest basis set to the largest is not smooth. An apparent basis set error of ~ 0.08 kcal/mol for some of the split-valence basis sets compared to the largest basis set calculated (aug-pc-3) is significant, if one keeps in mind the small energy differences that we are interested in.

Using the larger correlation-consistent basis sets the energy appears to be converged at the cc-pVQZ (quadruple-zeta) and the aug-cc-pVQZ level at 0.547 kcal/mol and 0.535 kcal/mol, respectively. The cc-pVQZ and aug-cc-pVQZ basis sets are considerably larger than the biggest Pople basis set though. Adding diffuse functions to cc-pVDZ, i.e. aug-cc-pVDZ, causes some ΔE deviation, worse in fact than the similarly small split-valence basis sets.

The cc-pV($n+d$)Z basis sets by Wilson et al. have a noticeable effect on the convergence for the double and triple-zeta basis sets but a very small effect on the quadruple-zeta basis set. These basis sets are designed to better describe second-row elements and thus it seems possible that they might be more important if a molecule includes even more second-row elements. This was explored in conjunction with calculations in chapter 2 and results can be found in appendix 1.3.

Using the polarization-consistent basis sets by Jensen we obtained converged ΔE values at 0.549 and 0.553 kcal/mol using the pc-3 and aug-pc-3 basis sets, respectively. This is very similar to the correlation-consistent basis set results. It's a very encouraging result, that the by far largest basis set, aug-pc-3 (see number of functions in table 6) yields a ΔE value that is almost the same as the smaller pc-3 and cc-pV(Q+d)Z values and very close to pc-2 and cc-pV(T+d)Z values as well.

Diffuse functions seem to have larger effects on the ΔE values when the polarization level of the basis set is low or medium and often seem to result in ΔE values that deviate more from the basis set limit (compare cc-pVDZ and aug-cc-pVDZ). When the polarization level is high, diffuse functions have small effects (compare cc-pVQZ vs. aug-cc-pVQZ and pc-3 vs. aug-pc-3). Diffuse functions thus do not seem necessarily

very useful for approaching the basis set limit of molecules like ours, although we note that the aug-pc-2 value is closer to the basis set limit than the pc-2 value.

The effects of diffuse functions were considered for some of our molecules that contain fluorine, an element where diffuse functions are sometimes recommended, due to the high electronegativity of the element and its non-bonding electron pairs. The effects are, however, still very small and approaching the basis set limit with increasing polarization functions only, seems more convenient^{vii}. Diffuse functions are mainly important when calculating anions, excited states, acidities or electron affinities [63].

Grimme has also argued [64] that diffuse functions are non-ideal for neutral organic molecules where intramolecular basis set superposition error can occur, especially with small basis sets (due to an unbalanced basis). A study of functionals and different basis sets by Merz et al. on conformational energy differences showed that for all functionals compared, cc-pVTZ resulted in smaller average errors (%) than aug-cc-pVTZ [41]. It seems likely that addition of diffuse functions to incompletely polarized basis sets (or perhaps also basis sets that have not been developed for DFT like the cc-pVnZ basis sets) can result in unbalanced basis sets that are subject to basis set superposition errors.

Generally it is rather easy, based on these results, to approach the basis set limit of our DFT calculations. A triple-zeta basis set with properly selected polarization functions can be rather close to the limit. The split-valence basis sets seem to yield similar results as the systematic basis sets but care should probably be taken in selecting properly polarized basis sets.

As the pc-*n* basis sets are designed for systematically approaching the basis set limit, using balanced polarization functions optimized for DFT, with *d*-functions properly optimized for second-row elements and appear to converge nicely, they have become our basis sets of choice. We also decided generally not to use diffuse basis sets due to the drawbacks discussed before.

This basis set study only compares the energy difference of a single molecule and obviously is not a complete basis set study. In our experience, however, these results are general for the molecules and properties we are interested in, a similar table for the basis set convergence of 1-fluoro-1-methyl-1-silacyclohexane is available in appendix 1.1.

^{vii} There have also been SCF convergence problems in our calculations with augmented diffuse functions.

The basis set convergence of the pc-*n* basis sets (and occasionally aug-pc-*n*) as well as other basis sets with other functionals are also discussed more later and more data are available in appendices.

The errors of our B3LYP calculations seem not to be related to the basis set used. It seems quite easy to approach the basis set limit with the functional using several basis sets families but this doesn't seem to improve the overall deviation of the functional very much. In fact using larger basis sets than used in table 5 (6-311+G(d,p)) give larger deviations from the experimental (and MP2) results.

The functional approximation must thus be the main reason for the bad performance of B3LYP.

1.4.2 Problems with DFT in computational organic chemistry

During the past few years there have been many papers in the chemical literature about problems with density functionals regarding calculations of enthalpies of formation and isomerization energies of medium to large organic molecules.

These papers grabbed our attention as they seemed relevant to our own results with the B3LYP functional.

Gilbert et al. noted the systematic underestimation of reaction energies by the B3LYP functional and other functionals as the number of carbon-carbon bonds increased while the MP2 method did not show this trend. Gilbert concluded that “*a computational chemist cannot trust a one-type DFT calculation*” [65].

A particularly frightening graph from a paper by Schleyer et al. [66], showed a systematic trend for density functionals to overestimate isodesmic stabilization energies of *n*-alkanes by increasing *n*. Notable is that B3LYP performs not much better than Hartree-Fock in this comparison.

Schleyer concluded: “*Energies computed by B3LYP and other popular DFT functionals are flawed by systematic errors, which can become considerable for larger molecules... Newer functionals, designed to describe weak interactions, give somewhat better agreement with experiment, but are not fully satisfactory*”.

In the same issue of *Organic Letters* as the Schleyer paper [66], Schreiner et al. noted the failure of many density functionals to give reliable isomer energy differences of large hydrocarbons [67]. Schreiner concluded with “*Our recommendation is to use higher level, non-DFT energy single points on DFT- or MP2-optimized structures.*”

Grimme has argued that while atomization energies (or heats of formation) may represent a worst-case scenario for quantum chemical methods, it is much more informative and much more related to typical chemistry to look at reaction energies or barriers [64]. Atomization energies involves calculating both the free (open-shell) atoms as well as the closed-shell molecules and such calculations can be subject to systematic errors [68].

Isomerization energies on the other hand are well-defined and accompanied by small to large changes in electronic structure (but still closed shell reactions). Grimme looked at 34 different isomerization reactions and showed how poor a performer B3LYP and many other density functionals can be for calculations of relative energies, sometimes not performing much better than Hartree-Fock theory [64].

Grimme has also studied specifically the performance of computational methods for the isomerization energies of branched to linear alkanes in a 2006 paper [69] and found that the inability of density functionals to predict accurate ΔE values (or even the right sign; no standard DFT method predicted the correct sign for the isomerization energy of *n*-octane \rightarrow 2,2,3,3-tetramethylbutane reaction), stems mainly from the inability of them to describe nonlocal electron correlations between localized sigma-bonds at medium range; i.e. the inability of density functionals to describe stereoelectronic effects properly. Using localized molecular orbitals as the basis in MP2 calculations, Grimme showed that it is possible to partition the correlation energy to different regions in space and by plotting the correlation energy as a function of the distance between MOs, it is evident that the main correlations that determine the relative energy of octane isomers (branched vs. linear forms) are on the medium-range length scale (1.5-3.5 Å).

This is a very persuasive argument and a sound explanation why so many current density functionals fail for this seemingly simple isomerization reaction. Grimme argues that long-range van der Waals interactions which are often put to blame for deficiencies of

DFT are only of secondary importance here but medium-range interactions are on the other hand crucial.

Grimme also looked at branched and linear forms of pentane and octane, with a carbon and silicon skeleton, respectively, and hydrogen, chlorine and fluorine substituents and found that these deficiencies of current functionals don't seem to be element specific [136].

Schreiner summarized in an *Angewandte* highlight "Relative Energy Computations with Approximate Density Functional Theory - A caveat!" the many recent failures of density functionals and possible solutions and ways forward [70].

All these results on the deficiencies of density functionals (and especially B3LYP) seemed to be relevant to us. Even though, in the conformational analysis of cyclohexanes, we are not dealing with isomerization energies where the electronic structure changes nearly as much as e.g. the isomerization reaction of *n*-octane, we are nevertheless dealing with energy differences of a very small magnitude and to satisfactorily describe the energy differences, the computational method must describe the electronic structure of each conformer well enough. While some cancellation of errors, due to the similarity of conformers, undoubtedly takes place (which is beneficial), the description of the diverse electronic structure must still be good enough, or else simple Hartree-Fock or semi-empirical methods would work just as well.

It seemed thus clear that our disappointing DFT results for conformational energies were part of a bigger problem and MP2 now seemed a much more reliable (although more expensive and more basis-set dependent) method and we had almost given up on using density functional theory for achieving accurate conformational energies when we noticed the recent appearance of new density functionals, designed to take into account some of the many problems with the density functionals mentioned before.

1.4.3 Recent functionals

There are many different strategies currently used for functional development and this is reviewed in a book chapter by Scuseria and Stavearov [71]. Mainly there are six strategies: (1) local density approximation, (2) density-gradient expansion, (3) constraint satisfaction, (4) modelling the exchange-correlation hole, (5) empirical fits and (6) mixing of approximate exchange and exact Hartree-Fock exchange.

The group of Donald Truhlar has been working on functional development since 2000 and the group's most recent M06 functionals are based on constraint satisfaction, modelling the exchange-correlation hole, empirical fits and the mixing of approximate and Hartree-Fock exchange [72]. The group's main objective has been to develop density functionals that can describe noncovalent interactions well, at the same time as describing main-group thermochemistry and barrier heights. The M06 functionals are meta-GGA functionals (include kinetic energy density in the functional), of which M06, M06-2X and M06-HF are hybrid meta-GGA functionals that incorporate some HF exchange while the M06-L functional is a local functional with no HF exchange. M06-2X is parameterized against main-group chemistry especially. The functionals are considerably complex and are also heavily parameterized against a number of diverse databases, developed in the Truhlar group, for many different energetic properties [73]. Truhlar et al. evaluated the M06 functionals (and the previous M05 functionals of similar composition) against several databases and well known troublesome reactions (not used in the training set) and found that the functionals show excellent results compared to other well known functionals [74], [75]. It is argued that while the M05/6 functionals do not describe properly the dispersion-dominated noncovalent interactions at distances larger than 6 Å, most noncovalent interactions in organic molecules take place at distances less than ~5 Å, so called medium-range correlation, that the M05/6 functionals describe very well due to a better correlation functional than most current functionals [74].

Looking at cases relevant to our own conformational systems, the M06 functionals have been shown to predict much more satisfying conformational energy differences for the challenging systems of alanine tetrapeptide and the 1,3-butadiene [72]. We also note that the difficult problem of the isomerization energy of octane, singled out by Grimme,

is predicted within 0.2 kcal/mol by the M06-2X functional compared to the ~10 kcal/mol deviation of the B3LYP functional.

Density functional development work of the Truhlar group is summarized in a recent *Accounts of Chemical Research* review [72].

The group of Stefan Grimme introduced in 2006 the double hybrid functionals [76], [77] where the typical hybrid GGA approximation (Becke exchange/mPW exchange and LYP correlation and a percentage of exact HF exchange) was combined with a perturbative second-order correlation part (PT2) that is dependent on Kohn-Sham orbitals. Part of Grimme's motivation was to build a functional that could describe non-local medium- and long-range interactions and introducing orbitals into the functional can do that to some extent. This would classify these functionals as fifth-rung functionals according to the Jacob's ladder scheme. Results for the G3/05 test set of experimental enthalpies of formation, where mean absolute deviations (MAD) of 2.1 and 2.5 kcal/mol for B2-PLYP and mPW2-PLYP respectively, were obtained, are excellent compared to the 4.4 kcal/mol MAD for the B3LYP functional. An MAD of 3.8 kcal/mol was the lowest result of other standard DFT functionals [77].

Analytical derivatives for the double-hybrid functionals were implemented in the program Orca and in the same 2007 paper it was found that B2-PLYP and mPW2-PLYP predict excellent geometries, even superior to standard DFT functionals and MP2 [78]. In another 2007 paper [79], the doubly hybrid functionals were extended by implementing a classical dispersion correction [80], [81] in order to describe medium- and long-range correlation that the perturbation-correction does not completely take care of.

It also turned out that this classical dispersion correction in combination with the standard DFT functionals had generally very positive results as well, with the MAD of B3LYP being 5.6 kcal/mol for the G3/99 set (enthalpies of formation), but the dispersion corrected functional B3LYP-D, having a MAD of 3.1. The B2PLYP-D and mPW2PLYP-D functionals both had an even lower MAD of 1.7 kcal/mol which is quite close to chemical accuracy (1 kcal/mol).

Conformational analysis of a tripeptide was also explored by Grimme et al. [79] where it was found that the dispersion correction resulted in dramatic improvements for

B3LYP, B2-PLYP and mPW2PLYP, compared to CCSD(T) reference values. The combination of the classical dispersion correction and a orbital-dependent perturbation correction (in the double hybrid functionals) to achieve especially accurate conformational energies was highlighted.

The DFT development work in the Grimme group is summarized in a recent *Accounts of Chemical Research* review [82].

1.4.4 Benchmarking density functionals

The apparent excellent performance of these new functionals from the groups of Stefan Grimme and Donald Truhlar for a number of properties (including conformational energies) and a plausible reason for the failure of other density functionals (improper description of medium-range correlation for stereoelectronic effects) for simple organic isomerization reactions, indicated that these new functionals might perform better for our low-magnitude conformational energy differences of heterocyclic systems.

The M06 functionals recently became available in the NWChem electronic structure software [40].

The B2PLYP functional and the classical dispersion correction was recently incorporated into the Orca program^{viii}.

Doing some initial trial calculations with the M06-2X functional in NWChem, we obtained very interesting results for our troublesome 1-silyl-1-silacyclohexane molecule. The ΔE value of B3LYP was +0.549 kcal/mol with the large pc-3 basis set as shown in table 6. The M06-2X/pc-3 calculation (on the same B3LYP/6-311+G(d,p) geometry) gave -0.003 kcal/mol which is much closer to the GED free energy difference ($A = -0.17(15)$ kcal/mol).

We noticed immediately that different size of the integration grid had strong effects on the conformational energies for several basis sets when doing the M06-2X calculations in NWChem. The default grid size turned out to result in, not only oscillating convergence, but also “wrong” energy differences, as shown in table 7. When the larger

^{viii} <http://www.thch.uni-bonn.de/tc/orca/>

‘xfine’ grid is used instead, the convergence is normal. This is quite surprising. It’s unclear if this is related to the M06 functionals, the implementation of the functionals in NWChem or general integral accuracy in NWChem. This extreme effect is, however, not noticed for B3LYP calculations in NWChem where the difference between the default and xfine grid is on the order of 0.02 kcal/mol. To be on the safe side, the xfine grid has been used in all NWChem calculations ever since and similarly large grids have been used in other programs.

This deserves to be mentioned especially, as users might not necessarily pay sufficient attention to grid size when doing DFT calculations. A recent paper on the precision of several DFT codes in electronic structure software is also well worth mentioning [83].

Table 7. B3LYP and M06-2X calculations on 1-silyl-1-silacyclohexane using the default grid and the xfine grid in NWChem. ΔE values in kcal/mol.

	B3LYP			M06-2X	
Basis set:	default grid	xfine grid	Basis set:	default grid	xfine grid
pc-0	+0.162	+0.184	pc-0	-0.617	-0.396
pc-1	+0.466	+0.474	pc-1	-0.398	-0.084
pc-2	+0.507	+0.520	pc-2	+0.493	-0.061
pc-3	+0.525	+0.549	pc-3	-0.575	-0.003

Recently, results of Tschumper et al. came to our attention, where CCSD(T) calculations had been carried out on a few monosubstituted 1-silacyclohexanes [84]. Before, the same group had done similar calculations on monosubstituted cyclohexanes and tetrahydropyrans [85].

Tschumper’s approach involved calculating complete basis set (CBS) extrapolated CCSD(T) values using low basis CCSD(T) calculations and large basis MP2 calculations, which can be described as a composite method, mentioned before. CCSD(T) calculations are among the most accurate calculations one can do and have been used for example for calculating the atomization energy of benzene within one 1 kcal/mol of the experimental result (1306.6 kcal/mol vs. 1305.7 kcal/mol) [86]. Also recently, the heats of formation of the alkanes pentane, hexane and octane were calculated within 0.3 kcal/mol [87]. The accuracy of CCSD(T) is thus well documented but this *ab initio* method is very expensive and out of reach for us.

Tschumper et al. also noted the rather erratic results when comparing earlier calculations of monosubstituted cyclohexanes, including several B3LYP calculations and the CCSD(T) calculations were thus intended to set the record straight for the conformational energies of several monosubstituted cyclohexanes and tetrahydropyrans.

This collection of conformational energies of cyclohexanes and heterocycles, calculated with a highly accurate ab initio method, seemed to us a good benchmark database to validate the recent DFT methods by Truhlar and Grimme and other functionals as well and to see if they are capable of predicting accurate axial/equatorial energy differences of six-membered rings.

Using the same geometries that the CCSD(T) single-point energy calculations were done on, MP2/6-311G(2d,2p) (from the supporting material of Tschumper et al. [84], [85]), and leaving out thermal and ZPE corrections, we could evaluate the error associated with our single-point DFT calculations much better than by comparing to experimental free energies.

We decided to do a thorough evaluation of the following methods:

B3LYP: the very popular density functional.

B3LYP-D : B3LYP with Grimme's classical dispersion correction as implemented in Orca.

B97-1 : another hybrid functional that often performs slightly better than B3LYP [45].

B2PLYP: The double-hybrid functional by Grimme.

B2PLYP-D : B2PLYP with the the dispersion correction as implemented in Orca.

M06-2X : Truhlar's hybrid meta-GGA functional as implemented in NWChem.

We decided to use very large basis sets to ensure the convergence of the relative energies. This was done to effectively remove the basis-set error and evaluate the performance of the functional only and also to see the basis set convergence of the new functionals for a set of molecules.

The pc-*n* basis set were used with the B97-1 and M06-2X functionals up to pc-4 with NWChem.

The def2-basis sets [88], up to def2-QZVPP, were used for the B3LYP and B2PLYP calculations in the Orca program. These basis sets have been used before, for B2PLYP and B3LYP calculations by Grimme [78] and def2-QZVPP was found to be sufficiently large for the energy differences to be converged^{ix}. Density fitting basis sets [89] were used for the perturbation step in the B2PLYP calculations as implemented in Orca to speed up the perturbation step. This involves using the resolution-of-identity (RI) approximation that has been shown to give negligible errors at a dramatical speed-up [90].

Table 8. Electronic energy differences (ΔE) in kcal/mol between the axial and equatorial conformers of monosubstituted cyclohexanes, tetrahydropyrans and 1-silacyclohexanes on MP2/6-311G(2df,2pd) geometries.

	CCSD(T)/CBS ^a	MP2/CBS ^a	B97-1	B3LYP	B3LYP-D	B2PLYP	B2PLYP-D	M06-2X
Cyclohexanes								
Methyl	1.75	1.73	2.15	2.37	1.31	2.09	1.54	1.72
Fluoro	0.20	0.23	0.51	0.50	0.21	0.35	0.20	0.16
Methoxy	0.21	0.03	0.97	1.11	0.32	0.64	0.23	0.11
Hydroxy	0.56	0.52	1.01	1.07	0.70	0.81	0.62	0.50
Tetrahydropyrans								
2-Methyl	2.82	2.90	3.12	3.38	2.24	3.18	2.58	2.60
2-Fluoro	-2.45	-2.45	-2.15	-2.29	-2.55	-2.42	-2.56	-2.45
2-Methoxy	-1.27	-1.37	-0.46	-0.37	-1.17	-0.81	-1.23	-1.31
2-Hydroxy	-0.86	-0.88	-0.33	-0.35	-0.72	-0.61	-0.81	-0.87
1-Silacyclohexanes								
Methyl	0.21	0.14	0.53	0.70	-0.03	0.45	0.07	0.10
Fluoro	-0.09	-0.05	-0.11	-0.13	-0.26	-0.15	-0.23	-0.17
Methoxy	-0.15	-0.23	0.20	0.30	-0.31	0.06	-0.26	-0.24
Hydroxy	0.03	0.01	0.13	0.16	-0.07	0.06	-0.06	-0.06
Chloro	-0.40	-0.58	-0.01	0.14	-0.41	-0.20	-0.49	-0.64
MAD	ref.	0.11	0.63	0.76	0.29	0.38	0.16	0.14
MD	ref.	-0.07	0.63	0.75	-0.16	0.36	-0.12	-0.14
MaxD	ref.	-0.18	0.81	0.90	-0.58	0.46	-0.24	-0.24

^a Extrapolated MP2 and CCSD(T) energies to the complete basis set limit [84], [85].

Table 8 shows the calculated conformational energies of 15 different rings for the DFT methods compared to the reference CCSD(T) values. The most informative part of the table is the mean absolute deviation (MAD) and maximum deviation of the density functional calculations, compared to the CCSD(T) values.

^{ix} We noticed during these calculations that using the def2-aug-TZVPP basis set resulted in energy differences that were very close to the def2-QZVPP values but at considerably lower cost.

The MAD for the B3LYP column^x is a good confirmation of our suspicion that the B3LYP functional is inadequate for calculating conformational energies of this type. A mean deviation of 0.76 kcal/mol is a disastrous result for conformational energies of cyclohexanes and heterocyclic compounds. The B97-1 functional (MAD=0.63 kcal/mol) is a small improvement over B3LYP but neither functional can be considered trustworthy of predicting accurate conformational energy differences, based on these results. An almost 1 kcal/mol maximum deviation for the B3LYP functional is a completely unacceptable error.

Applying the empirical dispersion correction to the B3LYP functional improves the performance significantly. The MAD drops from 0.76 kcal/mol to 0.29 kcal/mol. The performance of the more expensive B2PLYP functional is a definite improvement over the B3LYP and B97-1 functionals, the MAD of B2PLYP is 0.38 kcal/mol and notable is also the quite low maximum deviation of 0.46 kcal/mol (which is actually smaller than the MAD of B3LYP and B97-1).

When applying the dispersion correction to the B2PLYP functional the MAD drops considerably like before and the MAD is now only 0.16 kcal/mol and a maximum deviation of only -0.24 kcal/mol. This is a very positive result and shows a clear difference in performance of density functionals.

The M06-2X functional interestingly achieves almost the exact same result as the B2PLYP-D method. This is important also due to the less expensive nature of M06-2X compared to B2PLYP-D.

This density functional comparison of conformational energies has yielded a clear result that the M06-2X and the B2PLYP-D functionals are much more capable functionals of reproducing complete basis set estimated CCSD(T) conformational energy differences, at least for the axial/equatorial energy differences of six-membered systems, than popular functionals like B3LYP and B97-1.

Both methods have in common that they were designed to take into account a better description of nonbonding interactions, medium- or longrange.

^x We note that our B3LYP results are different from Tschumper's B3LYP values because the latter values were calculated on B3LYP optimized geometries. The difference is as large as 0.3 kcal/mol in some cases. We opted for using the same (MP2) geometries in all our calculations.

It thus seems highly likely that this is the main reason for the bad performance of other DFT functionals for these conformational systems and perhaps relative energies of organic molecules in general.

Woodcock et al. recently studied computationally another tetrahydropyran, the 2-ethoxy substituted one [91]. This ring is a model carbohydrate system that mimics the glycosyl linkage in disaccharides and glycolipids and the authors wanted to evaluate several theoretical methods for calculating the axial/equatorial energy difference. Using a similar methodology as Grimme, they calculated the CBS extrapolated CCSD(T) energy difference of 2-ethoxytetrahydropyran. Comparison with the experimental results involved taking into account thermal and solvation effects, that will not be discussed here, but again a dramatic difference between B3LYP calculations and the CBS extrapolated CCSD(T) energy difference is notable, deviations of 0.84 and 1.03 kcal/mol from the CCSD(T) value, using basis sets 6-311+G(d,p) and cc-pVTZ, respectively. The B3LYP calculations are in fact no better than HF calculations.

As a further confirmation of the ability of the functionals B2PLYP-D and M06-2X to reproduce CCSD(T) results, we calculated the energy difference of 2-ethoxy tetrahydropyran in the same way as before (table 9). The CCSD(T) calculations were done on MP2/cc-pVTZ geometries that we recalculated as well.

Table 9. The axial/equatorial electronic energy difference of 2-ethoxy-tetrahydropyran with different density functionals on MP2/cc-pVTZ geometries. Values in kcal/mol.

	ΔE	Deviation
CCSD(T)/CBS	1.42	-
M06-2X/pc-3	1.30	0.12
B2PLYP-D/def2-TZVPP	1.28	0.14
B2PLYP/def2-TZVPP	0.78	0.64
B3LYP-D/def2-TZVPP	1.25	0.17
B3LYP/def2-TZVPP	0.30	1.12

^a The B3LYP and B2PLYP values might not be completely converged at the def2-TZVPP level (but probably within 0.1 kcal/mol). There were problems with the SCF convergence using the def2-QZVPP basis set.

Again, we have a very positive result for the M06-2X and B2PLYP-D functionals as they are very close to the CCSD(T)/CBS value. The B3LYP-D functional performs also very well, showing that the classical dispersion correction can improve B3LYP results

significantly. The M06-2X and B2PLYP-D functionals thus seem quite capable methods of accurate conformational energies of carbohydrate model systems.

One might also speculate about the nature of the stabilization of the axial and equatorial conformers in six-membered rings from all these results. It is very noteworthy in table 8 that B97-1 and B3LYP functionals, always (except 1-fluorosilacyclohexane) overestimate the stabilization of the equatorial conformer (or underestimate the stabilization of the axial conformer).

Applying a dispersion correction or using functionals that take into account medium-range correlation (like M06-2X and B2PLYP-D) functionals then this effect disappears. Thus it seems likely that nonbonding interactions that generally seems to stabilize the axial conformer to some extent and that B3LYP and B97-1 account badly for, play a key role in the conformational equilibrium of these monosubstituted six-membered rings. This will be discussed further in chapter 2.

We have not discussed the MP2/CBS column in table 8 so far. The CCSD(T) calculations of Tschumper et al. are based on these extrapolated MP2 energies with an applied low-basis CCSD(T) correction. It turns out that MP2 actually performs very well, with a slightly less MAD than M06-2X and B2PLYP-D, meaning the CCSD(T) calculation acts only as a slight correction of higher order correlation in Tschumper's composite method. Jensen recently recommended MP2/aug-cc-pVTZ as a method/basis combination capable of predicting accurate amino acid conformational energies based on results that compared MP2 and B3LYP to CCSD(T) conformational energies [42]. It thus seems that MP2 conformational energies can be quite reliable when carried out with large enough basis sets (low-basis MP2 calculations have previously yielded erroneous energy differences for carbohydrate model systems [92], [93]).

Large basis set MP2 calculations are sometimes required to achieve complete convergence, often up to the 5Z level, as well as extrapolation to the basis set limit for optimal results. This is especially notable for the 1-silacyclohexane calculations. Meanwhile, the M06-2X calculations are completely converged at the pc-3 level, the pc-4 level numbers most likely only being numerical fluctuation (less than 0.01 kcal/mol). Comparison of the basis set convergence of M06-2X and MP2 is shown in

appendix 1.2. This smaller basis set dependence is one of the great benefits of density functional theory.

To summarize, we have done a comparison of several density functionals and found that two recent functionals described in the literature predict very accurate conformational energies compared to CCSD(T) results and represent a clear improvement over B3LYP results. These functionals have been thoroughly tested elsewhere and found to be generally accurate for thermochemistry and they are perhaps the most accurate density functionals for main-group chemistry right now. The MP2 method seems also to be very reliable for conformational energies. We note that MP2 and B2PLYP-D both are more basis set dependent than M06-2X (MP2 and B2PLYP include a perturbation step) and both methods scale as N^5 compared to M06-2X that scales as N^4 .

It appears, based on the results presented in table 8, that we might expect errors around 0.15 kcal/mol in ΔE values with these methods. This is much more acceptable than an error of 0.75 kcal/mol that might be expected by the B3LYP method.

1.5 Obtaining accurate molecular geometries

The previous section dealt with obtaining accurate single-point electronic energies on previously calculated molecular geometries. Doing accurate single-point calculations is often much more important than getting accurate structures as the electronic energy is more basis set dependent than bond lengths and angles [58], [59].

Nevertheless, we felt it was important to explore how best to calculate accurate molecular geometries for our systems and see how differently calculated structures affect the single-point energies. Usually MP2 or DFT (B3LYP being most popular) is used for structure optimization. Just like for energies, CCSD(T) calculations are more accurate but are usually only possible for very simple molecules.

We thus evaluated the basis set dependence of our molecular geometries, how differently calculated geometries affect single-point energies and compared our calculated geometries to recent gas-phase electron diffraction (GED) results of 1-silacyclohexanes.

It is important to begin with, discussing the difference between the geometries obtained from quantum calculations and those obtained from GED experiments.

Optimizing a molecular geometry with quantum calculations involves numerous single-point energy calculations, and is thus always done with an economic basis set and method. The gradient, the differentiated energy with respect to atomic coordinates, is calculated in each step and the molecular geometry changed in order to minimize the gradient until one reaches a minimum that is defined by boundary conditions. A good starting geometry is important, both to ensure that the optimization finds the correct minimum on the potential energy surface and it is also beneficial to reduce the number of optimization steps.

A calculated geometry, obtained by minimizing the gradient of the electronic energy is, however, a theoretical (or even fictional) geometry. It is obtained at 0 K (i.e. no external thermal energy) and ‘assumes’ that the nuclei don’t possess any vibrational motion. This is called the equilibrium geometry (r_e).

The experimental geometry from the GED experiment (r_a), however, is usually obtained at room temperature and the diffraction pattern obtained in the experiment is the statistical average of all vibrational conformers in the gas phase.

The experimental geometry is thus often refined using harmonic force constants from calculations (e.g. quantum calculations) so that it can be related to the r_e geometry. There are several problems associated with this, however, as vibrational motion is for example not always harmonic. New and better refinement methods in GED analysis have been developed in the last years and this continues to be an important field of study [94].

We carried out a set of calculations for comparison with experimental geometries, including MP2 with different basis sets, and a few density functionals and basis set combinations, some that are quite popular and are for example used for the geometry optimization step in the composite method G3B3 (B3LYP/6-31G(d)).

While a thorough analysis should involve comparing many different molecules we only calculated two molecules, the axial conformer of 1-silyl-1-silacyclohexane and 1-fluoro-1-silacyclohexane. We were mainly interested in seeing the basis set dependence

and if there are large differences between different functionals and MP2 theory. We also included calculations from the semi-empirical methods PM3 and the very recently developed method PM6 (includes new and updated parameters for over 70 elements) [95].

We then calculated the mean absolute deviation from the GED geometry for bond lengths and angles separately.

Our intent was to judge the quality of the equilibrium geometries by comparing with the GED geometry by assuming that an accurate equilibrium geometry would have lower MAD from the GED geometry than a less accurate one, bearing in mind, however, that the geometries are by definition different.

Vibrational averaging of the gas-phase geometry should mainly involve larger angles than the calculated angles, as the low-frequency motions of molecules usually are bending or torsional modes rather than stretching modes. Bond lengths should thus be less affected.

The results are given in table 10.

1.5.1 Bond lengths

Increasing the basis set from a double-zeta basis to triple-zeta nearly always lowers the MAD. This is consistent with reviews that have pointed out that a triple-zeta basis set nearly always give better geometries. Interestingly, the MAD for both the 1-fluoro and the 1-silyl molecule increases somewhat between B3LYP/6-31G(d) and B3LYP/6-311+G(d,p). When using both the pc-1 and pc-2 basis set instead (for 1-fluoro) the MAD gets lower and is completely converged at the pc-3 level. Thus, despite B3LYP/6-311+G(d,p) being a larger basis set (triple-zeta) than pc-1 (double-zeta) the pc-1 basis set appears to be better balanced (yielding a lower MAD); it is possible that the diffuse functions are responsible for this effect. A clear trend toward basis set convergence of the geometry is also observed for the B97-1 functional calculations from pc-1 to pc-3 on 1-silyl-1-silacyclohexane.

Increasing from a triple-zeta basis set (pc-2) to a quadruple-zeta basis set (pc-3) appears to generally have a negligible effect on the MAD. It appears that doing geometry

optimization with a quadruple-zeta basis set has very little effect on molecular geometries. This is rather fortunate since such optimizations are very expensive. This result was expected and has been pointed out before [50], [58], [59].

An interesting comparison is shown for the semi-empirical methods PM3 and the very recently released PM6 method. Not unexpectedly, the methods perform generally worse than the DFT and MP2 methods. For the 1-fluoro molecule the PM6 performs better than PM3 (and actually yields a rather low MAD) but then fails badly for the 1-silyl molecule and especially for the Si-Si bond length. It appears that the silicon parameters are worse in PM6 and neither method can be considered reliable for geometry optimization of our molecules.

While it seems that B3LYP and B97-1 give low MAD with appropriate basis sets (pc-2 seems a good choice) the best performing functionals for both molecules, however, are interestingly the same functionals that gave the lowest MAD for energies in chapter 1.4.4, B2PLYP-D/def2-TZVPP and M06-2X. MP2 methods performs also very well. In the paper describing the GED geometry of 1-fluorosilacyclohexane [96], MP2/6-31G(d,p) and B3LYP/6-31G(d,p) calculated geometries were compared to the experimental geometry and it was found that both methods overestimate the Si-C and Si-F bond lengths. We note that B2PLYP-D and M06-2X methods do not overestimate these crucial parameters as much, in combination with triple-zeta basis sets.

Another very positive result was the excellent result of the M06-L functional, with and without density fitting, that gave a very good MAD, similar to B3LYP and B97-1 functional. Local functionals (no HF exchange), like M06-L, always scale more favorably (N^3) than hybrid functionals (N^4) and one has the possibility to use density fitting to speed-up calculations even more without significant loss of accuracy [97]. Using this functional with density fitting for initial optimization or for doing geometry optimization on large molecules seems promising.

1.5.2 Angles

The two semi-empirical methods gave notably worse angles than all other methods with deviations of 1.5 - 2.3 °.

While we didn't expect comparing angles would be of much use, the methods that predict lowest MAD's for bond lengths generally seem to predict the lowest angle deviations as well. We note that both bond lengths and bond angles are generally worse predicted for the 1-silyl-1-silacyclohexane. The MAD of angles do not show normal convergence with respect to increasing basis set, however, as seen if one inspects the B3LYP/pc-*n* and B97-1/pc-*n* series. Angles are thus probably bad indicators of accurately calculated geometries of these kind of molecules.

1.5.3 Effect of geometries on the single-point energy

We also wanted to see what effect different geometries have on the single-point electronic energy differences.

We thus did single-point energy M06-2X/pc-3 calculations on a few differently calculated geometries of 1-silyl-1-silacyclohexane to see if there was some variation. This is shown in table 11.

Table 11. M06-2X/pc-3 single-point energy calculations on different geometries of 1-silyl-1-silacyclohexane. ΔE values ($E_{ax} - E_{eq}$) in kcal/mol.

Geometry:	ΔE
B3LYP/6-31G(d)	+0.039
B3LYP/6-311+G(d,p)	-0.003
B3LYP/pc-1	+0.033
B3LYP/pc-2	+0.031
B3LYP/aug-cc-pVTZ	+0.035
B2PLYP-D/def2-TZVPP	-0.077
MP2/cc-pVTZ	-0.129
M06-2X/pc-2	-0.138

Interestingly, there is a visible trend in the M06-2X/pc-3 calculated ΔE values on different geometries. Geometries calculated with M06-2X/pc-2 and B2PLYP-D/def2-TZVPP, that showed the lowest MAD's from the GED geometries and predicted more axial stabilization (hence lower ΔE values) than other functionals in chapter 1.4.4, are here responsible for further lowering of the ΔE values while the B3LYP geometries with

different basis sets all yield very similar ΔE values. This much variation is unexpected and suggests that functionals such as M06-2X and B2PLYP-D that describe medium-range correlation better than other functionals and hence yield better energies, can also have significant effects on molecular structure. This effect is here ~ 0.15 kcal/mol if one compares the M06-2X/pc-2 geometry and B3LYP/6-31G(d) geometry entries in table 11, which is significant if one keeps in mind the low-magnitude conformational energies we are interested in.

The results reported in this section are based on tests done on just 2 molecules. This is, however, strong indication that geometry optimization of six-membered rings should be done on a well-balanced triple-zeta basis set (like pc-2) with MP2 or a density functional that is not plagued by the deficiencies mentioned in chapter 1.4.2. This should be explored further.

1.6 Obtaining corrections to enthalpy and free energy

Calculating single-point electronic energy differences on optimized geometries gives the electronic energy difference that is hopefully already quite comparable to the energy difference between conformers that can be obtained experimentally.

However, the electronic energy difference is not zero-point energy corrected and it doesn't include enthalpic and entropic effects. The ΔE is thus not the same energy difference as the enthalpy difference (ΔH) or the free energy difference (ΔG or A) that are the thermodynamic quantities one usually obtains from experiments.

Traditionally, a frequency calculation is carried out on the optimized geometry (where the first derivatives are zero) where one obtains the harmonic vibrational frequencies of the molecule in question. This involves calculating the second derivatives of energy with respect to atom coordinates. The vibrational frequencies can then be used to calculate the thermodynamic corrections to the electronic energy and hence get calculated zero-point energy corrected energies, enthalpies and free energies.

Zero-point (vibrational) energy is an important correction as it is the vibrational energy of a molecule at 0 K.

$E_{\text{zpe}} = \frac{1}{2} \sum \omega_i$, where ω_i is the i th normal-mode vibrational frequency.

The thermal correction to energy, E^{corr} , includes the zero-point energy and also the energy associated with all vibrations, rotations and translations of the system at a specific temperature: $E^{\text{corr}} = E_{\text{zpe}} + E_{\text{vib}} + E_{\text{rot}} + E_{\text{trans}}$.

The thermal correction to enthalpy, H^{corr} , includes the thermal correction to energy and also the RT term, where the assumption of an ideal gas has been made:

$$H^{\text{corr}} = E^{\text{corr}} + RT.$$

The thermal correction to free energy is the thermal correction and an entropy term, $-TS_{\text{tot}}$, where S_{tot} is the total entropy associated with all vibrational, rotational and translational motion: $G^{\text{corr}} = H^{\text{corr}} - TS_{\text{tot}}$.

The calculated vibrational frequencies enter into most of the above terms and are thus the main ingredients in the thermodynamical corrections to the electronic energy. Calculations of vibrational frequencies involve, however, the use of a harmonic potential to solve the Schrödinger equation for vibrations of molecules. The harmonic approximation is a simple approximation, where an exact solution can be given and other potentials are too complicated to be solved easily.

The question, however, arises, how good the harmonic approximation is?

The harmonic approximation is actually a very good approximation for many systems at normal temperatures. Typically, Hartree-Fock calculations systematically overestimate frequencies by around 10 % due to anharmonicity, but this can be corrected for by scaling factors.

However, problems arise when a system has several low-frequency motions. Low-frequency motions would contribute very little to the zero-point vibrational energy but unfortunately, if one examines the vibrational entropy term closely (equation 1-11),

$$S_{\text{vib}} = R \sum_{i=1}^{3N-6} \left[\frac{h\omega_i}{k_B T (e^{h\omega_i/k_B T} - 1)} - \ln(1 - e^{-h\omega_i/k_B T}) \right] \quad (1-11)$$

it can be shown that as frequencies go to zero, the vibrational entropy goes to infinity (equation 1-12) [63].

$$\begin{aligned}\lim_{\omega \rightarrow 0} [-R \ln(1 - e^{-h\omega_i/k_B T})] &= \lim_{\omega \rightarrow 0} \left\{ -R \ln \left[1 - 1 + \frac{h\omega}{k_B T} - \frac{1}{2!} \left(\frac{h\omega}{k_B T} \right)^2 + \dots \right] \right\} \\ &= \lim_{\omega \rightarrow 0} \left[-R \ln \left(\frac{h\omega}{k_B T} \right) \right] = \infty\end{aligned}\quad (1-12)$$

This means that small errors in the low-frequency modes can lead to large errors in entropies. Unfortunately, errors in the low-frequency modes can be expected due to the common anharmonicity of such modes. Low-frequency modes are often torsions about single bonds with small barriers. These modes are often considered as free or hindered rotors.

The systems we are interested in unfortunately include a fair share of low-frequency motions (typically classified as $< 625 \text{ cm}^{-1}$ ^{xi}), 1-silyl-1-silacyclohexane including 12 low-frequency vibrations. While we make no attempt here of classifying these vibrations (some of them might be described as ring-puckering or ring-breathing modes) it is worth noting that these low-frequency modes might not be best calculated with the harmonic approximation and could thus be a significant source of error in the calculation of free energies.

The influence of low-frequency modes on free energy corrections in conformational analysis has been studied by De Almeida et al. for several molecules including 1,2-dihaloethanes [98], cyclodecane [99], cyclononane [100], cyclooctane [101] and cycloheptane [102]. For cycloheptane and cyclooctane the authors found that the free energy correction was very sensitive to low-frequency modes and that excluding the lowest modes from the free energy correction gave much more satisfactory results compared to experiment. This procedure was not found to work well for 1,2-difluoroethane and cyclononane, however.

Several different ways exist to treat specially low-frequency vibrations that can be classified as free rotors or hindered rotors and a black-box approach now exists in the

^{xi} http://www.gaussian.com/g_whitepap/thermo.htm

Gaussian program for the treatment of hindered rotors in the frequency calculation [103]. These procedures are, however, not intended for ring systems where coupling of modes occur.

Also implemented in Gaussian [28] is a second-order perturbation approach to go beyond the harmonic approximation by perturbation treatment of the vibrational frequencies [104]. Such methods are extremely expensive however and probably not suitable for low-frequency modes.

Recently, path integral Monte Carlo (PIMC) methods have begun to make an appearance that make it possible to go beyond the harmonic approximation and include all rotation-vibration interactions and anharmonicities [105], [106], [107], [108].

Using the disubstituted 1-fluoro-1-methyl-1-silacyclohexane (another molecule that we have used for benchmarking) we calculated harmonic frequencies with several methods, table 12. Frequency calculations are quite expensive and bigger basis sets than triple-zeta are out of reach.

Table 12. Relative corrections to enthalpy and free energy calculated by several different methods. The conformational equilibrium is with respect to methyl substituent. Values are in kcal/mol.

Method/basis	ΔH^{corr}	ΔG^{corr}
B3LYP/6-31G(d) ^a	0.0571	0.2046
B3LYP/6-31G(d) ^b	0.0194	0.0345
B3LYP/6-311+G(d,p) ^a	0.0483	0.0621
B3LYP/6-311+G(d,p) ^b	0.0307	0.0508
B3LYP/aug-cc-pVDZ ^b	0.0075	0.0119
B3LYP/aug-cc-pVTZ ^b	0.0176	0.0426
MP2/6-311+G(d,p) ^b	0.0220	0.0828
B3LYP/pc-2 ^c	0.0260	0.0552
B97-1/aug-cc-pVTZ ^{c,d}	0.0496	0.1908
B97-1/pc-2 ^{c,d}	0.0307	0.1884

^a Calculated in Gaussian 03 [28] with default optimization criteria and grid.

^b Calculated in Gaussian 03 [28] with tight optimization criteria and ultrafine grid (does not apply to MP2).

^c Calculated in NWChem 5.1 with tight optimization criteria and xfine grid.

^d Numerical frequencies calculated.

As can be seen from table 12, some fluctuation is witnessed between methods. The free energy correction is especially sensitive. There is a notable difference between B3LYP/6-31G(d) with the default optimization criteria and default grid and B3LYP/6-31G(d)

with tight optimization criteria and a larger grid. The B3LYP calculations with triple-zeta basis sets are, however, quite consistent and the MP2 value is not far off. The B97-1 calculations with triple-zeta basis sets aug-cc-pVTZ and pc-2 are consistent at ~ 0.19 kcal/mol but at odds with the B3LYP calculations where the correction is notably smaller. The enthalpic correction is of small magnitude and with generally smaller variation.

Radom et al. [109] recently did an evaluation of methods for predicting harmonic frequencies for several molecules and suggested scale factors for each method. B3LYP is generally recommended for predicting low-frequency vibrations (as well as possible within the harmonic approximation) and enthalpies and entropies. The B97-1 functional performed better overall, but only marginally.

We note that scale factors are of little use to us, scaling of the frequencies only results in corrections that are less than 0.001 kcal/mol.

With all this in mind, we decided that calculating harmonic frequencies was best done with B3LYP/pc-2, with tight optimization criteria and a large integration grid to be on the safe side. We chose B3LYP instead of B97-1, due to analytical frequencies being only available for B3LYP in NWChem, which decreases calculation time considerably, compared to calculating frequencies numerically (unfortunately we have no way of knowing whether the free energy correction calculated by B3LYP is more correct than B97-1). MP2 frequencies are also very expensive.

The pc-2 basis set was chosen due to it being a well-balanced basis set (as we have shown for energies and geometries), and Jensen has shown that it is closer to the basis set limit for harmonic frequencies than similar triple-zeta split-valence and correlation-consistent basis sets [50].

We do note, however, that a special treatment of low-frequency vibrations has not been carried out in these calculations and we are relying on cancellation of errors to some extent.

1.7 Modelling a low-temperature conformational equilibrium in solution

Some of our experimental energy differences have been carried out in solution. The Dynamic NMR experiments that have been carried out in our group, have been carried out at 100-150 K temperature, usually in a freon mixture, see results in table 3. When comparing free energies from the GED experiment and free energies from the DNMR experiment there are significant differences in the free energies, so much that in the gas phase experiment the axial conformer of the CF_3 -1-silacyclohexane is in slight excess ($A = -0.19$ kcal/mol) while in the low-temperature freon solution NMR experiment, the equatorial conformer is in excess ($A = +0.4$ kcal/mol).

Several other 1-silacyclohexanes have now been measured by GED and DNMR and a similar effect takes place, the DNMR experiment generally predicts a more stabilized equatorial conformer compared to GED results.

Our initial suspicion regarding these different results, were the different experimental conditions. The DNMR experiments do take place in solution, most in polar freon solvents, thus making possible several intermolecular effects that might stabilize the equatorial conformer more than the axial conformer.

Attempts to correct for this effect with a continuum solvation model (IPCM/PCM [110], [111], [112],) have been done previously in our group [22], [96], where the solvent is modelled as a dielectric medium similar to the experimental solvents and the solvation free energy added to the gas phase electronic energy.

For 1-trifluoromethyl-1-silacyclohexane [22], a shift from a negative A value to a positive value that agrees very well with the solvated NMR experiment, was obtained. Since then, calculation of solvation free energies for other 1-silacyclohexanes have been carried out, in order to explain the difference between the GED and DNMR results but with mixed results (table 13).

Table 13. *A* values from DNMR experiments compared with calculated *A* values with solvent corrections (IPCM).

	DNMR (<i>A</i> / mol % axial) ^a	QC (<i>A</i> with solvent effects ^b)
CH ₃	0.23 (2) / 26(1) %	0.08 to 0.09
	<i>T</i> = 110 K	
CF ₃	0.4 (1) / 17(2) %	0.37 to 0.50
	<i>T</i> = 113 K	
F	-0.13 (2) / 64(2) %	-0.61 to -0.53
	<i>T</i> = 112 K	
F-Me ^c	0.26(7) / 25(5) %	0.72
	<i>T</i> = 126 K	

^a Low-temperature NMR measurements were done in a 1:1:3 solvent mixture of CD₂Cl₂, CHFC1₂, and CHF₂Cl.

^b MP2/aug-cc-pVTZ//B3LYP/6-311+G(d,p) energies calculated with solvent effects for both a CH₂Cl₂ and a CHCl₃ solution with the IPCM/PCM solvation model (B3LYP/6-311+G(d,p)) as implemented in Gaussian 03 [28].

^c Equilibrium with respect to methyl substituent.

Recent results from Raman analysis of the 1-silacyclohexanes, where conformational enthalpy differences were obtained in different solvents, sheds new light on the problem (table 14) [23]. According to the Raman results, the conformational enthalpy differences don't seem to be very dependent on the solvent. Very similar values are obtained whether the measurements are carried out in a nonpolar medium (*n*-pentane or *n*-heptane), a polar medium (dichloromethane or THF) or as a neat liquid.

Table 14. ΔH values ($H_{ax} - H_{eq}$) for several monosubstituted 1- silacyclohexanes obtained from Raman experiments in different solvation phases [23]. All values in kcal/mol.

	Vibrational mode	Method of deconvolution	Neat liquid (ΔH)	Pentane solution (ΔH)	Heptane solution (ΔH)	CH ₂ Cl ₂ solution (ΔH)	THF solution (ΔH)
F	ν_s SiC ₂	Peak heights	-0.25	-0.21	-	-0.25	-
		Peak areas	-0.26	-0.24	-	-0.30	-
Cl	ν_s SiCl	Peak heights	-0.48	-	-0.35	-	-0.58
		Peak areas	-0.69	-	-0.46	-	-0.62
Br	ν_s SiBr	Peak heights	-0.69	-	-0.33	-	-0.31
		Peak areas	-0.57	-	-0.47	-	-0.89
SiH ₃	ν_{as} SiSi	Peak heights	-0.19	-	-0.22	-	-0.19
		Peak areas	-0.29	-	-0.09	-	-0.10
OMe	ν_s SiC ₂	Peak heights	-0.08	-	-0.06	-	-0.06
		Peak areas	-0.15	-	-0.11	-	-0.10
N(Me) ₂	ν_s SiC ₂	Peak heights	0.27	-	0.31	-	0.29
		Peak areas	0.30	-	0.27	-	0.28

Based on these results, it thus seems that solvent effects are relatively non-important for conformational enthalpy differences. This suggests that a solvation entropy effect of some magnitude takes place in the low-temperature freon-solution NMR experiment. As most continuum solvation models are mainly based on modelling electrostatic effects, they only take into account a rough estimate of the solvation entropy [113]. Furthermore, as we are modelling the solvated phase as being homogeneous (either CHCl_3 or CH_2Cl_2) we might be missing crucial solvation entropy effects that might take place in the actual heterogeneous freon solution. It is also quite likely that before mentioned errors in entropies due to low-frequency modes play a role here as well. A recent low-temperature NMR experiment of 1-silyl-1-silacyclohexane in our group, utilized SiD_4 as the solvent, with good results. This might be a simpler system to model by solvation models, but solvation parameters unfortunately do not yet exist. Recently, a solvation model, SM8 was introduced that claims high accuracy of calculated solvation free energies [114]. It will be interesting to see how that model performs for our systems.

Since it appears that modelling the low-temperature solvent phase is very hard to carry out, the DNMR results for the 1-silacyclohexanes, while still very interesting, do not help in our understanding of which electronic or steric effects are responsible for the difference between cyclohexanes and silacyclohexanes as the environmental factors of the experiment are too complicated to account for.

It will nonetheless be very interesting in the future, as solvation modelling progresses, to see if the low-temperature NMR experiment can one day be successfully modelled.

1.8. Theory vs. experiment

We can now return to our main objective in this chapter that involved calculating conformational enthalpies and free energies for direct comparison with experiment. Table 15 contains the experimental results of table 3 with added quantum chemical calculations and additional recent data on disubstituted silacyclohexanes.

Table 15. Experimental data of mono- and disubstituted 1-silacyclohexanes [23] with added values from quantum chemical calculations. Values in kcal/mol.

Substituent(s)	GED (A / mol % axial)	DNMR (A / mol % axial)	Raman (ΔH)	QC(ΔH) ^b	QC ($A-\Delta G$) ^b
CH ₃	0.45(14) / 32 (7) %	0.23 (2) / 26(1) %	0.15 (neat)		
	$T = 298$ K	$T = 110$ K ^c	0.15 (pentane) 0.16 (CH ₂ Cl ₂)	0.15 (M06-2X) 0.12 (B2PLYP-D)	0.20 (M06-2X) 0.17 (B2PLYP-D)
CF ₃	-0.19(29) / 58 (12) %	0.4 (1) / 17(2) %	-0.53 (neat)		
	$T = 293$ K	$T = 113$ K ^c	-0.51 (pentane) -0.62 (CH ₂ Cl ₂)	-0.50 (M06-2X) -0.71 (B2PLYP-D)	-0.30 (M06-2X) -0.51 (B2PLYP-D)
F	-0.31(20) / 63 (8) %	-0.13 (2) / 64(2) %	-0.25 (neat)		
	$T = 293$ K	$T = 112$ K ^c	-0.22 (pentane) -0.28 (CH ₂ Cl ₂)	-0.18 (M06-2X) -0.25 (B2PLYP-D)	-0.16 (M06-2X) -0.23 (B2PLYP-D)
SiH ₃	-0.17(15) / 57(7) %	0.12 (3) / 45(3) %	-0.19 (neat)		
	$T = 321$ K	$T = 100$ K ^d	-0.22 (heptane) -0.19 (THF)	-0.14 (M06-2X) 0.11 (B2PLYP-D)	-0.12 (M06-2X) 0.12 (B2PLYP-D)
F and CH ₃ ^a	0.11(13) / 45(6) %	0.26(7) / 25(5) %	0.50 (neat)		
	$T = 282$ K	$T = 126$ K ^c	0.48 (hexane) 0.51 (THF)	0.19 (M06-2X) 0.28 (B2PLYP-D)	0.22 (M06-2X) 0.31 (B2PLYP-D)
CF ₃ and CH ₃ ^a	-0.02(11) / 51(5)%	not available yet	0.73 (neat)		
	$T = 262$ K		0.67 (hexane) 0.78 (THF)	0.49 (M06-2X) 0.70 (B2PLYP-D)	0.29 (M06-2X) 0.50 (B2PLYP-D)

^a Conformational equilibrium defined with respect to methyl substituent.

^b Electronic energies calculated on M06-2X/pc-2 geometries. Enthalpic and entropic corrections calculated at the B3LYP/pc-2 level. M06-2X energies calculated with pc-3 basis set. B2PLYP-D energies calculated with def2-aug-TZVPP basis set.

^c Low temperature NMR measurements were performed in a 1:1:3 solvent mixture of CD₂Cl₂, CHCl₃, and CHF₂Cl.

^d SiD₄ was used as solvent for the low temperature measurements.

Calculated values generally compare quite favorably. The largest discrepancies occur between calculated A values and A values from the GED experiments for CH₃ and CF₃/CH₃ cases. We note that these are cases where comparison of the Raman ΔH values and the GED A values suggests especially large entropic factors, $\Delta(-TS_{\text{tot}})$, to contribute to the free energy difference. For the F/CH₃ case, experiments also suggest a notable $\Delta(-TS_{\text{tot}})$ factor that the harmonic calculations do not account for. It is thus likely that the harmonic B3LYP/pc-2 calculations are a source of error here.

There are also slight differences in the ΔE values of B2PLYP-D and M06-2X (maximum 0.25 kcal/mol) and sometimes M06-2X performs better for one case while B2PLYP-D performs better for another.

Four recently synthesized molecules have only been analyzed by Raman spectroscopy. Results are shown in table 16 and compared to M06-2X and B2PLYP-D ΔH values.

Table 16. Raman ΔH values ($H_{ax}-H_{eq}$), compared to calculated ΔH values of monosubstituted 1-silacyclohexanes. All values in kcal/mol.

Substituent		Raman (ΔH)	M06-2X (ΔH) ^{a,b}	B2PLYP-D (ΔH) ^{a,b}
Cl	Peak heights	-0.48	-0.67	-0.51
	Peak areas	-0.69		
Br	Peak heights	-0.69	-0.78 ^d	-0.60
	Peak areas	-0.57		
OMe	Peak heights	-0.08	-0.26	-0.31
	Peak areas	-0.15		
N(Me) ₂	Peak heights	+0.27	-0.03	-0.28
	Peak areas	+0.30		

^a Enthalpic corrections at the B3LYP/pc-2 level.

^b Electronic energies at M06-2X/pc-3//M06-2X/pc-2 level.

^c Electronic energies at B2PLYP-D/def2-aug-TZVPP//M06-2X/pc-2 level.

^d Electronic energies at M06-2X/def2-QZVPP//M06-2X/def2-TZVPP level. pc-*n* basis sets don't include third-row elements.

In table 16 we note that there is some uncertainty present in the experimental values as there is a significant discrepancy between values obtained using peak height comparison and peak area comparison for the Cl and Br cases. In fact the Raman experiment alone is unable to determine which molecule has lower conformational ΔH value. Both calculation methods suggest 1-bromo-1-silacyclohexane to have lower ΔH .

The 1-silacyclohexanes represent very difficult cases for a quantitative comparison between theory and experiment, due to the very low-magnitude energy difference between conformers and errors associated with the experiments as well as the theoretical methods. The harmonic frequency calculations are probably a source of error, as are our calculated ΔE values with the M06-2X and B2PLYP-D functionals. We do think these calculations are improvements over similar calculations with the B3LYP functional, because as we showed in table 8, the B3LYP functional is subject to systematic errors that can become very high in magnitude for several cases.

B2PLYP-D and M06-2X, represent in our belief, the best density functionals for conformational analysis of this kind. MP2 can also be recommended.

Chapter 2 – Silicon substitution effects on the conformational properties of the cyclohexane ring: From cyclohexane to cyclohexasilane

2.1 Introduction

Chapter 1 focused on calculating accurate conformational free energy and enthalpy differences for direct comparison with experiment. We argued that accurate calculations of the electronic energy difference can be done by recently developed density functionals that predict electronic energy differences that are very close to the CBS estimated CCSD(T) values. The electronic energy difference is the main factor behind the conformational equilibrium of the cyclohexanes and tetrahydropyrans as the enthalpic and entropic effects are only small shifts from the ΔE values. Similarly, for the 1-silacyclohexanes the electronic energy difference is the reason for the conformational equilibrium. The fact that accounting for enthalpic and entropic effects are more important for them is only because the ΔE values are so near zero.

Looking at the bigger picture, getting very accurate conformational energies that agree perfectly with experiment, is perhaps not the most important objective of our silacyclohexane investigation. More important is to describe and try to understand the dramatic ΔE difference that occurs when a carbon atom is replaced with silicon in monosubstituted cyclohexanes and how ΔE changes with different substituents. We wanted to investigate systematically this phenomenon for more silicon-containing heterocycles, by purely computational methods, now that our computational investigation in chapter 1 suggests that DFT can be a tool to obtain reliable conformational energies. The ultimate goal is to identify the major factor that is responsible for the different conformational properties of silacyclohexanes. Instead of calculating free energies and enthalpies, the focus in this chapter is purely on electronic energies (zero-point energy exclusive) as experimental data for the compounds is not available for comparison anyway. Should experimental data become available for some of the molecules in this chapter, our ΔE values can easily be related to ΔH and A values by independent frequency calculations.

The conformational properties of many heterocycles have been investigated and a lot of models been proposed for differing conformational properties, while silacyclohexanes

have not been subject to many such experimental or theoretical investigations outside our group as is evident in a recent review by Kleinpeter [10].

The concept of stereoelectronic effects has become an important model in the conformational analysis of cyclohexanes, heterocycles and similar molecules, as an alternative to the steric repulsion model for explaining conformational behaviour. The anomeric effect in carbohydrates is often explained by hyperconjugative interactions between lonepairs and antibonding orbitals [7], [10].

We will attempt to relate some of this knowledge to the conformational properties of silacyclohexanes.

2.2 Trends in ΔE values of silacyclohexane families

2.2.1 Choosing families and substituents and setting up the calculations

We have mainly been concerned with the monosilacyclohexane family until now, where the substituent is bonded to the silicon. But what about other silacyclohexane families? Does silicon in the 1-position cause a unique effect, or does silicon have similar effects in other positions? What happens if one adds 2 or 3 silicon atoms? How does an $\text{Si}_6\text{H}_{11}\text{X}$ ring compare to a $\text{C}_6\text{H}_{11}\text{X}$ ring?

The polysilacyclohexane families are numerous and we decided only to consider families that retain C_s symmetry when monosubstituted (except some of the monosilacyclohexanes), as both the conformational analysis and the calculations get too complicated without it. Only monosubstituted rings were considered. The families investigated are shown in figure 6.

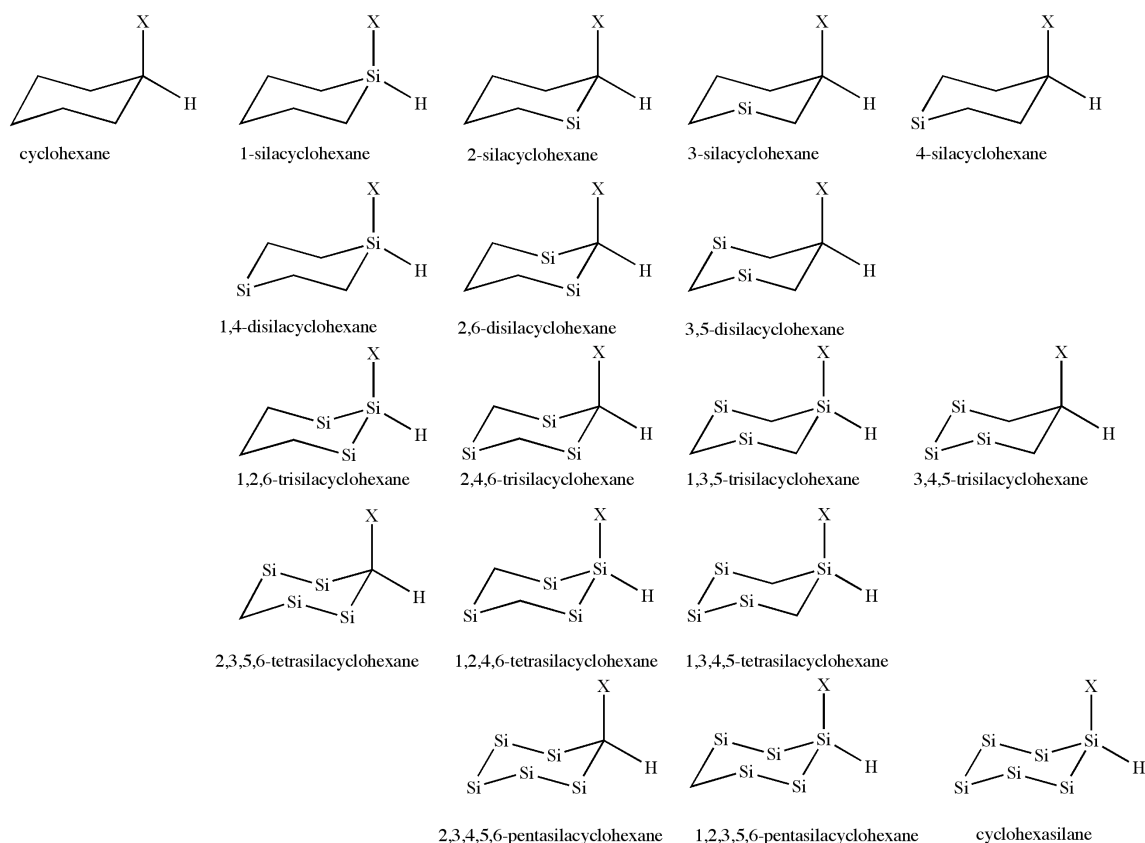
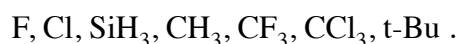


Figure 6. The monosubstituted silacyclohexane families investigated.

We adopted our own naming system for distinguishing between families. It is useful, for our purposes, to define the atom bonded to the substituent as being always in the 1-position, to avoid confusing nomenclature when additional silicon atoms are added.

We wanted to investigate a few interesting substituents:



Most of these substituents were chosen as they have been investigated experimentally for cyclohexane and 1-silacyclohexane and are chemically diverse, but we decided not to include substituents that break the symmetry and for which several rotamers are possible, thus complicating both the conformational analysis and the number of calculations needed to be carried out. We wanted to include the tertbutyl substituent as this is the classic bulky substituent in organic chemistry and results of this substituent could give us valuable information about the importance of steric repulsion on the conformational properties of silacyclohexanes.

In order to do these calculations as conveniently as possible we set up a standardized input file (Appendix 2.1). The input files for all molecules and their conformers differed only in the cartesian coordinates that define the different geometry for each conformer, thus ensuring that the calculations are carried out identically.

The different ring systems with different substituents were calculated at the same level of theory that was chosen as being both economic and accurate enough. Geometries were thus optimized at the M06-2X/pc-2 level, a theory level that we had previously shown to be able to predict accurate geometries compared to GED results. Single-point energies were then calculated with the same functional up to the pc-3 level, a basis set that we considered to be large enough for the energy difference to be converged. As a continuing analysis on the basis set convergence of our calculations, we always did calculations with basis sets from pc-0 to pc-3. Generally, it seems quite clear that the pc-2 basis set is satisfactory and the use of pc-3 changes substantially, only in a few cases, the ΔE value.

Starting geometries were either built in Gaussview 3.0 or modified manually with a text editor. Due to the starting geometries often being far from the optimized ones, pre-optimization with the M06-L functional was carried out, using density fitting, to reduce the number of optimization steps at the M06-2X/pc-2 level. This turned out to be a convenient way of optimizing accurate geometries quite quickly.

2.2.2 Monosilacyclohexane families

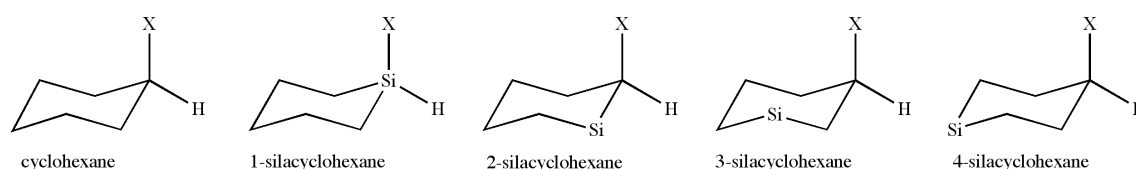


Figure 7: The monosilacyclohexane families and cyclohexane.

The focus of the experimental work in our group has mainly been on monosubstituted silacyclohexanes with the silicon in the 1-position (bonded to the substituent). This is an interesting family and both experimental and theoretical results were presented in

chapter 1. But what effect has it on the conformational properties if the silicon occupies another position? The 1-position is clearly special as the substituent is not only “interacting” with a different ring system but it is also connected to the heteroatom directly, thus subject to different bond polarization and different bond length if compared to the cyclohexane reference system.

Placing silicon in the 2-, 3-, or 4- position should result in different properties but how different?

It seems rather difficult to predict offhand what will happen as we don’t understand the conformational properties of 1-silacyclohexane to begin with. It should be noted that 5-silacyclohexane and 6-silacyclohexane are also possible ring systems, they, however, are enantiomers of 2- and 3-silacyclohexane and as such have identical energetic properties. Calculations were performed for the four monosilacyclohexane families and the cyclohexane system and the results are shown in table 17.

Table 17. M06-2X/pc-3 calculated ΔE values ($E_{ax}-E_{eq}$) of different monosilacyclohexane families (and cyclohexane) for a few substituents. Values in kcal/mol.

	cyclohexane	1-sila	2-sila	3-sila	4-sila
F	+0.12	-0.15	-0.37	+0.94	-0.05
Cl	+0.23	-0.64	-0.43	+0.82	-0.44
SiH ₃	+1.26	-0.14	+0.34	+1.55	+0.70
CH ₃	+1.70	+0.12	+0.86	+1.33	+1.10
CF ₃	+2.26	-0.50	+0.69	+2.41	+1.52
CCl ₃	+4.87	+0.30	+2.11	+4.65	+3.87
t-Bu	+5.39	+1.03	+2.44	+4.08	+4.91

While it is informative to look at the numbers it is easier to discover trends in the numbers using a graphical representation. We thus plot the energy values for each family on a single graph, figure 8. The x-axis is not a real numerical axis as we don’t attempt to relate the different substituents to any single chemical property. The connecting lines between points similarly have no meaning and their only purpose is to distinguish clearly between families. The substituents were ordered according to ascending energy values of the cyclohexane family. The resulting graph is easy to understand and one can see the different trends in the families. The same graphical representation will be used for other families in this chapter.

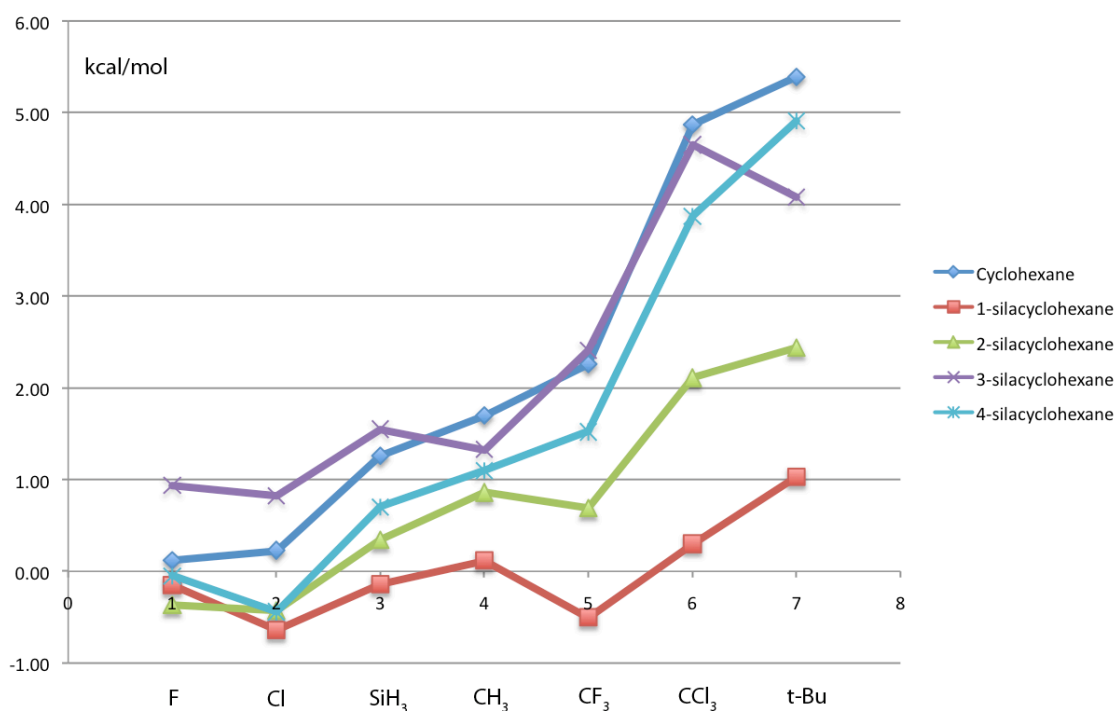


Figure 8. Graph showing the trends in ΔE values of the monosilacyclohexane families compared to cyclohexane.

From the graph it is quite clear that 1-silacyclohexane is unique in being the family where the equatorial conformer is the least predominant in the conformational equilibrium. Two substituted 1-silacyclohexanes were not discussed in chapter 1, these are the CCl_3 and t-Bu molecules. Comparing the 1-silacyclohexane values for these substituents with the cyclohexane values is very interesting, with large differences in ΔE values of ~ 4.5 kcal/mol between families.

The 2-silacyclohexane family is also very interesting as it decreases the ΔE values of the cyclohexane family considerably, despite the silicon atom not being directly bonded to the substituent as in the 1-silacyclohexane family. Silicon in the 4-position is the farthest away from the substituent. It still has a noticeable lowering effect on the ΔE value.

Especially interesting are the results of the 3-silacyclohexane family. One might perhaps guess beforehand that the 3-silacyclohexane family might behave somewhat inbetween the 2-silacyclohexane family and the 4-silacyclohexane. Instead, however, the energy values closely resemble the cyclohexane values and interestingly for four substituents of 3-silacyclohexane, the ΔE values are higher than for cyclohexane. Placing a silicon in the 3-position thus seems to have a peculiar effect that seems different from placing silicon in the other positions.

We were interested in seeing if the energy values of the different families might correlate. We thus plotted the energy values of cyclohexane vs. each monosilacyclohexane family. Interestingly, plots of 2-, 3- and 4-silacyclohexane vs. cyclohexane correlate rather well while the correlation is noticeably worse for 1-silacyclohexane vs. cyclohexane.

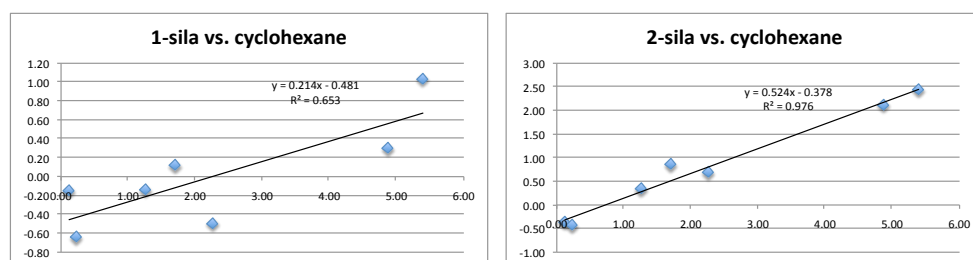


Figure 9. Left: Plot of ΔE values of 1-silacyclohexane vs. cyclohexane. Both axes are in units of kcal/mol.

Figure 10. Right: Plot of ΔE values of 2-silacyclohexane vs. cyclohexane. Both axes are in units of kcal/mol.

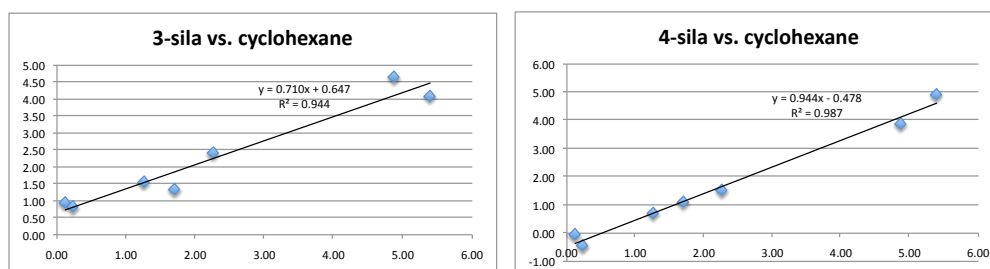


Figure 11. Left: Plot of ΔE values of 3-silacyclohexane vs. cyclohexane. Both axes are in units of kcal/mol.

Figure 12. Right: Plot of ΔE values of 4-silacyclohexane vs. cyclohexane. Both axes are in units of kcal/mol.

It is an interesting observation that the 1-silacyclohexane family shows notably worse correlation with cyclohexane than the other monosilacyclohexane families. As mentioned before, the silicon occupying position 1 is unique in being directly bonded to the substituent.

The correlations between cyclohexane and 2-, 3- and 4-silacyclohexane energy values are interesting and suggest that silicon has a systematic effect on the cyclohexane system and the overall conformational properties, one that perhaps might be explainable by simple means. This also suggests that it might be possible to build an empirical model that could predict energy differences of heterocyclic systems containing silicon. One would have to relate the substituents to some chemical property though for this to be useful (steric size, electronegativity, Lewis base/acidity etc.)

2.2.3 Disilacyclohexane families

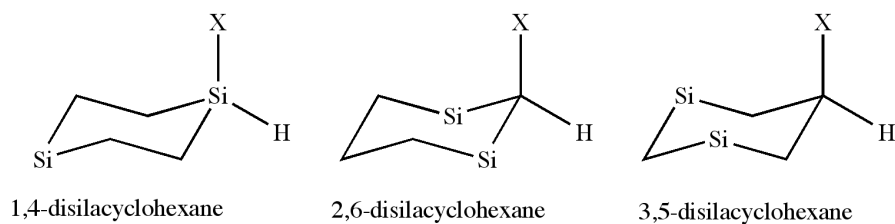


Figure 13: The disilacyclohexane families.

Three disilacyclohexane families (figure 13) were selected and calculated for the same substituents. They are interesting systems, mainly because they can be directly related to the monosilacyclohexanes discussed before (and the polysilacyclohexane families in the later subchapters).

Table 18. M06-2X/pc-3 calculated ΔE values ($E_{ax}-E_{eq}$) of the disilacyclohexane families. Values in kcal/mol.

	1,4-disila	2,6-disila	3,5-disila
F	-0.26	-0.48	+1.49
Cl	-0.84	-0.90	+1.35
SiH ₃	-0.24	-0.06	+1.86
CH ₃	+0.12	+0.26	+1.04
CF ₃	-0.58	-0.36	+2.55
CCl ₃	+0.36	+0.15	+4.62
t-Bu	+1.50	+1.42	+4.95

Results for the disilacyclohexane families are given in table 18 and figure 14.

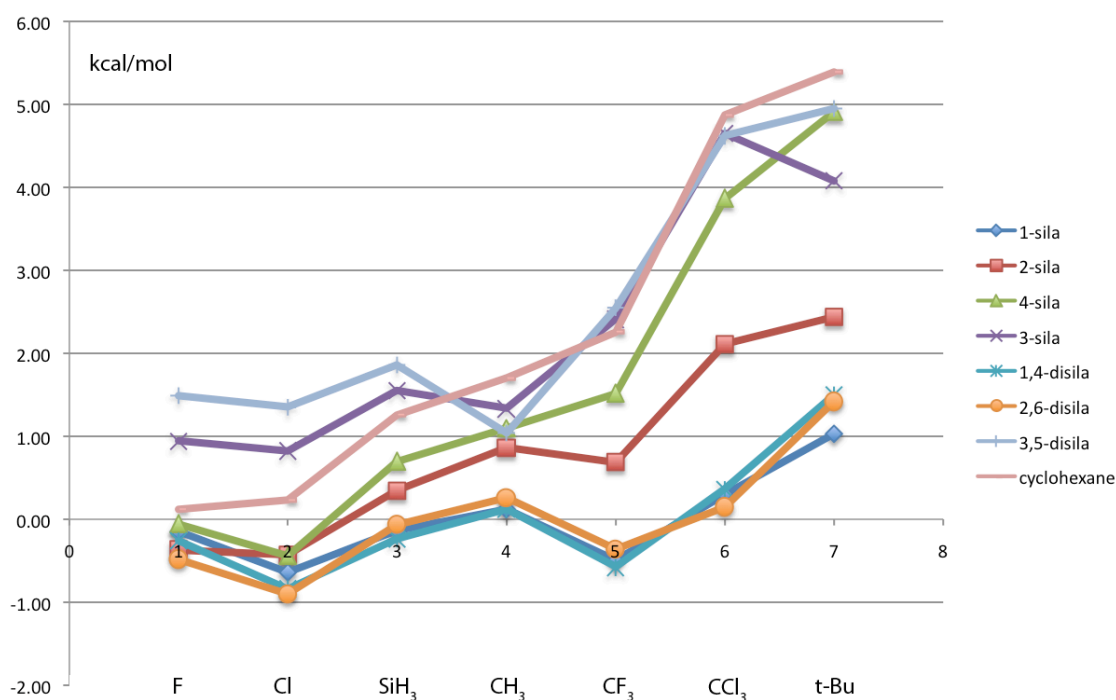


Figure 14. Graph showing the trends in ΔE values of the monosilacyclohexane and disilacyclohexane families compared to the cyclohexane family.

In figure 14 we show the energy values of cyclohexane, all monosilacyclohexanes and the disilacyclohexanes in one plot for direct comparison.

The 1,4-disilacyclohexane system has rather low energy values and comparing this system to the related 1-silacyclohexane and 4-silacyclohexane families one sees that:

1. adding a silicon to the 4-position of 1-silacyclohexane causes a very small ΔE lowering effect for all cases but curiously not for the CCl_3 and t-Bu cases.
2. Adding a silicon atom to the 1-position of 4-silacyclohexane causes considerable ΔE lowering.

Adding a second silicon atom to the 2-silacyclohexane family in to the symmetrically equivalent 6-position, resulting in 2,6-disilacyclohexane, causes considerable lowering of ΔE values. The 2,6-disilacyclohexane and the 1,4-disilacyclohexane families in fact behave rather similarly, which is interesting as the silicon atoms are in different positions of both rings. The 1-silacyclohexane family also behaves similarly. Interestingly, it takes 2 silicon atoms in the 2- and 6- positions to get energy lowering of the same magnitude as placing a single silicon atom in the 1-position. We do note that 1-silacyclohexane and

2,6-disilacyclohexane both have two Si-C bonds, next to the substituent, in common, and it is possible that this might explain the similarity in conformational properties.

The 3,5-disilacyclohexane family is very interesting. Adding another silicon to the 5-position (symmetrically equivalent to the 3-position) causes ΔE to increase for the same four substituents of the 3-silacyclohexane that had higher ΔE values than cyclohexane. ΔE decreases for the methyl substituent, however.

Placing silicon atoms in positions 3 and 5 appear to have completely different effects than placing silicon atoms in other positions of the ring.

We note that the ΔE lowering effect of adding silicon atoms (into the 1- and 4- position, 2- and 6- position, and 3- and 5- positions) is not an additive effect as is easily demonstrated by adding e.g. the $\Delta\Delta E$ difference between 1-silacyclohexane and cyclohexane on one hand and the $\Delta\Delta E$ difference between 4-silacyclohexane and cyclohexane on the other, to the cyclohexane ΔE values.

Like before we did notice correlation between families. 1,4-silacyclohexane and 1-silacyclohexane families correlate strongly while 1,4-silacyclohexane and 4-silacyclohexane don't correlate nearly as well.

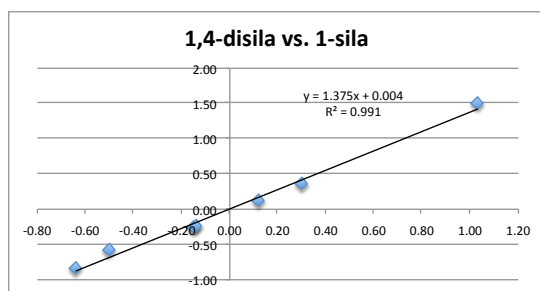


Figure 15. Left: Plot of ΔE values of 1,4-disilacyclohexane vs. 1-silacyclohexane. Both axes are in units of kcal/mol.

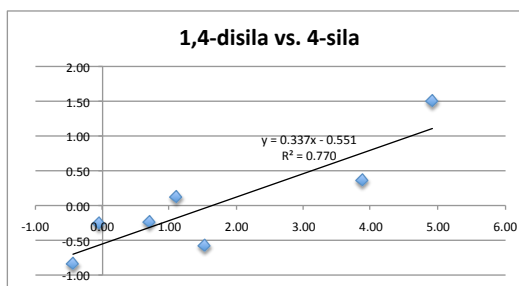


Figure 16. Right: Plot of ΔE values of 1,4-disilacyclohexane vs. 4-silacyclohexane. Both axes are in units of kcal/mol.

This seems to be related to the fact that we similarly had small correlation between cyclohexane and 1-silacyclohexane families before. This suggests that placing silicon in the 1-position generally has a non-linear effect on the conformational equilibrium.

The 2,6-disilacyclohexane family vs. the 2-silacyclohexane family don't correlate as well as one would have expected, mainly due to one point breaking the trend. The point corresponds to the ΔE values of the CCl_3 substituent.

The 3,5-disilacyclohexane family correlates, however, well with the 3-silacyclohexane family.

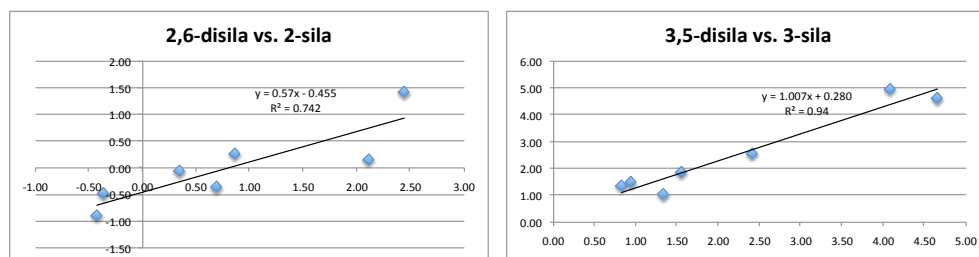


Figure 17. Left: Plot of ΔE values of 2,6-disilacyclohexane vs. 1-silacyclohexane. Both axes are in units of kcal/mol.

Figure 18. Right: Plot of ΔE values of 3,5-disilacyclohexane vs. 3-silacyclohexane. Both axes are in units of kcal/mol.

Interestingly, the 1,4-disilacyclohexane family and the 2,6-disilacyclohexane family correlate rather well and same goes for 2,6-disilacyclohexane and 1-silacyclohexane. This is strange because these families don't even have a single silicon position in common. More points should be calculated here to confirm that a correlation actually exists.

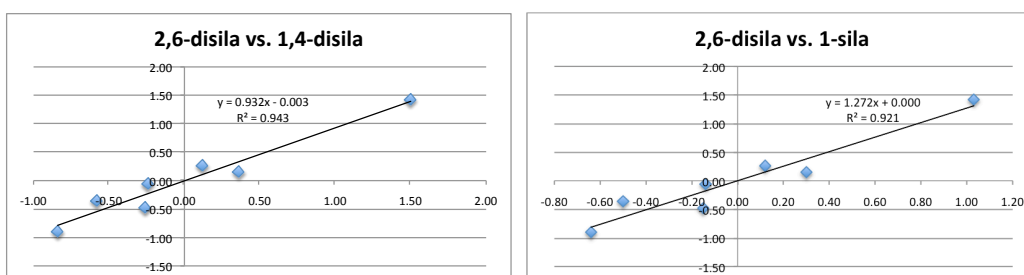


Figure 19. Left: Plot of ΔE values of 2,6-disilacyclohexane vs. 1,4-disilacyclohexane. Both axes are in units of kcal/mol.

Figure 20. Right: Plot of ΔE values of 2,6-disilacyclohexane vs. 1-silacyclohexane. Both axes are in units of kcal/mol.

2.2.4 Trisilacyclohexanes

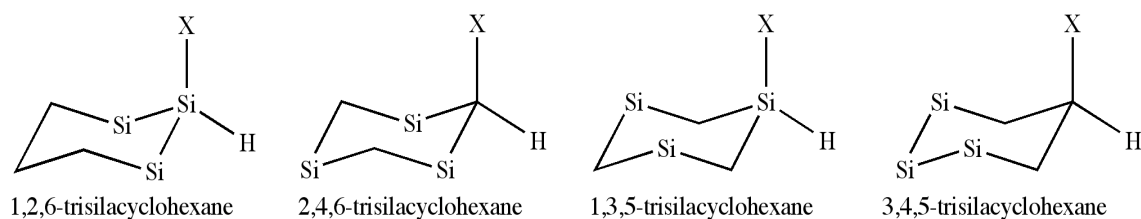


Figure 21: The trisilacyclohexane families.

Four trisilacyclohexane families were calculated. Two of these, 1,3,5-trisilacyclohexane and 2,4,6-trisilacyclohexane, have a homogeneous ring skeleton, i.e. consisting only of Si-C bonds.

Table 19. M06-2X/pc-3 calculated ΔE values ($E_{ax} - E_{eq}$) of the trisilacyclohexane families. Values in kcal/mol.

	1,2,6-trisila	2,4,6-trisila	1,3,5-trisila	3,4,5-trisila
F	+0.13	-1.00	+0.49	+1.04
Cl	+0.15	-1.30	+0.10	+0.47
SiH ₃	-1.24	-0.24	+0.14	+1.22
CH ₃	-0.44	+0.16	-0.15	+1.23
CF ₃	-0.84	-1.11	+0.99	+0.57
CCl ₃	-1.32	-0.38	+1.90	+1.97
t-Bu	-0.23	+0.96	+1.69	+2.45

Inspecting the 1,3,5-trisilacyclohexane ring and using the information gathered from the mono- and disilacyclohexane families before, we would expect that the 1,3,5-trisilacyclohexane family would have lower ΔE values than 3,5-disilacyclohexane, since we are placing a silicon in the 1-position. The ΔE values would be higher than the 1-silacyclohexane values due to silicon occupying the 3- and 5- positions. Similarly placing a silicon in the 4-position of 3,5-disilacyclohexane would also lower the ΔE values of the resulting 3,4,5-trisilacyclohexane. This is approximately what happens.

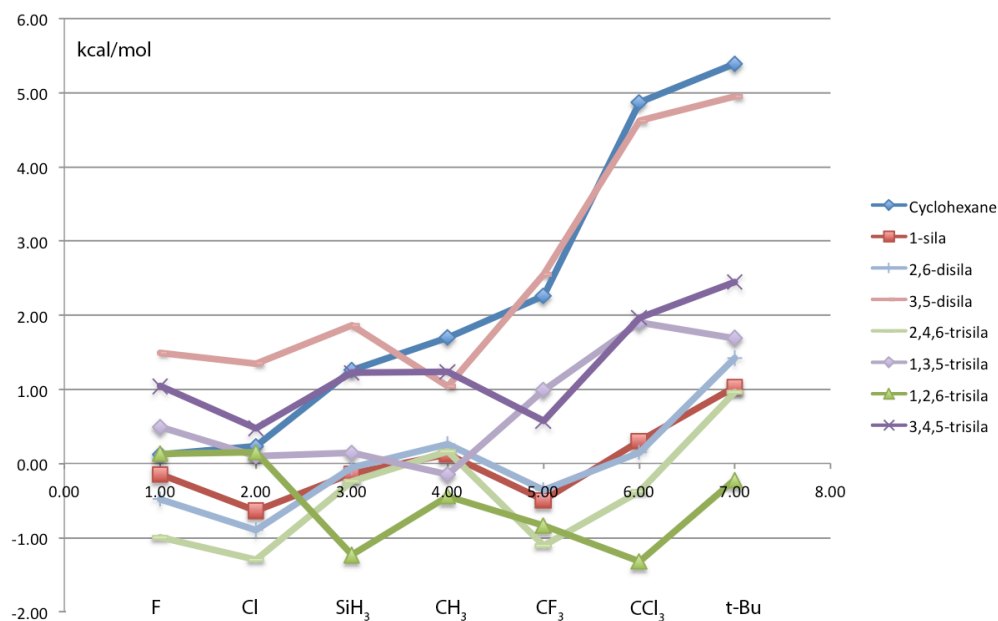


Figure 22. Graph showing the trends in ΔE values of the trisilacyclohexane families compared to some of the monosila- and disilacyclohexane families.

Placing a silicon in the 4-position yields considerable ΔE lowering when comparing cyclohexane and 4-silacyclohexane. The effect is not as big when comparing 1-silacyclohexane and 1,4-disilacyclohexane.

However when comparing 2,6-disilacyclohexane and 2,4,6-trisilacyclohexane, the effect is quite notable again, yielding ΔE values that are generally lower than 1-silacyclohexane. Even more interesting is the 1,2,6-trisilacyclohexane system where, apart from F and Cl substituents, very low ΔE values are obtained. Especially noteworthy is the CCl_3 case with $\Delta E = -1.32$ kcal/mol and the t-Bu case that yields remarkably a slightly negative ΔE value.

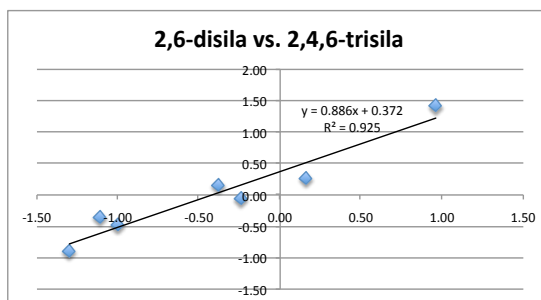


Figure 23. Plot of ΔE values of 2,6-disilacyclohexane vs. 2,4,6-trisilacyclohexane. Both axes are in units of kcal/mol.

The 2,6-disilacyclohexane and 2,4,6-trisilacyclohexane ΔE values correlate as shown in figure 23. 3,5-disilacyclohexane and 1,3,5-trisilacyclohexane families also correlate well, in contrast to previous graphs where the correlation was not so good when comparing families with and without silicon in the 1-position.

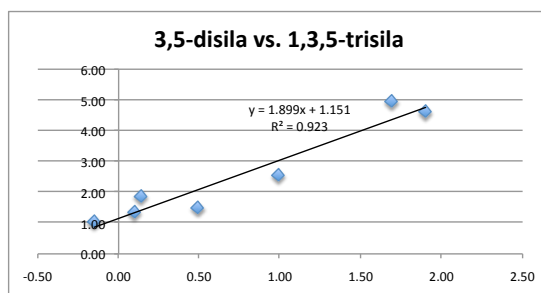


Figure 24. Plot of ΔE values of 3,5-disilacyclohexane vs. 1,3,5-trisilacyclohexane. Both axes are in units of kcal/mol.

2.2.5 The tetra- and pentasilacyclohexanes and cyclohexasilane

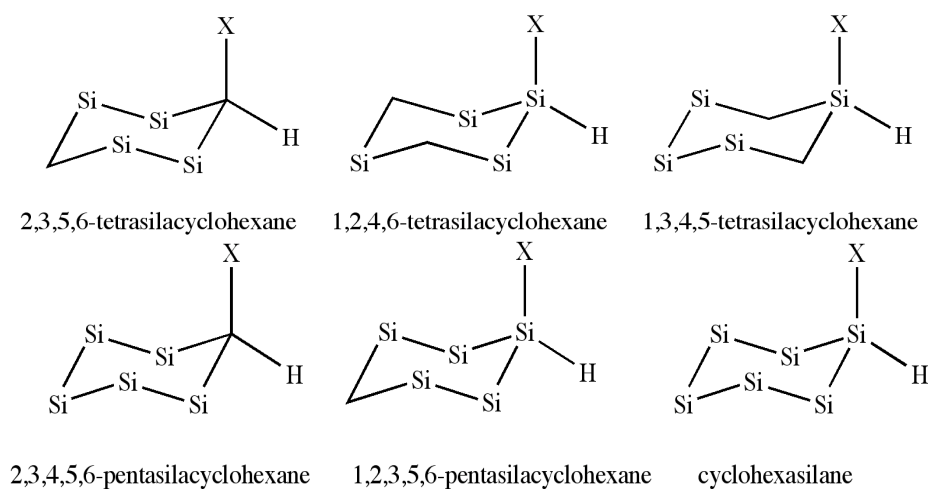


Figure 25: The tetra- and pentasilacyclohexane families and cyclohexasilane.

Lastly, we consider three tetrasilacyclohexane families, two pentasilacyclohexane families and finally cyclohexasilane, a family where the ring skeleton consists exclusively of silicon atoms. The results are shown in tables 20 and 21 and figure 26.

Table 20. M06-2X/pc-3 calculated ΔE values ($E_{ax}-E_{eq}$) of the tetrasilacyclohexane families. Values in kcal/mol.

	2,3,5,6-tetrasil	1,2,4,6-tetrasil	1,3,4,5-tetrasil
F	+0.34	-0.25	+0.36
Cl	-0.03	-1.24	-0.22
SiH ₃	-0.35	-0.45	+0.78
CH ₃	+0.14	+0.15	-0.13
CF ₃	-0.34	-1.57	-0.07
CCl ₃	-0.12	-1.50	+1.29
t-Bu	+0.75	+0.05	+1.99

Table 21. M06-2X/pc-3 calculated ΔE values ($E_{ax}-E_{eq}$) of the pentasilacyclohexane families and cyclohexasilane. Values in kcal/mol.

	2,3,4,5,6-pentasil	1,2,3,5,6-pentasil	cyclohexasilane
F	-0.10	+0.50	+0.12
Cl	-0.33	-0.13	-0.59
SiH ₃	-1.44	-0.54	-0.22
CH ₃	-0.22	-0.23	-0.22
CF ₃	-0.68	-0.37	-0.79
CCl ₃	-1.45	-0.53	-0.84
t-Bu	-0.32	+0.21	+0.29

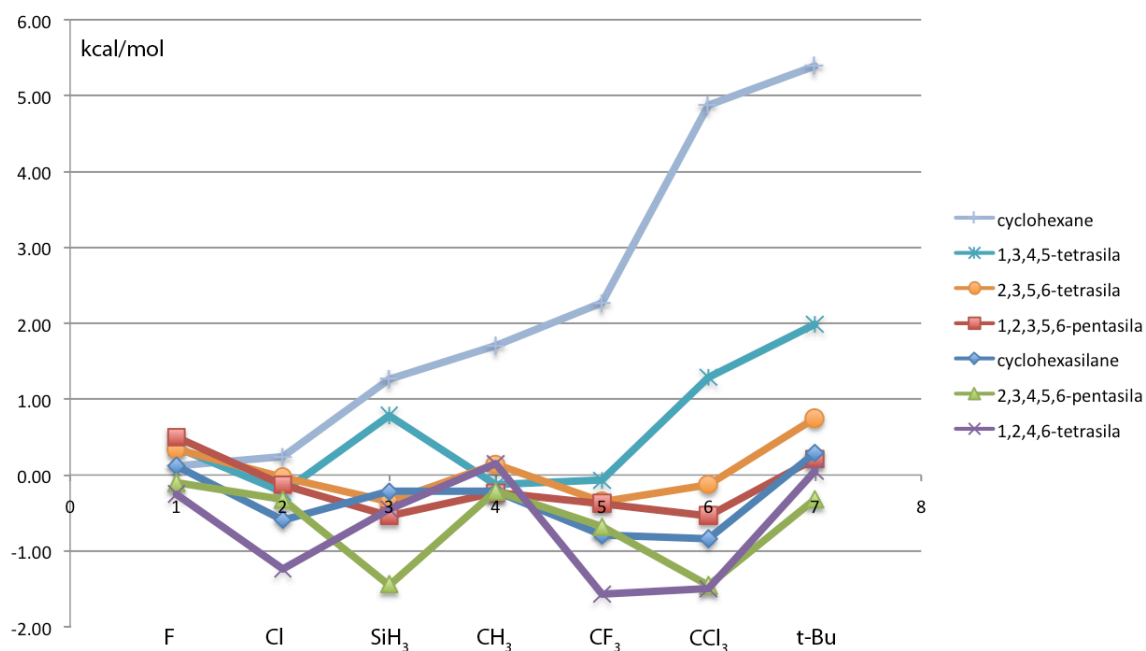


Figure 26. Graphical representation of the trends in ΔE values of the tetra- and pentasilacyclohexane and cyclohexasilane families compared to the cyclohexane family.

The tetra-, penta- and hexasilacyclohexane families (except the 1,3,4,5-tetrasilacyclohexane family) show a general tendency for negative ΔE values. 1,2,4,6-tetrasilacyclohexane show the lowest ΔE values for CF_3 and CCl_3 substituents for any silacyclohexane family so far (and in fact for any substituent as well). 2,3,4,5,6-pentasilacyclohexane family shows a very low ΔE for the SiH_3 substituent, -1.44 kcal/mol and the lowest ΔE value for the t-Bu substituent of all silacyclohexanes, -0.32 kcal/mol.

The cyclohexasilane family does not stick out if compared to the tetra- and pentasilacyclohexane families but it is nonetheless interesting to compare it to its carbon analogue, cyclohexane, that shows completely different conformational properties.

2.2.6 General observations

The conformational data just discussed, was obtained very recently and the above discussion only reflects a first impression of the results. Clearly, however, silicon introduces a very interesting effect on the conformational properties of the cyclohexane ring. Especially interesting is the sharp contrast between CCl_3 -substituted cyclohexane and 1,2,6-trisila, 1,2,4,6-tetrasila and 2,3,4,5,6-pentasilacyclohexanes, where there is a clear preference for the axial conformer for the mentioned silacyclohexanes but a very high preference for the equatorial conformer in cyclohexane. It is also remarkable to regard the cases where the t-Bu substituent has a slight axial preference or the ΔE is close to zero for a few of the silacyclohexanes.

The last systems calculated here are obviously quite different from the cyclohexanes, tetrahydropyrans and 1-silacyclohexanes, that we used to benchmark density functionals in chapter 1.4.4, as the systems consist here mostly of Si-Si and Si-H bonds and could hardly be called organic molecules anymore. The question springs to mind whether the M06-2X functional is as accurate for these systems. While we don't have CCSD(T) values to compare to, we decided to pick one molecule with a ring skeleton consisting mainly of silicon atoms and calculate the energy difference with B3LYP, B97-1,

B2PLYP-D and MP2 and see how the methods compare now. B2PLYP-D, M06-2X and MP2 methods have generally resulted in very similar values while we found that the B3LYP and B97-1 functionals suffered from equatorial overstabilization. We decided thus to see how a molecule would compare, that showed surprisingly much axial stabilization, 1-CCl₃-2,3,4,5,6-pentasilacyclohexane, with $\Delta E = -1.45$ kcal/mol, according to the M06-2X calculations.

Table 22. The axial/equatorial energy difference of 1-CCl₃-2,3,4,5,6-pentasilacyclohexane with different methods.

Method	ΔE	Deviation from M06-2X
M06-2X/pc-3	-1.45	-
B3LYP/pc-3	+0.56	2.01
B97-1/pc-3	+0.12	1.57
B2PLYP-D /aug-def2-TZVPP	-0.86	0.59
MP2/cc-pV(Q+d)Z	-1.21	0.24

The results in table 22 show that the M06-2X and MP2 methods are very much in agreement and B2PLYP-D is not far off. The B3LYP and B97-1 functionals, however, appear to show disastrous failure for this system. This is a worrying result, and suggests that the B3LYP functional can fail even worse than our comparison in chapter 1 indicated.

The reliability of B3LYP for doing conformational analysis of heterocyclic systems seems thus questionable.

Finally, while this is the first systematic investigation of this kind on the silicon substitution effect on the cyclohexane system, it is far from complete. We have given no attention to geometry effects, how the geometries of the ring systems change with different substituents and how particular bonds and angles change when carbon is substituted for silicon. A systematic study of geometry changes (bonds, angles and intramolecular distances) of the systems discussed in this chapter would be very interesting and could yield valuable information regarding possible stereoelectronic or steric effects. All of this geometric data exists but has yet to be analyzed.

No calculations were done to describe the potential energy surfaces of the different ring systems or to calculate activation barriers.

To the best of our knowledge, there exist no experimental results for any of these molecules (except cyclohexane and 1-silacyclohexane families). It would definitely be interesting to confirm some of these observations with experiments.

2.3 Stereoelectronic effects

Inspection of the tables and figures in chapter 2.2 reveals that steric effects, like 1,3-diaxial repulsion that is used to explain the conformational properties of cyclohexanes, don't seem to apply to the conformational properties of silacyclohexanes. While silicon introduces longer bonds in the molecule (both in the ring and also in the substituent when silicon is in the 1-position) that would certainly diminish such steric effects, this is not a satisfactory explanation for the conformational properties of silacyclohexanes because it doesn't explain why CF_3 -substituted cyclohexane for example, with a large equatorial preference ($\Delta E = +2.26$), "changes" into a slight axial preference ($\Delta E = -0.5$ kcal/mol) when silicon occupies the 1-position. This is also a larger effect than CH_3 -substituted cyclohexane vs. 1-silacyclohexane. The large axial preference of several substituents of the polysilacyclohexane families also point to 1,3-diaxial interactions not playing a significant role. It would thus appear that some conformational effect is stabilizing the axial substituent more in silacyclohexanes, or perhaps destabilizing the equatorial substituent.

While we are not necessarily questioning the fact that 1,3-diaxial steric repulsion effects might play a role in systems like these, they do not appear to play a major role.

What is then the major factor(s) behind the conformational properties of silacyclohexanes? While other steric effects are definitely possible (we again note that a proper investigation of geometric effects of the silacyclohexanes in chapter 2.2 has not been performed), much work in the recent years has revolved around stereoelectronic effects like hyperconjugation, for explaining conformational problems. The stabilization of the gauche conformer of 1-fluoropropane for example, is explained by an

hyperconjugative electron-donating interaction into an antibonding $\sigma^*(\text{C-F})$ bond by a $\sigma(\text{C-H})$ donor [115].

Hyperconjugation as a major factor behind conformational properties remains a controversial subject, however. A discussion took place recently in the literature about the origin of the rotational barrier of ethane, whether it is of hyperconjugative or steric origin [116], [117], [118], [119]. Hyperconjugation as an explanation for the anomeric effect, mentioned in the introduction, has also been accepted for some time but has recently been questioned from recent QTAIM calculations (quantum theory of atoms in molecules) [8] [9].

Recent research on the conformational properties of monosubstituted cyclohexanes has also revealed several surprises. Wiberg et al. [120] suggested, based on geometric analysis, that there was no evidence for 1,3-diaxial interactions in monosubstituted cyclohexanes and Ribeiro et al. [121] came to the same conclusion and suggested a hyperconjugative explanation for the conformational properties involving the axial hydrogens.

Cuevas et al. [122] also demonstrated by QTAIM analysis that the 1,3-diaxial interactions are not repulsive but are instead attractive, generally. They also suggested that substituents generally are stable in the axial positions but in turn they destabilize the cyclohexyl ring that results in the observed conformational properties.

Taddei et al. [123], [124] investigated the role of hyperconjugative interactions in substituted cyclohexanes using natural bond orbital analysis (NBO) [125] and found that the hyperconjugative effect is often more important for O-including substituents than alkyl substituents.

Alabugin et al. have investigated stereoelectronic effects of σ -bonds in general [126], and stereoelectronic effects in heterocycles [127], [128] with many interesting findings.

It seems especially hard to relate our results to the numerous studies on cyclohexane and heterocycles just mentioned, as the conformational properties of cyclohexane are perhaps just beginning to be understood fully. Heterocyclic systems that have been studied (excluding silicon heterocycles) usually include heteroatoms with lonepairs and their conformational properties are usually explained by hyperconjugative interactions involving them [129], [128]. The silacyclohexanes do not include lone pairs but yet

exhibit interesting conformational properties and the work presented in this chapter should contribute valuable knowledge to the continuing investigation of the conformational properties of six-membered rings. It is possible that the conformational properties of our systems might be explained by something as simple as donor- acceptor hyperconjugative interactions involving the Si-C bonds or perhaps the hydride character of the hydrogens connected to silicon but this awaits further study.

We did attempt NBO calculations using the NBO 5.G^{xii} package, that was implemented in NWChem with the help of NWChem programmers. Natural bond orbital analysis involves transforming the molecular orbitals of a quantum calculation into localized orbitals. Filled localized orbitals, that describe as much as possible of the total electron density correspond to the Lewis structure of the molecule. The rest would involve delocalization of electron density and by comparing the nature and magnitude of the delocalization energy one can explain different chemical properties of conformers for example.^{xiii} Unfortunately we ran into problems involving the convergence of the delocalization energy, that we do not understand completely how to solve.

Finally, while we had hoped during the course of this project to be able to shed some light on the heteroatom effects that silicon has on the conformational properties of the cyclohexane ring we are still very much in the dark on this and future studies should definitely focus on identifying these effects. Natural bond orbital analysis [125], BLW(Block-localized wave function) [130] or QTAIM [131] approaches seem to be viable methods for such investigations. We have, however, using a computational method that we consider trustworthy for calculating energy differences of these systems, explored the conformational properties of silacyclohexanes considerably, with sometimes counterintuitive results.

^{xii} <http://www.chem.wisc.edu/~nbo5/>

^{xiii} http://www.chem.wisc.edu/~nbo5/tur_ch.htm

Chapter 3 – Disilacyclohexanes - physical properties, energy surfaces and NMR spectra

3.1 Introduction

Monosubstituted disilacyclohexanes were discussed in the previous chapters. This chapter, however, is about the parent (unsubstituted) disilacyclohexanes.

Three configurational isomers of the disilacyclohexanes exist:

1,2-disilacyclohexane, 1,3-disilacyclohexane and 1,4-disilacyclohexane.

These molecules were synthesized for the first time by graduate student Pálmar I. Gudnason in the research group of Ingvar Arnason. The synthesis of all three rings was a challenging problem that required novel synthetic procedures as well as uncommon starting materials [132].

In his M.Sc. thesis, *Silicon-containing six-membered rings* [24], Gudnason describes the conformational energy surfaces as well as the lowest energy pathways of the chair-chair equilibrium of all three molecules. Conformational energy surfaces (CES) were calculated using Gaussian 98 by varying two dihedral angles of the ring and calculating the energy of each conformation with the B3LYP/STO-3G method. While this basis set is very incomplete, it served its purpose for this rough description of the potential energy surface and all important minima and maxima of the three molecules were located. The lowest energy pathways were then obtained from the data of the CES-scan. The critical points were also re-optimized with additional methods, using more complete basis sets. While the work done serves well as a general description of the CES and most stationary points of these molecules were located, Gudnason did run into a few computational obstacles, mainly related to his modest computational facilities (a single 1.15 GHz PC).

Our work has involved the following:

- We wanted to solve the problems that Gudnason ran into, as well as confirm the lowest energy pathways using modern optimization- and saddle-point location techniques and finally recalculate the conformational energies of the minima and saddle points with higher level methods.

- Gas electron diffraction data for the disilacyclohexanes also became available recently and the structures were compared to calculated structures.
- Enthalpies of formation for the molecules were calculated and are discussed.
- Another interesting aspect of the disilacyclohexanes concerns their NMR spectra that interestingly enough are very complicated. Simulations of the spectra were carried out by Gudnason but were not completely successful. Using different simulation techniques, the spectra were simulated with better results.

3.2 Potential energy surfaces

The conformational energy surfaces were mapped with the B3LYP functional and the STO-3G basis set by Gudnason. The STO-3G basis is a minimal basis set, meaning that it contains the minimum number of basis functions that are needed to describe each atom. This small basis set was chosen due to the large amount of points that needed to be calculated for each surface. By varying two dihedral angles of the rings in steps of 5° from -90° to +90° and calculating the energy at each point, surfaces were obtained that include essentially all the important conformations that can be expected from a six-membered heterocyclic ring.

While the 3D surfaces have their uses, they are not as easy to understand as the 2D lowest energy pathways, that Gudnason shows in his thesis. They were made using the information from the calculated energy surfaces and reoptimization of the stationary points (minima and maxima) with DFT methods using larger basis sets.

We wanted to confirm these pathways: make sure that the correct saddle points had been found, that the path was possible and recalculate the energy of the stationary points with the M06-2X functional that we used successfully for the axial/equatorial energy differences in chapter 1 and 2. In the Gaussian 03 software [28], the synchronous transit-guided quasi-newton (STQN) method [133] is implemented that enables one to locate and optimize saddle points conveniently, by using as input the approximate

geometries of the reactant and product (QST2 keyword) and possibly also a good guess for the saddle point geometry (QST3 keyword) if needed.

We used the B3LYP method with the 6-311+G(d,p) basis set, this functional/basis combination has been used previously in our group for calculating lowest energy pathways for substituted monosilacyclohexanes [4], [22], [96]. Starting structures for the minima were built by hand in Gaussview. QST2 calculations, with no symmetry constraints, were carried out for locating and optimizing saddle points and the option added to minimize in the same calculation, the reaction path from structure A to B with 8 extra intermediate conformers (Gaussian keyword path=11). Frequency calculations were then carried out on the geometry of all stationary points to confirm that they were either minima or maxima. A saddle point should have exactly one imaginary frequency while a minimum should have no imaginary frequencies. Calculated pathways are shown in figures 27-29, where the dots indicate the different conformations. They are essentially the same pathways that Gudnason presented in his thesis.

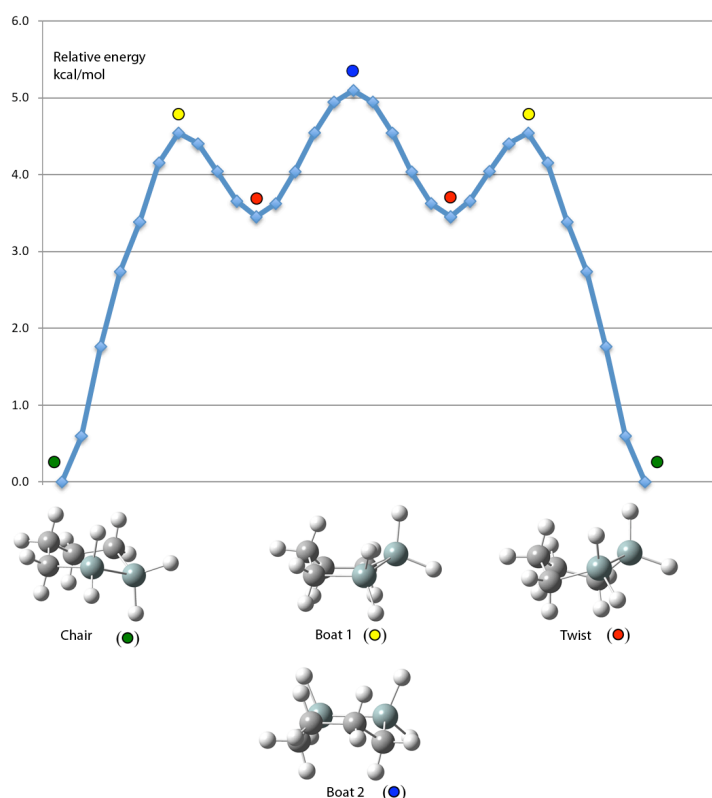


Figure 27. B3LYP/6-311+G(d,p) calculated lowest-energy path of 1,2-disilacyclohexane using the QST2 method.

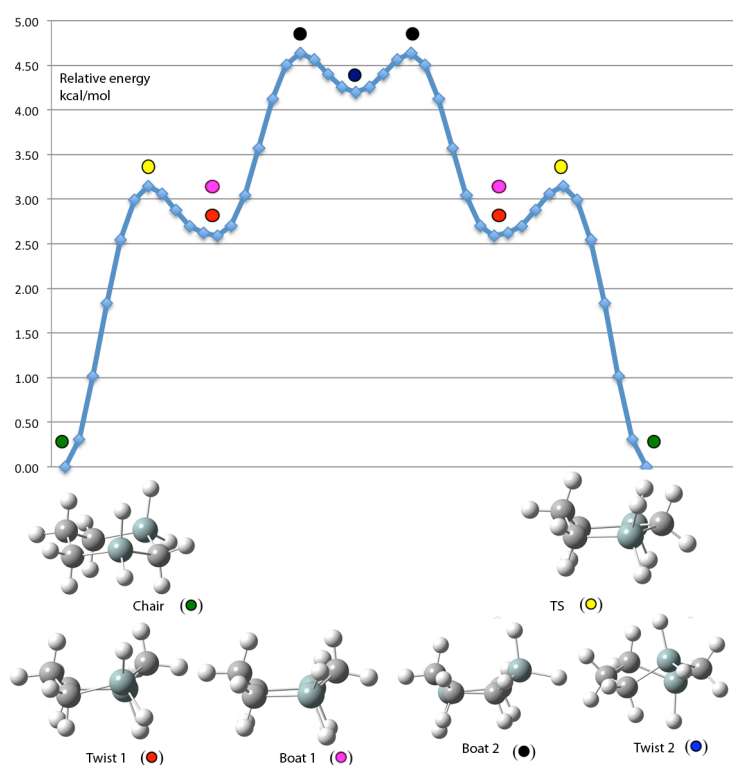


Figure 28. B3LYP/6-311+G(d,p) calculated lowest-energy path of 1,3-disilacyclohexane using the QST2 method.

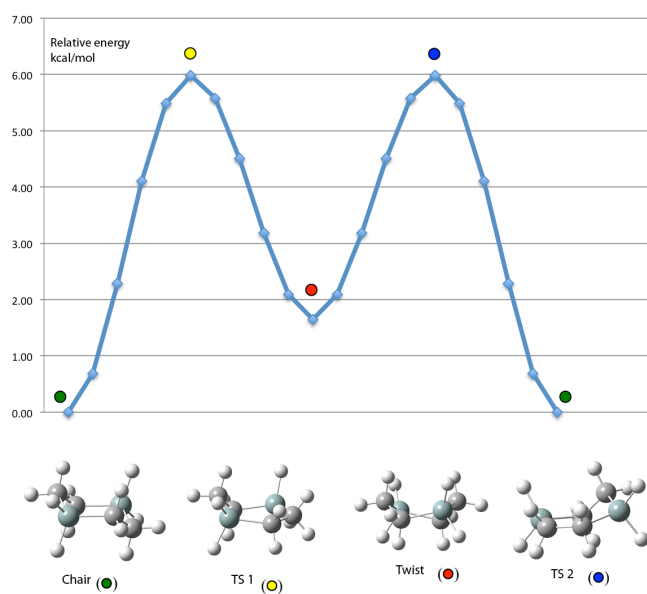


Figure 29. B3LYP/6-311+G(d,p) calculated lowest-energy path of 1,4-disilacyclohexane using the QST2 method.

The 1,3-disilacyclohexane pathway and surface was, however, improved upon. Two low energy conformers, Twist-1 and Boat-1 are very similar in energy, so similar that it was unclear which conformer was lower than the other, according to Gudnason's

calculations. By doing tight geometry optimizations (keyword: opt=vtight) and using a large grid (keyword: int=ultrafine), we were able to accurately locate both conformers unambiguously and relate them to each other by a QST3 calculation. It turned out that Boat-1 was a connecting saddle point between two conformers of type Twist-1, i.e. Twist-1a and Twist-1b. The transformation from Twist-1a to Twist-1b through Boat-1 is the same kind of pseudorotation as the well known twist-boat-twist transformation for cyclohexane along the equator of the conformational globe, that was mentioned in the introduction. In this case, however, we note a very subtle pseudorotation with an extremely low activation barrier of 0.04 kcal/mol (B3LYP/6-311+G(d,p) (figure 30).

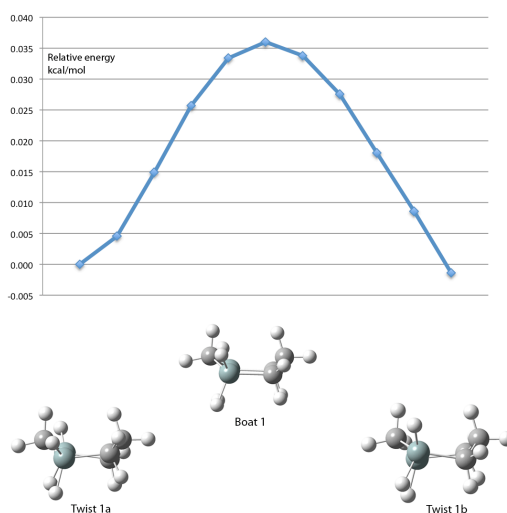


Figure 30. B3LYP/6-311+G(d,p) calculated path between the two equivalent twistforms (Twist-1a and Twist-1b).

Single-point M06-2X/pc-3 calculations were then carried out on the B3LYP/6-311+G(d,p) geometries for all stationary points. These calculations were performed in NWChem 5.1.

Table 23-25 shows the relative energies of all stationary points for all three disilacyclohexanes. Compared are the B3LYP/6-311+G(d,p) calculations and the M06-2X/pc-3//B3LYP/6-311+G(d,p) calculations^{xiv}.

The M06-2X energies are qualitatively similar to the B3LYP energies with some variation for a few conformers. We note that the activation barrier for the pseudorotation of Twist 1a to Twist 1b is higher according to the M06-2X calculations than the B3LYP calculations predicted (0.20 kcal/mol vs. 0.04 kcal/mol). We believe that the M06-2X

^{xiv} The relative energies are generally very similar to the DFT calculations by Gudnason with the variations most likely being only due to different basis sets used for energy evaluation and geometry optimization.

energies are more accurate, based on the arguments presented in chapter 1, due to a better functional and a more complete basis set.

Table 23. Relative energies (in kcal/mol) of conformers of 1,2-disilacyclohexane with different methods.

	B3LYP/6-311+G(d,p)^a	M06-2X/pc-3^b
Chair-1	0.00	0.00
Boat-1	4.54	4.71
Twist	3.45	2.96
Boat-2	5.10	5.00

^a B3LYP/6-311+G(d,p)//B3LYP/6-311+G(d,p) .

^b M06-2X/pc-3//B3LYP/6-311+G(d,p) .

Table 24. Relative energies of conformers of 1,3-disilacyclohexane with different methods.

	B3LYP/6-311+G(d,p)	M06-2X/pc-3
Chair	0.00	0.00
TS	3.15	3.76
Twist-1	2.59	2.67
Boat-1	2.62	2.87
Boat-2	4.63	4.73
Twist-2	4.20	3.99

Table 25. Relative energies of conformers of 1,4-disilacyclohexane with different methods.

	B3LYP/6-311+G(d,p)	M06-2X/pc-3
Chair	0.00	0.00
TS	5.98	6.70
Twist	1.65	1.72

3.3 Structure and stability

The disilacyclohexanes were measured by gas electron diffraction in the group of Heinz Oberhammer, University of Tübingen, in order to determine their structures in gas phase. According to the calculations in the previous chapter, no conformer of 1,2- and 1,3-disilacyclohexane, except the chair form, is low enough in energy to be significantly populated at room temperature to be detectable in the GED experiment in the previous chapter. The twist-form of 1,4-disilacyclohexane has a relative energy of 1.72 kcal/mol and might thus be detectable, but wasn't found during the course of the experiment.

We optimized the molecular structure of the chair form of all three disilacyclohexanes at the M06-2X/pc-2 level as this method seemed to give accurate bond lengths of two monosilacyclohexanes in chapter 1.5. MP2/6-31G(d,p) and B3LYP/6-311+G(2d,p) calculations were performed by Heinz Oberhammer.

Experimental and theoretical bond lengths and angles are shown in tables 26-28.

Table 26. Experimental and calculated geometric parameters of 1,2-disilacyclohexane. Bond lengths in Å and angles and dihedral angles in °. Error limits are 3 σ values and refer to the last digit.

	GED (r_{h1})	MP2/ 6-31G(d,p)	B3LYP/ 6-311+G(2d,p)	M06-2X/ pc-2
Si-Si	2.324(4)	2.328	2.347	2.326
Si-C	1.884(3)	1.899	1.900	1.888
C3-C4	1.548(3)	1.539	1.545	1.538
C4-C5	1.544(3)	1.553	1.540	1.534
(Si-H) _{mean}	1.468(10)	1.481	1.487	1.482
(C-H) _{mean}	1.105(5)	1.094	1.095	1.093
Si1-Si2-C3	101.5(11)	101.9	102.2	101.9
Si2-C3-C4	113.8(13)	113.5	114.5	113.5
C3-C4-C5	115.8(18)	115.7	116.0	115.3
H-Si-H	108.0	108.0	107.9	108.2
(H-C-H) _{mean}	106.3(36)	106.1	105.8	106.1
τ (C6-Si1-Si2-C3)	40.5(46)	38.0	35.7	37.9
τ (Si1-Si2-C3-C4)	-49.5(28)	-47.9	-46.0	-48.0
τ (Si2-C3-C4-C5)	66.2(22)	67.0	65.8	67.5
τ (C3-C4-C5-C6)	-73.0(42)	-75.9	-75.0	-76.6

Table 27. Experimental and calculated geometric parameters of 1,3-disilacyclohexane. Bond lengths in Å and angles and dihedral angles in °. Error limits are 3σ values and refer to the last digit.

	GED (r_{hi})	MP2/ 6-31G(d,p)	B3LYP/ 6-311+G(2d,p)	M06-2X/ pc-2
Si1–C2	1.870(1)	1.883	1.885	1.873
Si1–C6	1.878(1)	1.891	1.891	1.880
C–C	1.552(4)	1.538	1.543	1.538
(Si–H) _{mean}	1.485(10)	1.482	1.486	1.482
(C–H) _{mean}	1.101(5)	1.093	1.095	1.093
Si1–C2–Si3	110.5(3)	109.2	110.0	109.1
C2–Si3–C4	109.0(16)	108.2	108.9	108.3
Si3–C4–C5	113.6(10)	113.7	114.5	113.6
C4–C5–C6	112.5(11)	113.6	114.0	113.4
H–Si–H	108.1	108.1	107.9	108.3
(H–C–H) _{mean}	105.5(23)	106.3	106.1	106.5
τ(Si1–C2–Si3–C4)	42.4(22)	45.5	43.0	45.8
τ(C2–Si3–C4–C5)	- 53.8(19)	- 54.9	- 52.9	-55.2
τ(Si3–C4–C5–C6)	66.7(17)	65.8	64.1	65.9

Table 28. Experimental and calculated geometric parameters of 1,4-disilacyclohexane. Bond lengths in Å and angles and dihedral angles in °. Error limits are 3σ values and refer to the last digit.

	GED (r_{hi})	MP2/ 6-31G(d,p)	B3LYP/ 6-311+G(2d,p)	M06-2X/ pc-2
Si–C	1.877(1)	1.892	1.893	1.881
C–C	1.559(4)	1.546	1.550	1.544
(Si–H) _{mean}	1.467(8)	1.492	1.486	1.482
(C–H) _{mean}	1.103(5)	1.097	1.095	1.093
C–Si–C	109.4(6)	108.2	108.4	108.2
Si–C–C	112.4(5)	112.2	112.9	112.1
H–Si–H	108.3	108.3	108.4	108.7
H–C–H	106.8(24)	105.9	105.8	106.1
τ(Si–C–C–Si)	56.0(6)	57.9	56.2	58.0
τ(C–C–Si–C)	- 54.4(9)	- 55.7	- 54.4	-55.8

M06-2X calculated geometric parameters do not always show the smallest deviation from the GED structure, but interestingly M06-2X predicts Si-Si and Si-C bond lengths that are considerably closer to the GED values than the B3LYP and MP2 calculations.

The three disilacyclohexanes are configurational isomers and differ specifically in the distance between the silicon atoms. 1,2-disilacyclohexane also differs from the other isomers by the number of different bonds, table 29.

Table 29. The bond skeleton of the disilacyclohexanes. Number of different bonds.

	C-C	Si-C	Si-Si
1,2-disilacyclohexane	3	2	1
1,3-disilacyclohexane	2	4	0
1,4-disilacyclohexane	2	4	0

In table 2, in the introduction of this thesis, the bond energies of organosilicon compounds are listed. The Si-C bond is a slightly weaker bond than the C-C bond (75 kcal/mol vs. 80 kcal/mol). The Si-Si bond is much weaker with a bond energy of 47 kcal/mol.

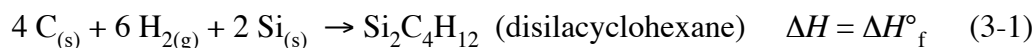
We were interested in knowing the different enthalpies of formation of the disilacyclohexanes, the enthalpy of formation being a measure of stability. It is possible to calculate enthalpies of formation of organic molecules by a simple group increment method that assumes that bond energies are roughly additive. This method holds while the molecules are relatively strain-free (a highly strained molecule like cyclopropane shows, for example, significant deviation between its group increment ΔH_f° and the experimental ΔH_f°) [2]. A six-membered ring is, as mentioned in the introduction, almost strain-free. Unfortunately, group increments for organosilicon groups are not available.

By inspection of the above mentioned bond energies, we might guess, that 1,2-disilacyclohexane would be less stable than the other disilacyclohexanes due to the low bond energy of the Si-Si bond. 1,3-disilacyclohexane and 1,4-disilacyclohexane have the same number of bonds, however, and should by this very rough model have a similar ΔH_f° .

We decided to calculate the enthalpies of formation for the disilacyclohexanes by quantum chemical calculations. The enthalpy of formation of a molecule is essentially

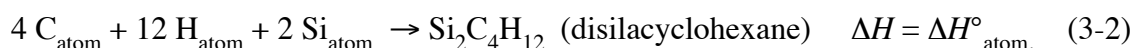
the reaction energy (enthalpy change) of the elements in their standard state reacting to form the molecule in question.

We are thus interested in the reaction energy of this reaction.



This reaction energy is obviously not calculated directly, as calculating an infinite graphite or silicon surface is not practical. The enthalpies of formation for the reactants in the above equation are all zero by definition. To calculate the enthalpy of formation of the product we need to relate the above reactants to something we can calculate.

The atomization enthalpy of a reaction is an easier equation to deal with:



The equation for the atomization enthalpy can then be given as:

$$\Delta H^\circ_{\text{atom.}} = H(\text{Si}_2\text{C}_4\text{H}_{12}) - [4H(\text{C}) + 12 H(\text{H}) + 2H(\text{Si})] \quad (3-3)$$

The enthalpies of formation of the atoms is then what you need to relate the atoms to the elements in their standard states. They have been obtained from experiment. A diagram that explains the whole calculation is shown in figure 31.

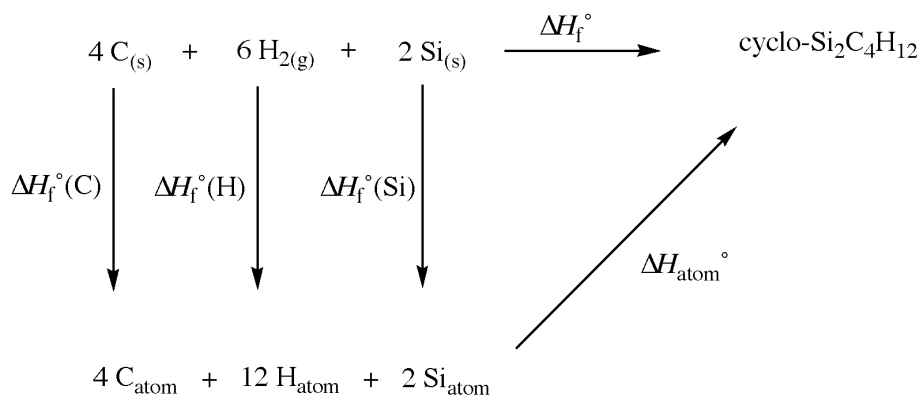


Figure 31. Diagram for the calculation of enthalpies of formation of the disilacyclohexanes.

The final equation to get the enthalpy of formation of a molecule is then:

$$\Delta H_{\text{atom}}^{\circ} = \Delta H_{\text{f}}^{\circ}(\text{Si}_2\text{C}_4\text{H}_{12}) - [4\Delta H_{\text{f}}^{\circ}(\text{C}) + 12\Delta H_{\text{f}}^{\circ}(\text{H}) + 2\Delta H_{\text{f}}^{\circ}(\text{Si})] \quad (3-4)$$

The quantities that need to be calculated by quantum mechanics are then the enthalpy of the molecule and the enthalpies of the single atoms silicon, carbon and hydrogen, all at the same level of theory.

The geometries of disilacyclohexanes thus need to be optimized and then a single-point energy calculation as well as a frequency calculation to get the thermal correction to enthalpy (including zero-point energy).

The individual atoms need to be calculated at the same level of theory, i.e. a single-point energy and $H^{\text{corr}} = 5/2RT$ added.

Calculating enthalpies of formation of molecules can be very hard for quantum chemical calculations. In fact it is one of the hardest quantities to calculate, due to the immense change in electronic structure, from free atoms to covalent molecules.

Recently, it has been pointed out that calculating energies of free atoms might be one of the main weaknesses of DFT [68].

We tried out several different calculations: the composite methods G3B3 and CBS-QB3, MP2 calculations and the DFT functional B3LYP.

All methods agree on the ordering of stability of the disilacyclohexanes and the relative energies are quite close for all methods (table 31) but there is significant disagreement in the absolute values (table 30).

Table 30. Calculated enthalpies of formation for the disilacyclohexanes using different methods. Values in kcal/mol.

	G3B3	CBS	MP2/aug-cc-pVTZ	B3LYP/aug-cc-pVTZ
1,2	-0.8	-1.2	-17.4	+21.1
1,3	-15.1	-16.2	-32.8	+8.9
1,4	-9.2	-10.3	-27.2	+14.2

Table 31. Relative enthalpy differences for the disilacyclohexanes with respect to 1,3-disilacyclohexane. Values in kcal/mol.

	G3B3	CBS	MP2/aug-cc-pVTZ	B3LYP/aug-cc-pVTZ
1,2	+14.3	+15.0	+15.4	+12.2
1,3	0	0	0	0
1,4	+5.9	+5.9	+5.6	+5.3

Like expected, 1,2-disilacyclohexane is the least stable of the disilacyclohexanes. However, 1,3-disilacyclohexane is also substantially more stable than the 1,4-disilacyclohexane which is quite interesting as both molecules contain the same number of different bonds. Clearly the closer distance between silicons in 1,3-disilacyclohexane plays a role in the overall stability.

The G3B3 and CBS-QB3 calculations are in very good agreement (for both absolute and relative enthalpy differences) and we expect these values to be more accurate than the MP2 and DFT calculations as the composite methods are designed for very accurate computation of properties like enthalpies of formation.

3.4 NMR spectra and attempted simulation

The disilacyclohexanes are simple molecules. Yet, their ^1H NMR spectra have proven difficult to analyze. The spectra indicate strong second order coupling that makes analysis troublesome. Spectral analysis of complicated NMR spectra usually involves simulation with iteration methods where the parameters of a calculated spectrum are gradually changed in order to converge with the experimental spectrum. Traditionally, LAOCOON^{xv} spectral analysis has been used while Gudnason used gNMR 4.1^{xvi} for simulation of 1,3-disilacyclohexane [24].

As the calculated conformational energy surfaces of the compounds showed, low-lying transition states (4-6 kcal/mol) between conformers are characteristic for these compounds and low-lying twist conformers as minima and boat conformers as saddlepoints, are found on the potential energy surface. The low activation energy for the chair-chair inversion indicates a very dynamic system at room temperature.

Dynamic spin-systems are often simplified by measuring the NMR spectra at lower or higher temperature. Such a temperature analysis has been carried out from -90°C to +90°C in a toluene solution. No difference between spectra was detected, however. Judging from the NMR experiments and the DFT-calculations, the rings must be in a fast

^{xv} <http://qcpe.chem.indiana.edu> : QCPE 111

^{xvi} <http://www.adeptscience.co.uk/products/lab/gnmr/>

equilibrium between the conformers and couplings in the NMR spectra are average values of the couplings in the different conformers.

The simulation of a complicated NMR spectrum involves solving the non-linear equations [134]:

$$\begin{aligned} F_1(\nu, J, D, \Delta) &= O_1 \\ F_2(\nu, J, D, \Delta) &= O_2 \\ &\dots \\ F_n(\nu, J, D, \Delta) &= O_n \end{aligned} \quad (3-5)$$

where ν is the chemical shift, J the scalar coupling vector, D the dipolar coupling vector and Δ includes the linewidth and a few lineshape terms: i.e. Lorentzian contribution, normal dispersion and Gaussian. These equations are solved by iteration procedures, and in the case of LAOCOON analysis they would be solved by a plain Gauss-Newton type algorithm.

The Integral-Transform (IT) procedure [134] involves first transforming the NMR data into integral transforms that are fast to compute and differentiate. The frequency domain is multiplied with a set of basis functions, $f_i(\nu)$ and each product integrated to produce a set of integral transforms:

$$IT_i = \int f_i(\nu) I(\nu) d\nu \quad (3-6)$$

The integral transforms are then used as solutions to the non-linear equations above. The basis functions, $f_i(\nu)$, are A-shaped functions, $A(\nu_i, \text{SPAN})$ where ν_i is the midpoint of the A-function and SPAN the width of the function. By setting SPAN high in the beginning of the procedure (splittings are then completely dissolved) and then gradually decreasing until the IT spectrum approaches the original one, one gets good convergent behavior as demonstrated by Laatikainen et al. [134].

Using adequate starting parameters (chemical shifts and coupling constants) the IT-procedure can usually find a good solution for 2-14 spins.

Total-Line-Shape-fitting (TLS) [135] is another iteration procedure that involves changing the Δ parameter as well as fine-tuning of the couplings. It requires very good starting parameters and is typically performed after the IT-procedure if a good simulation, of a system that involves abnormal lineshape, is required. The IT and TLS

procedures are implemented in the program Perch^{xvii} and are available also as add-ons to the Topspin NMR software from Bruker-Biospin^{xviii}.

The experimental spectra (400 MHz ¹H NMR in toluene-d₈) was imported into the program Perch, Fourier-transformed, phase-corrected, baseline-corrected and solvent peaks were deleted. The experimental spectrum generally must be well prepared for a simulation to be successful [134]. The lineshape was then estimated. Based on the structure of the molecule one can obtain adequate starting parameters. DFT-optimized structures were used and starting parameters obtained by a simple empirical procedure in Perch. Perch also includes parameter estimation in combination with a molecular dynamics simulation that can give averaged parameters from several conformers. Even though the starting parameters are very crude (chemical shifts especially) the IT procedure appears to find a solution very quickly, fixes the chemical shifts and then moves on to tuning the coupling constants. The simulation was considered successful when the RMS% < 20 %.

A Total-Line-Shape analysis was then performed using the IT parameters which was of importance in order to obtain spectra with the correct lineshape.

The results of the simulations are shown in the following tables and figures.

^{xvii} Perch NMR Software: <http://www.perchsolutions.com>

^{xviii} <http://www.bruker-biospin.com/topspin.html>

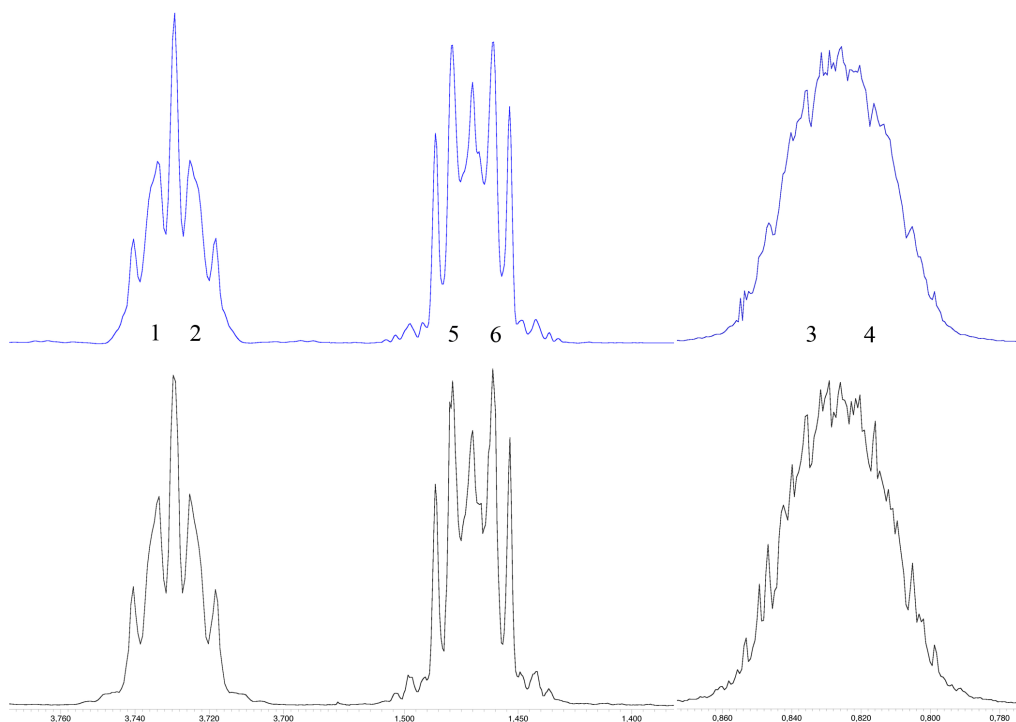


Figure 32. Measured (below) and simulated (above) spectrum of 1,2-disilacyclohexane.

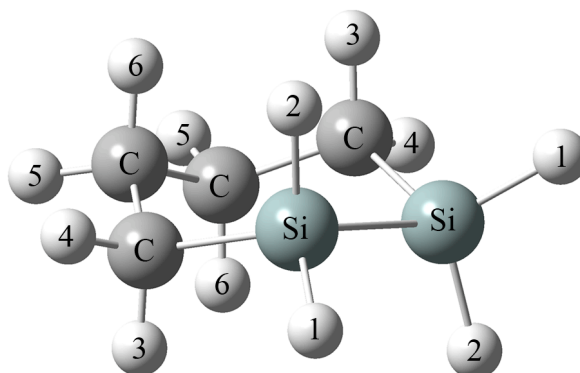


Figure 33. Ball-and-stick model of 1,2-disilacyclohexane with atom numbering used in simulation.

Table 32. Simulated coupling constants and linewidths of 1,2-disilacyclohexane in Hz.

Coupling constants (Hz)	1	2	3	4	5	6	Linewidth (Hz)
1	0.0	13.700	0.0	0.0	0.0	0.0	0.024
2	-18.101	0.004	14.667	6.419	0.0	0.0	1.433
3	0.119	0.0	0.0	0.0	0.0	0.0	4.924
4	0.0	0.0	0.0	0.0	2.817	0.0	0.384
5	0.0	0.0	0.001	4.160	0.156	-10.574	0.618
6	0.0	0.0	0.404	8.125	4.378	3.664	5.854

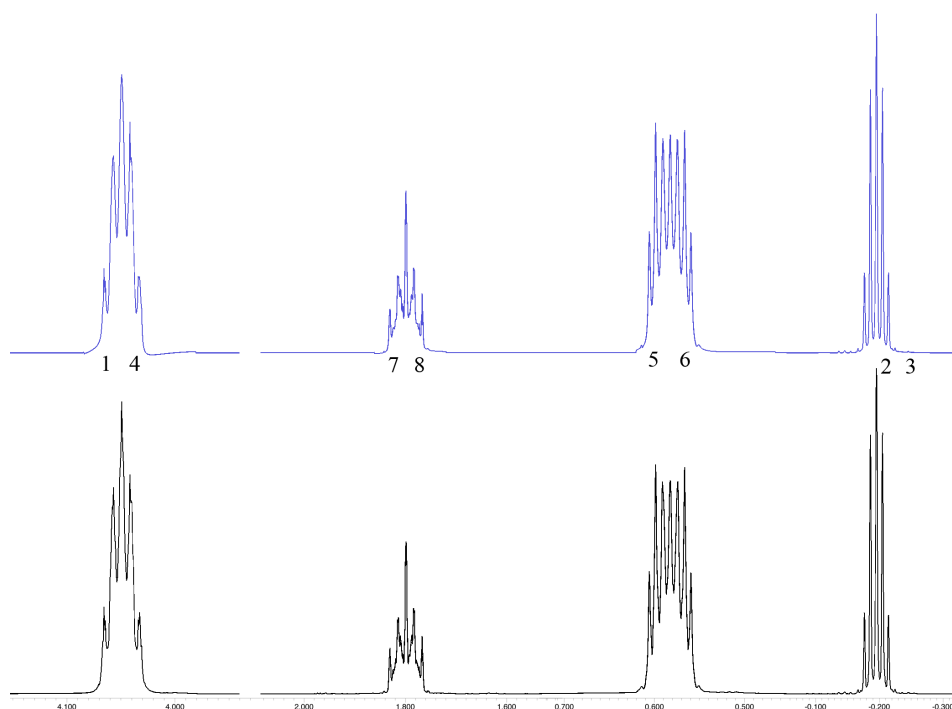


Figure 34. Measured (below) and simulated (above) spectrum of 1,3-disilacyclohexane.

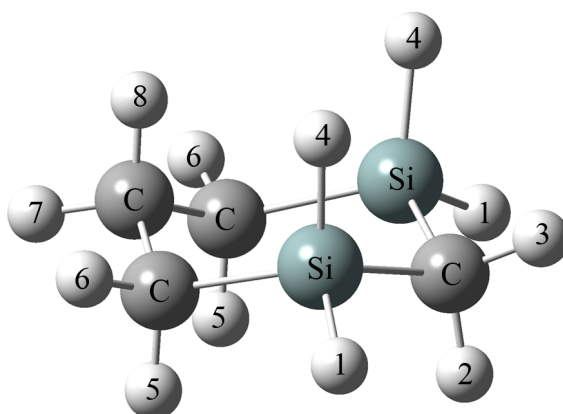


Figure 35. Ball-and-stick model of 1,3-disilacyclohexane with atom numbering used in simulation.

Table 33. Simulated coupling constants and linewidths of 1,3-disilacyclohexane in Hz.

Coupling constants (Hz)	1	2	3	4	5	6	7	8	Linewidth (Hz)
1	0.0	4.050	3.427	0.0	3.624	1.532	0.0	0.0	0.377
2	4.050	-	-6.684	3.459	0.0	0.0	0.0	0.0	0.868
3	3.427	-6.684	-	4.034	0.0	0.0	0.0	0.0	0.860
4	-6.509	3.459	4.034	0.0	0.0	0.0	0.0	0.0	2.877
5	0.0	0.0	0.0	1.425	0.0	-0.406	3.090	9.836	2.080
6	0.0	0.0	0.0	4.509	0.0	-0.479	10.188	2.694	0.317
7	0.0	0.0	0.0	0.0	3.090	10.188	-	-8.086	1.671
8	0.0	0.0	0.0	0.0	9.836	2.694	2.694	-	1.604

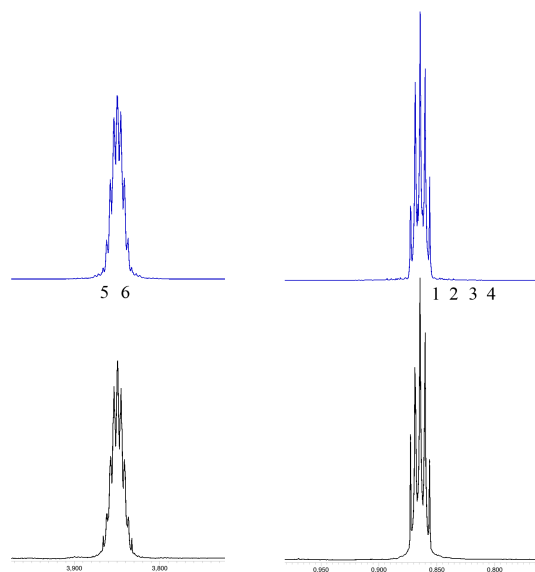


Figure 36. Measured (below) and simulated (above) spectrum of 1,4-disilacyclohexane.

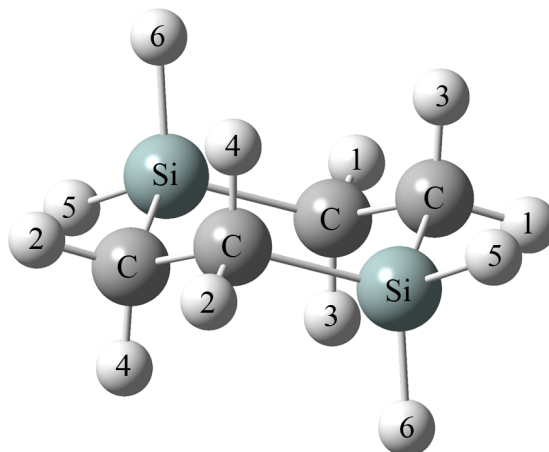


Figure 37. Ball-and-stick model of 1,4-disilacyclohexane with atom numbering used in simulation.

Table 34. Simulated coupling constants and linewidths in Hz.

Coupling constants (Hz)	1	2	3	4	5	6	Linewidth (Hz)
1	3.569	0.0	2.847	0.0	2.527	3.760	0.117
2	0.0	15.765	0.0	-8.891	4.754	2.629	0.434
3	-3.117	0.0	12.780	0.0	0.0	0.0	0.806
4	0.0	1.244	0.0	12.300	0.960	4.952	0.103
5	0.0	0.0	3.824	0.0	0.0	-10.049	0.479
6	0.0	0.0	2.905	0.0	0.0	0.0	0.355

While the simulated spectra look very much like the experimental spectra, the NMR simulation of the disilacyclohexanes continue to be a work in progress. Due to a bug in the program, the correct symmetry of 1,4-disilacyclohexane cannot be given, thus resulting in a wrong solution of the spin-system. Furthermore the coupling constants of 1,2- and 1,3-disilacyclohexanes show indications of wrong solutions and need to be critically evaluated to make sure that the correct solutions have been found. These simulations thus appear to be incomplete.

Summary

In this thesis, computational studies were carried out with the intent of calculating accurate conformational energy differences of substituted six-membered heterocycles, as an alternative to experiment. The computational strategy was used to predict conformational properties of silacyclohexanes that are currently out of reach for experimental methods.

The work done, while related to silacyclohexanes in general, can be summarized into three major themes, that are described below.

1. Calculating accurate conformational energies of substituted six-membered rings with computational methods that were critically evaluated:

We compared a few density functionals for conformational energy differences of 13 different monosubstituted six-membered rings and by comparing mean absolute deviations from accurate CCSD(T) values, we were able to show that recent functionals M06-2X and B2PLYP-D, are much more accurate than functionals like B3LYP for this kind of conformational analysis. Both functionals have in common, that they were intended to include a better description of medium-range correlation and it seems likely that this is the reason for the better performance. Basis sets were compared and systematic basis set expansion using e.g. the polarization-consistent basis sets was found to suit quite well for achieving converged relative energies. By comparing calculated geometries of the axial conformer of two silacyclohexanes with recent gas electron diffraction results, there is data to suggest that M06-2X and B2PLYP-D predict bond lengths that are closer to the experimental bond lengths for silacyclohexane systems. By calculating harmonic frequencies we could relate the electronic energy difference to recent experimental enthalpy and free energy differences of 1-silacyclohexanes and the comparison is quite favorable overall, although the question of the reliability of the harmonic approximation arises.

2. Mapping the conformational properties of silacyclohexanes systematically by step-by-step silicon substitution on the cyclohexane ring, with an accurate yet affordable computational method:

Using one of the computational methods, that we showed to be capable of predicting quite accurate conformational energy differences of cyclohexanes and heterocycles with one heteroatom, we calculated a considerable number of different silacyclohexanes, with silicon in differing positions and numbers, and with several different substituents. Our predictions suggest remarkably different conformational properties of several silacyclohexane families compared to cyclohexanes and other heterocycles, even more than for the 1-silacyclohexane family. A study of geometric parameters of all these silacyclohexane families and attempt to identify the dominating effects behind the conformational properties would be a highly interesting future study.

3. Investigating the structure, stability, magnetic resonance spectra and potential energy surfaces of the parent disilacyclohexanes:

Former graduate student Pálmar Guðnason, successfully synthesized the parent disilacyclohexanes and described the potential energy surfaces of the molecules. We contributed some additional calculations to this work.

The lowest energy pathways of chair-chair ring inversion were recalculated, using a reliable saddle-point locating technique implemented in Gaussian [28] and single-point energy calculations with M06-2X/pc-3 were carried out on stationary points.

Recent gas electron diffraction structural data of the disilacyclohexanes was compared to M06-2X/pc-2 calculated data. Calculations of enthalpies of formations of the molecules were carried out with interesting results.

We attempted simulation of the ^1H NMR spectra of the parent disilacyclohexanes, that have proven difficult to analyze. While we succeeded in obtaining simulated spectra that by visual inspection appear to be very close to the measured spectra, the parameters of the spin systems suggest that there is still work to be done.

References

- [1] Eliel, E. L. In *Conformational behavior of six-membered rings: analysis, dynamics, and stereoelectronic effects*; Juaristi, E., Ed.; VCH Publishers: New York, 1995; pp 19-20.
- [2] E. V. Anslyn, D. A. Dougherty, *Modern physical organic chemistry* (University Science, 2006), pp. 82-110.
- [3] Cremer, D., K. J. Szabo, In *Conformational behavior of six-membered rings: analysis, dynamics, and stereoelectronic effects*; Juaristi, E., Ed.; VCH Publishers: New York, 1995; pp 71-77.
- [4] Arnason, I.; Kvaran, A.; Bodi, A. *Int. J. Quantum. Chem.* **2006**, *106*, 1975-8.
- [5] Bushweller, C. H. In *Conformational behavior of six-membered rings: analysis, dynamics, and stereoelectronic effects*; Juaristi, E., Ed.; VCH Publishers: New York, 1995; pp 28-32.
- [6] J. D. Roberts, M. C. Caserio, *Basic principles of organic chemistry* (W. A. Benjamin, New York, 1964), pp. 453-457.
- [7] Franck, R. W. In *Conformational behavior of six-membered rings: analysis, dynamics, and stereoelectronic effects*; Juaristi, E., Ed.; VCH Publishers: New York, 1995; pp 181-188.
- [8] Vila, A.; Mosquera, R. A. *J. Comput. Chem.* **2007**, *28*, 1516-30.
- [9] Eskandari, K.; Vila, A.; Mosquera, R. A. *J. Phys. Chem. A* **2007**, *111*, 8491-9.
- [10] Kleinpeter, E. *Adv. Heterocycl. Chem.* **2004**, *86*, 41-127.
- [11] G. Fritz, E. Matern, *Carbosilanes: syntheses and reactions* (Springer-Verlag, New York, 1986), pp. 1-2.
- [12] Ohno, K.; Matsuura, H.; Endo, Y.; Hirota, E. *J. Mol. Spectrosc.* **1986**, *118*, 1-17.
- [13] Cordero, B.; Gomez, V.; Platero-Prats, A. E.; Reves, M.; et al. *Dalton. T.* **2008**, *21*, 2832-8.
- [14] Arnason, I. *Z. Anorg. Allg. Chem.* **1998**, *624*, 1973-6.
- [15] Arnason, I.; Kvaran, A. *Z. Anorg. Allg. Chem.* **1998**, *624*, 65-73.
- [16] Arnason, I. *Z. Anorg. Allg. Chem.* **1999**, *625*, 97-101.
- [17] Arnason, I.; Matern, E. *J. Mol. Struct:Theochem* **2001**, *544*, 61-8.
- [18] Arnason, I.; Thorarinsson, G. K.; Matern, E. *J. Mol. Struct:Theochem* **1998**, *454*, 91-102.

- [19] Arnason, I.; Oberhammer, H. *J. Mol. Struct.* **2001**, 598, 245-50.
- [20] Arnason, I.; Thorarinsson, G. K.; Matern, E. *Z. Anorg. Allg. Chem.* **2000**, 626, 853-62.
- [21] Arnason, I.; Kvaran, A.; Jonsdottir, S.; Gudnason, P. I.; Oberhammer, H. *J. Org. Chem.* **2002**, 67, 3827-31.
- [22] Girichev, G. V.; Giricheva, N. I.; Bodi, A.; Gudnason, P. I.; et al. *Chem. - Eur. J.* **2007**, 13, 1776-83.
- [23] Wallevik, S. O. *Conformational behavior of substituted silacyclohexanes*, M.Sc. thesis, University of Iceland, 2008.
- [24] Gudnason, P. I. *Kísilinnihaldandi sexhringir*, M.Sc. thesis, University of Iceland, 2003.
- [25] Klaeboe, P. *Vib. Spectrosc.* **1995**, 9, 3-17.
- [26] Halgren, T. A. *J. Comput. Chem.* **1999**, 20, 730-48.
- [27] Leininger, M. L.; Allen, W. D.; Schaefer III, H. F.; Sherrill, C. D. *J. Chem. Phys.* **2000**, 112, 9213.
- [28] Frisch, M. J., Trucks, G. W., Schlegel, H. B., Scuseria, G. E., Robb, M. A., Cheeseman, J. R., Montgomery, J., A., J., Vreven, T., Kudin, K. N., Burant, J. C., Millam, J. M., Iyengar, S. S., Tomasi, J., Barone, V., Mennucci, B., Cossi, M., Scalmani, G., Rega, N., Petersson, G. A., Nakatsuji, H., Hada, M., Ehara, M., Toyota, K., Fukuda, R., Hasegawa, J., Ishida, M., Nakajima, T., Honda, Y., Kitao, O., Nakai, H., Klene, M., Li, X., Knox, J. E., Hratchian, H. P., Cross, J. B., Bakken, V., Adamo, C., Jaramillo, J., Gomperts, R., Stratmann, R. E., Yazyev, O., Austin, A. J., Cammi, R., Pomelli, C., Ochterski, J. W., Ayala, P. Y., Morokuma, K., Voth, G. A., Salvador, P., Dannenberg, J. J., Zakrzewski, V. G., Dapprich, S., Daniels, A. D., Strain, M. C., Farkas, O., Malick, D. K., Rabuck, A. D., Raghavachari, K., Foresman, J. B., Ortiz, J. V., Cui, Q., Baboul, A. G., Clifford, S., Cioslowski, J., Stefanov, B. B., Liu, G., Liashenko, A., Piskorz, P., Komaromi, I., Martin, R. L., Fox, D. J., Keith, T., Al-Laham, M. A., Peng, C. Y., Nanayakkara, A., Challacombe, M., Gill, P. M. W., Johnson, B., Chen, W., Wong, M. W., Gonzalez, C., Pople, J. A. *Gaussian 03*, revision C.02; Gaussian, Inc.: Pittsburgh, PA, 2003.
- [29] Curtiss, L. A.; Raghavachari, K.; Redfern, P. C.; Rassolov, V.; Pople, J. A. *J. Chem. Phys.* **1998**, 109, 7764.

- [30] Baboul, A. G.; Curtiss, L. A.; Redfern, P. C.; Raghavachari, K. *J. Chem. Phys.* **1999**, *110*, 7650.
- [31] Montgomery Jr, J. A.; Frisch, M. J.; Ochterski, J. W.; Petersson, G. A. *J. Chem. Phys.* **1999**, *110*, 2822.
- [32] Montgomery Jr, J. A.; Frisch, M. J.; Ochterski, J. W.; Petersson, G. A. *J. Chem. Phys.* **2000**, *112*, 6532.
- [33] Hohenberg, P.; Kohn, W. *Phys. Rev.* **1964**, *136*, B864-71.
- [34] Kohn, W.; Sham, L. J. *Phys. Rev.* **1965**, *140*, A1133-8.
- [35] W. Koch, M. C. Holthausen, *A chemist's guide to density functional theory* (Wiley-VCH, New York, 2001), pp. 3-91.
- [36] Stephens, P. J.; Devlin, F. J.; Chabalowski, C. F.; Frisch, M. J. *J. Phys. Chem.* **1994**, *98*, 11623-7.
- [37] Sousa, S. F.; Fernandes, P. A.; Ramos, M. J. *J. Phys. Chem. A* **2007**, *111*, 10439-52.
- [38] Tirado-Rives, J.; Jorgensen, W. L. *J. Chem. Theory. Comp.* **2008**, *4*, 297-306.
- [39] Perdew, J. P., K. Schmidt, In *Density Functional Theory and Its Applications to Materials*, Van Doren, V., Van Alsenoy, C., Geerlings, P., Eds. American Institute of Physics: New York, 2001.
- [40] Kendall, R. A.; Aprà, E.; Bernholdt, D. E.; Bylaska, E. J.; et al. *Comp. Phys. Comm.* **2000**, *128*, 260-83.
- [41] Riley, K. E.; Op' t Holt, B. T.; Merz Jr, K. M. *J. Chem. Theory. Comp.* **2007**, *3*, 407-33.
- [42] Kaminsky, J.; Jensen, F. *J. Chem. Theory. Comp.* **2007**, *3*, 1774-88.
- [43] Dunning, T. H. *J. Chem. Phys.* **1989**, *90*, 1007-23.
- [44] Woon, D. E.; Dunning, T. H. *J. Chem. Phys.* **1993**, *98*, 1358-71.
- [45] Boese, A. D.; Martin, J. M. L.; Handy, N. C. *J. Chem. Phys.* **2003**, *119*, 3005.
- [46] Dunning, T. H.; Peterson, K. A.; Wilson, A. K. *J. Chem. Phys.* **2001**, *114*, 9244-53.
- [47] Jensen, F. *J. Chem. Phys.* **2001**, *115*, 9113-25.
- [48] Jensen, F. *J. Chem. Phys.* **2002**, *116*, 7372-9.
- [49] Jensen, F. *J. Chem. Phys.* **2002**, *117*, 9234-40.
- [50] Jensen, F. *J. Chem. Phys.* **2003**, *118*, 2459-63.
- [51] Jensen, F.; Helgaker, T. *J. Chem. Phys.* **2004**, *121*, 3463-70.
- [52] Jensen, F. *Chem. Phys. Lett.* **2005**, *402*, 510-3.
- [53] Jensen, F. *Theor. Chem. Acc.* **2005**, *113*, 267-73.

- [54] Jensen, F. *J. Phys. Chem. A* **2007**, *111*, 11198-204.
- [55] Jensen, F. *J. Chem. Phys.* **1999**, *110*, 6601.
- [56] Christensen, K. A.; Jensen, F. *Chem. Phys. Lett.* **2000**, *317*, 400-3.
- [57] Kutzelnigg, W.; Morgan III, J. D. *J. Chem. Phys.* **1992**, *96*, 4484.
- [58] Wang, N. X.; Wilson, A. K. *J. Chem. Phys.* **2004**, *121*, 7632-46.
- [59] Wang, N. X.; Wilson, A. K. *Mol. Phys.* **2005**, *103*, 345-58.
- [60] Wang, N. X.; Venkatesh, K.; Wilson, A. K. *J. Phys. Chem. A* **2006**, *110*, 779-84.
- [61] Prascher, B. P.; Wilson, B. R.; Wilson, A. K. *J. Chem. Phys.* **2007**, *127*, -.
- [62] Prascher, B. P.; Wilson, A. K. *Mol. Phys.* **2007**, *105*, 2899-917.
- [63] C. J. Cramer, *Essentials of computational chemistry : theories and models* (Wiley, 2004, Chichester , 2004), pp. 596.
- [64] Grimme, S.; Steinmetz, M.; Korth, M. *J. Org. Chem.* **2007**, *72*, 2118-26.
- [65] Check, C. E.; Gilbert, T. M. *J. Org. Chem.* **2005**, *70*, 9828-34.
- [66] Wodrich, M. D.; Corminboeuf, C.; Schleyer, P. V. *Org. Lett.* **2006**, *8*, 3631-4.
- [67] Schreiner, P. R.; Fokin, A. A.; Pascal, R. A.; de Meijere, A. *Org. Lett.* **2006**, *8*, 3635-8.
- [68] Csonka, G. I.; Ruzsinszky, A.; Tao, J.; Perdew, J. P. *Int. J. Quantum. Chem.* **2005**, *101*, 506-11.
- [69] Grimme, S. *Angew. Chem. Int. Ed. Engl.* **2006**, *45*, 4460-4.
- [70] Schreiner, P. R. *Angew. Chem. Int. Ed. Engl.* **2007**, *46*, 4217-9.
- [71] C. E. Dykstra, *Theory and applications of computational chemistry : the first forty years* (Elsevier, Amsterdam ; Boston , 2005).
- [72] Zhao, Y.; Truhlar, D. G. *Acc. Chem. Res.* **2008**, *41*, 157-67.
- [73] Zhao, Y.; Truhlar, D. G. *Theor. Chem. Acc.* **2008**, *120*, 215-41.
- [74] Zhao, Y.; Truhlar, D. G. *J. Chem. Theory. Comp.* **2007**, *3*, 289-300.
- [75] Zhao, Y.; Truhlar, D. G. *Org. Lett.* **2006**, *8*, 5753-5.
- [76] Grimme, S. *J. Chem. Phys.* **2006**, *124*, 034108.
- [77] Schwabe, T.; Grimme, S. *Phys. Chem. Chem. Phys.* **2006**, *8*, 4398-401.
- [78] Neese, F.; Schwabe, T.; Grimme, S. *J. Chem. Phys.* **2007**, *126*, 124115.
- [79] Schwabe, T.; Grimme, S. *Phys. Chem. Chem. Phys.* **2007**, *9*, 3397-406.
- [80] Grimme, S. *J. Comput. Chem.* **2004**, *25*, 1463-73.
- [81] Grimme, S. *J. Comput. Chem.* **2006**, *27*, 1787-99.
- [82] Schwabe, T.; Grimme, S. *Acc. Chem. Res.* **2008**, *41*, 569-79.

- [83] Papas, B. N.; Schaefer, H. F. *J. Mol. Struct:Theochem.* **2006**, 768, 175-81.
- [84] Weldon, A. J.; Tschumper, G. S. *Int. J. Quantum. Chem.* **2007**, 107, 2261-5.
- [85] Weldon, A. J.; Vickrey, T. L.; Tschumper, G. S. *J. Phys. Chem. A.* **2005**, 109, 11073-9.
- [86] Parthiban, S.; Martin, J. M. L. *J. Chem. Phys.* **2001**, 115, 2051.
- [87] Pollack, L.; Windus, T. L.; de Jong, W. A.; Dixon, D. A. *J. Phys. Chem. A.* **2005**, 109, 6934-8.
- [88] Weigend, F.; Ahlrichs, R. *Phys. Chem. Chem. Phys.* **2005**, 7, 3297-305.
- [89] Eichkorn, K.; Weigend, F.; Treutler, O.; Ahlrichs, R. *Theor. Chem. Acc.* **1997**, 97, 119-24.
- [90] Weigend, F.; Haser, M.; Patzelt, H.; Ahlrichs, R. *Chem. Phys. Lett.* **1998**, 294, 143-52.
- [91] Woodcock, H. L.; Moran, D.; Pastor, R. W.; MacKerell, A. D.; Brooks, B. R. *Biophys. J.* **2007**, 93, 1-10.
- [92] Tvaroska, I.; Carver, J. P. *J. Phys. Chem.* **1994**, 98, 9477-85.
- [93] Tvaroska, I.; Carver, J. P. *Carbohydr. Res.* **1998**, 309, 1-9.
- [94] McCaffrey, P. D.; Mawhorter, R. J.; Turner, A. R.; Brain, P. T.; Rankin, D. W. H. *J. Phys. Chem. A.* **2007**, 111, 6103-14.
- [95] Stewart, J. J. *J. Mol. Model.* **2007**, 13, 1173-213.
- [96] Bodi, A.; Kvaran, A.; Jonsdottir, S.; Antonsson, E.; et al. *Organometallics.* **2007**, 26, 6544-50.
- [97] Skylaris, C. K.; Gagliardi, L.; Handy, N. C.; Ioannou, A. G.; et al. *J. Mol. Struct:Theochem.* **2000**, 501, 229-39.
- [98] Franco, M. L.; Ferreira, D. E. C.; Dos Santos, H. F.; De Almeida, W. B. *J. Chem. Theory. Comp.* **2008**, 728-39.
- [99] Ferreira, D. E. C.; De Almeida, W. B.; Dos Santos, H. F. *J. Chem. Theory. Comp.* **2007**, 6, 281-99.
- [100] Franco, M. L.; Ferreira, D. E. C.; Dos Santos, H. F.; De Almeida, W. B. *Int. J. Quantum. Chem.* **2007**, 107, 545-55.
- [101] Dos Santos, H. F.; Rocha, W. R.; De Almeida, W. B. *Chem. Phys.* **2002**, 280, 31-42.
- [102] Anconi, C. P. A.; Nascimento, C. S.; Dos Santos, H. F.; De Almeida, W. B. *Chem. Phys. Lett.* **2006**, 418, 459-66.

- [103] Ayala, P. Y.; Schlegel, H. B. *J. Chem. Phys.* **1998**, *108*, 2314.
- [104] Barone, V. *J. Chem. Phys.* **2004**, *120*, 3059-65.
- [105] Miller III, T. F.; Clary, D. C. *J. Chem. Phys.* **2003**, *119*, 68.
- [106] Miller, T. F.; Clary, D. C. *Mol. Phys.* **2005**, *103*, 1573-8.
- [107] Glaesemann, K. R.; Fried, L. E. *J. Chem. Phys.* **2005**, *123*, 34103.
- [108] Chempath, S.; Predescu, C.; Bell, A. T. *J. Chem. Phys.* **2006**, *124*, 234101.
- [109] Merrick, J. P.; Moran, D.; Radom, L. *J. Phys. Chem. A* **2007**, *111*, 11683-700.
- [110] Mierts, S.; Scrocco, E.; Tomasi, J. *Chem. Phys.* **1981**, *55*, 117-29.
- [111] Cossi, M.; Barone, V.; Cammi, R.; Tomasi, J. *Chem. Phys. Lett.* **1996**, *255*, 327-35.
- [112] Foresman, J. B.; Keith, T. A.; Wiberg, K. B.; Snoonian, J.; Frisch, M. J. *J. Phys. Chem.* **1996**, *100*, 16098-104.
- [113] Tomasi, J.; Mennucci, B.; Cammi, R. *Chem. Rev.* **2005**, *105*, 2999-3093.
- [114] Cramer, C. J.; Truhlar, D. G. *Acc. Chem. Res.* **2008**, *41*, 760-8.
- [115] Goodman, L.; Sauers, R. R. *J. Chem. Theory. Comput.* **2005**, *1*, 1185-92.
- [116] Pophristic, V.; Goodman, L. *Nature* **2001**, *411*, 565-8.
- [117] Bickelhaupt, F. M.; Baerends, E. J. *Angew. Chem. Int. Ed. Engl.* **2003**, *42*, 4183-8; discussion 4188-94.
- [118] Weinhold, F. *Angew. Chem. Int. Ed.* **2003**, *42*, 4188-94.
- [119] Mo, Y.; Gao, J. *Acc. Chem. Res.* **2007**, *40*, 113-9.
- [120] Wiberg, K. B.; Hammer, J. D.; Castejon, H.; Bailey, W. F.; et al. *J. Org. Chem.* **1999**, *64*, 2085-95.
- [121] Ribeiro, D. S.; Rittner, R. *J. Org. Chem.* **2003**, *68*, 6780-7.
- [122] Cortés-Guzmán, F.; Hernández-Trujillo, J.; Cuevas, G. *J. Phys. Chem. A* **2003**, *107*, 9253-6.
- [123] Taddei, F.; Kleinpeter, E. *J. Mol. Struct:Theochem.* **2004**, *683*, 29-41.
- [124] Taddei, F.; Kleinpeter, E. *J. Mol. Struct:Theochem.* **2005**, *718*, 141-51.
- [125] Reed, A. E.; Weinstock, R. B.; Weinhold, F. *J. Chem. Phys.* **1985**, *83*, 735-46.
- [126] Alabugin, I. V.; Zeidan, T. A. *J. Am. Chem. Soc.* **2002**, *124*, 3175-85.
- [127] Alabugin, I. V. *J. Org. Chem.* **2000**, *65*, 3910-9.
- [128] Alabugin, I. V.; Manoharan, M.; Zeidan, T. A. *J. Am. Chem. Soc.* **2003**, *125*, 14014-31.
- [129] Santos, F. P.; Tormena, C. F. *J. Mol. Struct:Theochem.* **2006**, *763*, 145-8.
- [130] Mo, Y.; Song, L.; Lin, Y. *J. Phys. Chem. A* **2007**, *111*, 8291-301.

- [131] Bader, R. F. W. *Chem. Rev.* **1991**, *91*, 893-928.
- [132] Gudnason, P.; Arnason, I. *Org. Lett.* , Manuscript in preparation.
- [133] Peng, C. Y.; Schlegel, H. B. *Israel. J. Chem.* **1993**, *33*, 449-54.
- [134] Laatikainen, R.; Niemitz, M.; Weber, U.; Sundelin, J.; et al. *J. Magn. Res. Ser. A.* **1996**, *120*, 1-10.
- [135] Laatikainen, R.; Niemitz, M.; Malaisse, W. J.; Biesemans, M.; Willem, R. *Magn. Reson. Med.* **1996**, *36*, 359-65.
- [136] Grimme, S.; Steinmetz, M.; Korth, M. *J. Chem. Theory. Comp.* **2007**, *3*, 42-5.

Publications and presentations regarding this thesis

1. Björnsson, R.; Arnason, I., **A computational study of the conformational properties of monosubstituted cyclohexanes and silacyclohexanes**; The 15th International Symposium on Organosilicon Chemistry, June 1-6, 2008, Jeju, Korea.
2. Wallevik, S. Ó.; Björnsson, R.; Arnason, I., **Conformational behavior of monosubstituted silacyclohexanes**; The 15th International Symposium on Organosilicon Chemistry, June 1-6, 2008, Jeju, Korea.
3. Björnsson, R.; Arnason, I., **NMR simulation of the parent disilacyclohexanes**; Natural Science Symposium 2008, March 14-15, 2008, Reykjavík, Iceland.
4. Wallevik, S. Ó.; Björnsson, R.; Kvaran, Á.; Jónsdóttir, S; Arnason, I.; Bodi, A.; Girichev, G. V.; Giricheva, N. I, **Conformational properties of 1-fluoro-1-methyl-1-silacyclohexane. Are A values additive?**; 12th European Symposium on Gas Electron Diffraction, June 24-28, 2007, Blaubeuren, Germany.
5. Björnsson, R.; Wallevik, S. Ó.; Arnason, I.; Bodi, A.; Hölbling, M., **Substituent effects in silacyclohexanes: Theory vs. experiment**; 12th European Symposium on Gas Electron Diffraction, June 24-28, 2007, Blaubeuren, Germany.

Papers in preparation:

1. Bodi, A.; Bjornsson, R.; Arnason, I.; **Predicting conformational energy change on the basis of molecular geometry change in monosubstituted propanes, silapropanes, cyclohexanes, silacyclohexanes, piperidines and phosphorinanes.** Manuscript in preparation.
2. Arnason, I.; Gudnason, P.; Bjornsson, R.; ... Oberhammer, H.; **Conformations of silicon-containing rings. Part X. Gas phase structures of disilacyclohexanes.** Manuscript in preparation.
3. Bjornsson, R.; Arnason, I.; **Reliable conformational energy differences of six-membered rings using density functional theory.** Manuscript in preparation.
4. Bjornsson, R.; Arnason, I.; **Silicon substitution effects on the axial/equatorial equilibrium of monosubstituted rings.** Manuscript in preparation.
5. Arnason, I.; Kvaran, A.; Jonsdottir, S.; Wallevik, S. Ó.; Bjornsson, R.; Bodi, A.; Oberhammer, H.; **Conformations properties of 1-silyl-1-silacyclohexane: Gas Electron Diffraction, Low-temperature NMR, Temperature-dependent Raman Spectroscopy and Quantum chemical calculations.** Manuscript in preparation.
6. Arnason, I.; Kvaran, A.; Jonsdottir, S.; Wallevik, S. Ó.; Bjornsson, R.; Bodi, A.; Girichev, G. V.; Giricheva, N. I.; Hassler, K. et al. **Conformations properties of 1-fluoro-1-methyl-1-silacyclohexane and 1-trifluoromethyl-1-methyl-1-silacyclohexane: Gas Electron Diffraction, Low-temperature NMR, Temperature-dependent Raman Spectroscopy and Quantum chemical calculations.** Manuscript in preparation.

Curriculum vitae

Ragnar Björnsson

Born on July 2nd, 1983 in Reykjavik, Iceland.

Nationality: Icelandic

E-mail address: ragnarbj@theochem.org

Research interests

Quantum chemical calculations, inorganic chemistry, bioinorganic chemistry, physical organic chemistry, NMR.

Educational record

- B.Sc. degree in Biochemistry spring 2006, from the University of Iceland.
- M.Sc. degree in Inorganic Chemistry fall 2008, from the University of Iceland.
 - 90 ECTS research project: *Theoretical studies of silicon-containing six-membered rings*. Supervisor: Prof. Ingvar Arnason.
 - A semester was spent at the University of Ottawa fall 2006, taking chemistry courses at the graduate level.

Professional experience

- Research assistant at the Science Institute, University of Iceland, parttime 2004-2006. Worked with Prof. Hannes Jónsson doing various computational work, including server and cluster maintenance, website management and computer programming.
- Research assistant at the Science Institute, University of Iceland, summer 2005 and 2006. Worked in synthetic inorganic chemistry with Prof. Ingvar Arnason. Synthesis, analysis and theoretical calculations of silicon- and germanium-containing organic rings.
- Teaching assistant 2006 - 2008, Department of Chemistry, University of Iceland
 - Spring 2006: TA in the laboratory part of Organic Chemistry 2.
 - Spring 2007: TA in the laboratory part of Instrumental Analysis.
 - Fall 2007: TA in the laboratory part of General Chemistry 1.
 - Spring 2008: TA in the laboratory part of Instrumental Analysis.

- Fall 2008: TA in the laboratory part of Inorganic Chemistry 3.

Advanced courses and conferences attended

- Radiochemistry - University of Ottawa fall 2006
- Mass Spectrometry - University of Ottawa fall 2006
- Organic Structure Determination Using NMR Spectroscopy - University of Ottawa fall 2006
- Surface and Nanotechnology - University of Ottawa fall 2006
- Catalysis in Organic Chemistry - University of Ottawa fall 2006
- Quantum Chemistry and Chemical Rate Theory - University of Iceland spring 2007
- Advanced Spectroscopy - University of Iceland spring 2006
- Organometallic Chemistry - University of Iceland fall 2007
- “New Materials for the Hydrogen Society” - summer school 2006
- NRENS and GRID Conference & GRID Workshop, 18-19 of October 2007
- 12th European Symposium on Gas Electron Diffraction, June 2007
- 12th European Symposium on Gas Electron Diffraction, June 2007
- The 15th International Symposium on Organosilicon Chemistry, June 1-6, 2008, Jeju, Korea.

Service and activities

- Website administrator for Hvarf, the Student Chemistry Society at the University of Iceland, 2004-2006.
- Editorial board member of Snefill, the student chemistry journal, 2004-2005.
- President and co-founder of Komplex, the Graduate Student Chemistry Society at the University of Iceland, 2007-2008.
- Student representative at departmental meetings (Chemistry), 2007-2008.
- Website design for :
 - Hvarf, the Student Chemistry Society, University of Iceland
 - Komplex, the Graduate Student Chemistry Society, University of Iceland
 - Chemistry Department, University of Iceland
 - Science Institute: Chemistry Division
 - The Icelandic Chemical Society
- Organization of the Natural Science Symposium in 2006.

- Member of the local organizing committee of the EIPAM 2007 conference: Electron Induced Process At the Molecular Level , Hveragerdi, May 25th-27th, 2007.
- Member of the local organizing committee of the Nordforsk conference: Fundamental Quantum Processes in Atomic and Molecular Systems , Nesbúð June 30th- July 2nd, 2007.
- Board member of the Icelandic Chemical Society (www.efn.is), 2008.

Appendix 1.1

Basis set convergence of 1-fluoromethyl-1-silacyclohexane.

ΔE values (in kcal/mol) of the axial/equatorial equilibrium of 1-fluoro-1-methyl-1-silacyclohexane. B3LYP calculations with different basis sets.

Basis set ^b	ΔE	Nr. functions ^a
Pople basis sets		
6-31G(d)	-0.571	142
6-31G(d,p)	-0.562	181
6-31++G(d,p)	-0.576	226
6-311G(d)	-0.482	191
6-311G(d,p)	-0.487	230
6-311++G(d,p)	-0.602	275
6-311++G(2d,2p)	-0.591	354
6-311++G(3df,3pd)	-0.528	554
cc-pVDZ	-0.682	181
cc-pVTZ	-0.499	426
cc-pVQZ	-0.489	834
aug-cc-pVDZ	-0.704	305
aug-cc-pVTZ	-0.521	671
aug-cc-pVQZ	-0.498	1242
cc-pV(D+d)Z	-0.643	186
cc-pV(T+d)Z	-0.491	431
cc-pV(Q+d)Z	-0.483	839
pc-0	+0.363	102
pc-1	-0.547	181
pc-2	-0.474	426
pc-3	-0.483	954
aug-pc-0	-0.719	147
aug-pc-1	-0.550	305
aug-pc-2	-0.502	671
aug-pc-3	-0.487	1362

^aTotal number of basis functions for describing 1-fluoro-1-methyl-1-silacyclohexane

^bThe aug-prefix means the basis set is augmented with diffuse functions.

Appendix 1.2

The basis set convergence of MP2/*anZ*^{xix} compared to M06-2X/*pc-n* for the 13-molecule test set in chapter 1.4.4.

The MP2/*anZ* [85], [85] and M06-2X basis set convergence of ΔE values (in kcal/mol) for the axial/equatorial equilibrium of several cyclohexanes, tetrahydropyrans and silacyclohexanes.

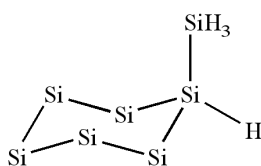
	MP2/aDZ	MP2/aTZ	MP2/aQZ	MP2/aSZ	MP2-CBS		M06-2X/pc-0	M06-2X/pc-1	M06-2X/pc-2	M06-2X/pc-3	M06-2X/pc-4
Cyclohexanes											
Methyl	-1.79	-1.70	-1.73	-1.73	-1.73		-0.86	-1.45	-1.69	-1.70	-1.72
Fluoro	0.27	-0.10	-0.17	-0.20	-0.23		2.25	0.79	-0.14	-0.15	-0.16
Methoxy	0.40	0.12	0.01	-0.01	-0.03		2.69	0.98	-0.05	-0.12	-0.11
Hydroxy	-0.08	-0.38	-0.49	-0.50	-0.52		2.31	0.47	-0.45	-0.50	-0.50
Tetrahydropyrans											
2-Methyl	-3.13	-2.92	-2.91	-2.91	-2.90		-0.52	-2.32	-2.60	-2.59	-2.60
2-Fluoro	3.13	2.59	2.51	2.48	2.45		6.57	3.81	2.50	2.46	2.45
2-Methoxy	1.80	1.51	1.40	1.39	1.37		5.93	2.55	1.35	1.31	1.31
2-Hydroxy	1.32	1.03	0.92	0.90	0.88		5.48	2.09	0.91	0.87	0.87
Silacyclohexanes											
Methyl	-0.28	-0.18	-0.18	-0.13	-0.14		0.74	-0.05	-0.08	-0.11	-0.10
Fluoro	0.29	0.10	0.00	0.11	0.05		-0.74	0.38	0.20	0.16	0.17
Methoxy	0.41	0.28	0.16	0.30	0.23		0.98	0.63	0.29	0.23	0.24
Hydroxy	0.18	0.08	-0.06	0.07	-0.01		0.57	0.37	0.10	0.06	0.06
Chloro	0.6	0.77	0.62	0.64	0.58		1.80	0.91	0.63	0.63	0.64
MAD	0.57	0.25	0.13	0.14	0.11		3.68	1.22	0.19	0.14	0.14
ME	0.46	0.22	0.08	0.12	0.07		3.47	1.22	0.19	0.14	0.14
MaxE	0.68	0.37	0.22	0.24	0.20		4.66	1.36	0.23	0.23	0.24

^{xix} Basis sets were mixed with aug-cc-pVnZ basis sets only used on O and F atoms, while cc-pVnZ basis sets were used on C and H atoms and cc-pV(n+d)Z used on Si atoms [85], [85].

Appendix 1.3

The basis set convergence of silylcyclohexasilane using cc-pVnZ and cc-pV(*n*+*d*)Z basis sets and functionals B3LYP and M06-2X.

Calculations were carried out in order to see if the conformational energy difference of a six-membered ring with many second-row atoms, is dependent on using basis sets with tight *d*-functions (cc-pV(*n*+*d*)Z basis sets).



silylcyclohexasilane

Effect of basis sets on the conformational energy difference of silylcyclohexasilane with B3LYP and M06-2X functionals. Values in kcal/mol.

B3LYP	ΔE		M06-2X	ΔE
cc-pVDZ	0.912		cc-pVDZ	-0.317
cc-pVTZ	1.111		cc-pVTZ	-0.234
cc-pVQZ	1.144		cc-pVQZ	-0.237
cc-pV(D+d)Z	0.913		cc-pV(D+d)Z	-0.311
cc-pV(T+d)Z	1.106		cc-pV(T+d)Z	-0.237
cc-pV(Q+d)Z	1.143		cc-pV(Q+d)Z	-0.240

The difference in ΔE values using the cc-pVnZ and the cc-pV(*n*+*d*)Z basis sets is very small for this example and can safely be ignored.

It appears that the cc-pV(*n*+*d*)Z basis sets do not offer any improvement over cc-pVnZ basis sets for conformational analysis of our systems, even those containing many silicon atoms.

Appendix 2.1

NWChem 5.1 input file, used for the M06-2X/pc-*n* calculations in chapter 2.

```
START
MEMORY 1950 MB
echo
GEOMETRY
*cartesian coordinates*
END
DRIVER
tight
maxiter 150
END
DFT
xc m06-l
direct
END

BASIS spherical
* library def2-tzvp file /home/ragnarbj/def2-grunnar/
END
BASIS "cd basis" spherical
* library "Ahlrichs Coulomb Fitting"
END
TASK dft optimize

BASIS spherical
* library def2-tzvp file /home/ragnarbj/def2-grunnar/
END
BASIS "cd basis" spherical
* library "Ahlrichs Coulomb Fitting"
END
TASK dft optimize

STOP
DFT
xc m06-2x
direct
tolerances tight
grid xfine
END
BASIS spherical
* library pc-2 file /home/ragnarbj/jensen/
END
TASK dft optimize

BASIS spherical
* library pc-0 file /home/ragnarbj/jensen/
END
TASK dft energy
BASIS spherical
* library pc-1 file /home/ragnarbj/jensen/
END
TASK dft energy
BASIS spherical
* library pc-2 file /home/ragnarbj/jensen/
END
TASK dft energy
BASIS spherical
* library pc-3 file /home/ragnarbj/jensen/
END
TASK dft energy
```